Uncovering roles for Caspar/dFaf1 in *Drosophila* development

A Thesis

submitted to

Indian Institute of Science Education and Research Pune in partial fulfilment of the requirements for the BS-MS Dual Degree Programme

by

Jyothish S

Indian Institute of Science Education and Research Pune

Dr. Homi Bhabha Road,

Pashan, Pune 411008, INDIA.

April, 2020

Supervisor: Dr. Girish Ratnaparkhi

Jyothish S

Certificate

This is to certify that this dissertation entitled “Uncovering roles for Caspar/dFaf1 in Drosophila development” towards the partial fulfilment of the BS-MS dual degree programme at the Indian Institute of Science Education and Research, Pune represents study/work carried out by Jyothish S at Indian Institute of Science Education and Research under the supervision of Dr. Girish Ratnaparkhi, Associate Professor, Department of Biology, during the academic year 2019-2020.

Dr. Girish Ratnaparkhi

Committee:

Dr. Girish Ratnaparkhi

Dr. Richa Ricky

I dedicate this thesis to my parents Mr. Sudhakaran P and Mrs. Bindhu V, who have pushed themselves beyond I could have asked for, to let me pursue my dreams. My sister, Karthika S, for that sweet sibling rivalry.

My teachers from preschool to college, especially Rajashree teacher, Sheeja teacher and Satheeesh sir, whom ensured that I get a fair chance at higher education. Thank you so much for paving my path and guiding me.

To Swati Choudhary for being the crazy friend that always has my back.

My friends, Zakhiya P C, Rajdeep Haldar, Shubhangi Khobragade, Aarti Kejriwal for their constant emotional support.

Dr. Girish Ratnaparkhi, for his quirks and enthusiasm that has enchanted me to mirthfully pursue my thesis project.

Declaration

I hereby declare that the matter embodied in the report entitled “Uncovering roles for Caspar/dFaf1 in Drosophila development” are the results of the work carried out by me at the Department of Biology, Indian Institute of Science Education and Research, Pune, under the supervision of Dr. Girish Ratnaparkhi and the same has not been submitted elsewhere for any other degree

Jyothish S

Date: 27-03-2020

Table of Contents

List of Tables

List of Figures

Abstract

Fas associating Factors (Faf1/Casp and Faf2) are members of the UBX domain containing proteasomal adaptors family of proteins. The primary sequence analysis suggests conservation of structure and function between flies and humans. Casp has been previously reported to be involved in *Drosophila* innate immunity and also has been characterized as a maternal effect gene in development. The physiological function of Faf2 is not well characterized in *Drosophila*.

In this study, we attempt to characterize the role of the different functional domains of Casp by generating Casp transgenic animals with targeted domain deletions. The deletions of interest were the ΔUBX, and a combined deletion ΔUASΔUBX. Our first attempt used CRISPR/Cas9 based genome editing, which did not succeed. As an alternative, we were successful in generating a number of overexpression transgenic animals, pUASP-ΔDomain flies, which we plan to express in a $Casp^{null}$ animal using the UAS Gal4 system. We are also redoing the CRISPR screen using a modified design. Additionally, a loss of function analysis using reverse genetics on the Casp homolog Faf2 suggest that Faf2 is a paternal effect gene. Zygotic copy of Faf2 is not sufficient to rescue the paternal phenotype. Faf2 knockdown does not cause sterility of the male germline as the embryos fathered by Faf2 knockdown males proceed through nuclear divisions. Paternal germline specific Faf2 knockdown results in embryonic developmental arrest at early stages of gastrulation.

Given that Faf2 is not present in the *Drosophila* sperm and that Faf2 influences protein dynamics in the cell, we hypothesize that Faf2 functions in the observed paternal effect phenotype by altering the chromatin architecture of paternal chromosomes.

Acknowledgments

First and foremost, I would like to express my sincere gratitude to Dr. Girish Ratnaparkhi, Department of biology, Indian Institute of Science Education and Research, Pune, for letting me work in his lab. I am extremely thankful that you let me join your lab on a short notice and for having immense faith in my abilities even at times when I was doubting myself. I am thankful to you for your constant support and guidance throughout my thesis project and for considering my ideas and allowing me to pursue them.

I am really thankful to Sushmitha Hegde and Neel Wagh for their constant guidance throughout my thesis work. I am thankful to Aarti Kejriwal for keeping me on my toes and making sure that I finish things on time. I am thankful to all the other members of Girish's lab for their help and suggestions. I convey my gratitude towards Dr. Richa Ricky, Department of biology, Indian Institute of Science Education and Research, Pune, for her valuable comments and inputs for my project. I convey my gratitude towards Dr. Anuradha Ratnaparkhi, Agharkar Research Institute, Pune for training me in transgenics generation. I would like to thank the IISER Pune fly facility and microscopy facility for their services. And Finally, I would like to thank my institute IISER Pune, for providing me with an amazing research environment.

Chapter 1

Introduction

Summary: In this Chapter I have introduced Casp, a protein that has not been studied in detail in *Drosophila*. I compare and contrast fly Casp/Faf1 with known mammalian functions for Faf1. Faf1 domain analysis suggest important roles for Casp in the Ubiquitin-Proteasomal pathway, and these are discussed in detail. Possible roles for *Drosophila* Faf2, a Faf1 homolog is also discussed.

Caspar: Caspar (Casp) is the *Drosophila* ortholog of mammalian fas associated factor 1 (Faf1). Faf1 is an evolutionarily conserved protein with a wide range of biological functions. Faf 1 was first identified as a Fas interacting protein. Faf1 is not sufficient to initiate apoptosis, but can enhance the process (Chu, Keting, et al. 1995). Over the past few decades, new roles for Faf1 are being discovered in immunity, oncogenesis and development with clear parallels being identified between mammalian and *Drosophila* systems.

Faf1 domains and functions: Faf1 has multiple interaction domains with most of them conserved in the *Drosophila* ortholog, Casp (Fig. 1). The various domains of Casp/Faf1 are as follows: N-terminal ubiquitin associating UBA domain, a fas interacting domain (FID) which includes ubiquitin like domains Ubl1 and Ubl2, a death effector domain interacting domain (DEDID) the UAS domain and the C-terminal Valosin binding Ubiquitin regulatory-x (Ubx) domain. Each of these domains have been shown to interact with specific interacting partners and assist with mediating different biological processes.

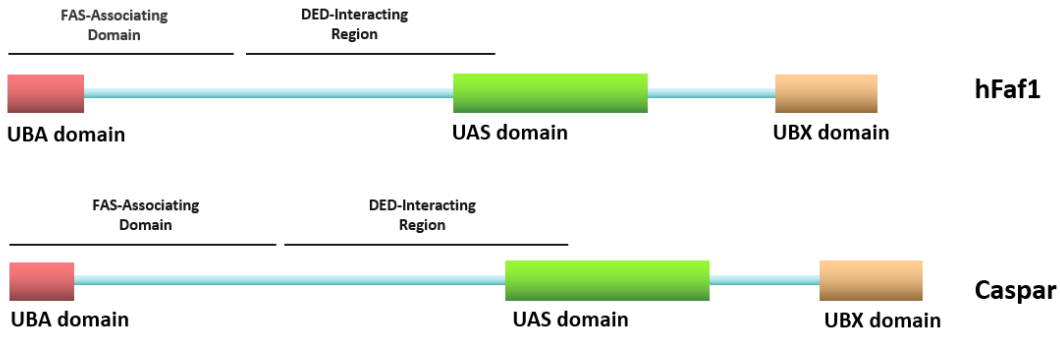

Figure 1: Casp is homologous to human Faf1. Bioinformatic studies suggest that Casp and human Faf1 have conserved UBA, UAS and the UBX domains. Overall, Casp has 54% sequence similarity with hFaf1 and 34% identity. Figure modified from Kim, Myungjin, et. al. 2006.

The UBA domain of Faf1 interacts with lysine 48 linked polyubiquitinated proteins (Song, Eun Joo et. al, 2005). The ubiquitin binding UBA domain of Faf1 is not completely conserved with the UBA domains of other ubiquitin binding proteins. Faf1 UBA domain conserves the characteristic three helical bundles and the hydrophobic surface that interacts with the 5-strand beta sheet present in ubiquitin but lacks the MGF motif. The affinity of Faf1 UBA domain was shown to be strongest towards tetra-ubiquitin and was shown to not interact at all with mono-ubiquitinated proteins (Fig. 2).

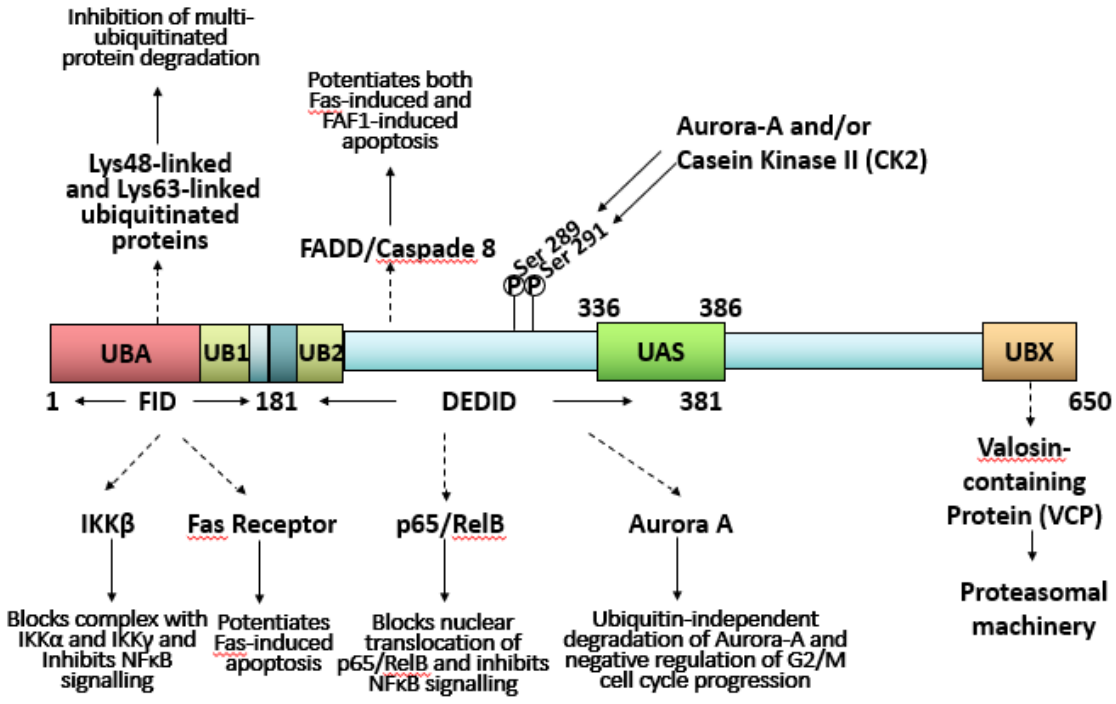

Figure 2: hFaf1 domains and their known functions. Faf1 shows the characteristic folds of a fas-interacting domain and the death effector domain interacting domain. FID fold contains the UBA domain that binds to polyubiquitinated proteins and the ubiquitin like folds UB1 and UB2. Faf1 has multiple phosphorylation sites. The DEDID region can physically interact with RelB and retain it within the cytoplasm resulting in an inhibition of Nf-κB signalling. I also can bind to Aurora A and result in its degradation. The UBX domain interacts with VCP which is a major subunit of the proteasomal machinery. Figure adapted from Song, Eun Joo, et al., 2005.

It has been shown that the binding of ubiquitinated proteins to the UBA domain of Casp stabilizes these substrates and prevent their degradation by the 26S

proteasomal machinery (Song, Eun Joo, et al. 2005). it is not clear as to whether all Lys-48 linked polyubiquitinated proteins are prevented from degradation by UBA domain of Faf1 or if this activity is substrate specific.

For instance, it has been shown that Faf1 aids in the ubiquitin mediated degradation of Hsp70 and negatively regulates tumorigenesis (Lee, Jae Jin, et. al, 2012). The UBA domain is necessary for the binding of ubiquitinated Hsp70, in addition to which the Ubl1 domain of Faf1 also interacts with Hsp70 (Lee, Jae Jin, et. al, 2012). Over-expression of Faf1 or its UBA domain alone results in enhanced degradation of Hsp70 and also shows inhibition of tumour colony growth and promotes tumour cell death. The observed cell death is assumed to be a result of increased cell stress due to the accumulation of a wide range of ubiquitin proteasomal substrates. The interaction of the Ubl1 domain with Hsp70 has been shown to reduce the chaperonic activity of Hsp70 to refold misfolded proteins. Which suggests that tumour suppressive activity of Faf1 might be resultant of its ability to regulate Hsp70 activity (Kim, Hee-Jung, et al. 2005). It has also been shown that the Ubl1 binding of Hsp70 enhances its ubiquitylation via various E3 ligases, one of which is C-terminal Hsp70 interacting protein (CHIP) and the ubiquitinated Hsp70 then binds to the UBA domain and is degraded eventually.

Faf1 is an antagonist of Nf-κB signalling. Ubl domains of Faf1 physically interact with Nf-κB subunit RelA (p65) and retain it in the cytosol (Park, Min-Young, et al. 2004). Faf1 also inhibits the inhibitory kappa kinase (IκK) activity as a result of which the phosphorylation and consequent excision of IκB from Rel to release RelA(p65) does not take place. As a result of which the downstream pro-inflammatory cytokine genes of Nf-κB signalling are not activated.

The UAS domain of Faf1 responds to cytosolic unsaturated long chain fatty acid levels. Under elevated levels of long chain unsaturated fatty acids, UAS domain causes polymerization of Faf1 (Kim, Hyeonwoo, et al. 2013). In the mammalian system, Faf1 and Faf2 (ubdx8) are the only proteins shown to have a UAS domain. Ubdx7 contains a primitive UAS domain but there isn't any sequence conservation with the other two UAS domains. Both Faf1 and Faf2 as well as their purified UAS domains formed oligomer to polymers in presence of long chain unsaturated fatty acids indicating that the UAS domain of Faf1 might act as a switch to alter the function

of the protein in various tissue types as well as in stress or other altered physiological conditions. Shorter unsaturated fatty acids as well as short and long saturated fatty acids could not elicit any protein polymerization. In support of this argument, it has been previously reported that elevated levels of long chain unsaturated fatty acids result in Nf-κB activation (Weigert, Cora, et al. 2004) also saturated fatty acids fail to produce similar results. One of the reasons for which could be the simple fact that monomeric Faf1 being an antagonist of Nf-κB signalling is inactivated by unsaturated fatty acids by mediating the UAS directed polymerization of Faf1.

The C-terminal Ubx domain of Faf1 interacts with valosin to associate with the 20S proteasomal machinery (Lee, Jae-Jin, et al. 2013). Ubx domain, which resembles ubiquitin in its tertiary structure binds to valosin-containing protein (VCP), a AAA (ATPase) family protein. This interaction requires the preassembly of VCP with Nuclear protein localization protein 4 (Npl4) and Ubiquitin recognition factor in ER associated degradation 1 (Ufd1) heterodimer. The Npl4-Ufd1 is a cofactor for the 20S proteasomal machinery. It has been observed that the interaction of the Ubx domain with VCP-Npl4-Ufd1 is a prerequisite for the ubiquitin binding of the UBA domain. This regulation seems not to require a direct interaction between UBA and Ubx domains. Faf1 lacking C-terminal Ubx domain highly stabilizes ubiquitinated proteins. It is debatable as to whether this is due to a lack of UBA binding to the ubiquitinated proteins or there is active stabilization of ubiquitin proteasomal substrates by the UBA domain since previous studies have shown that C-terminal truncated Faf1 and its UBA domain alone can successfully interact with multiple ubiquitinated target proteins (Song, Eun Joo et. al, 2005). In presence of both UBA and Ubx domains, proteasomal degradation takes place suggesting that Faf1 acts as a scaffolding protein that bring together the proteasomal machinery and its substrates to facilitate endoplasmic reticulum associated degradation (ERAD) (Fig. 3).

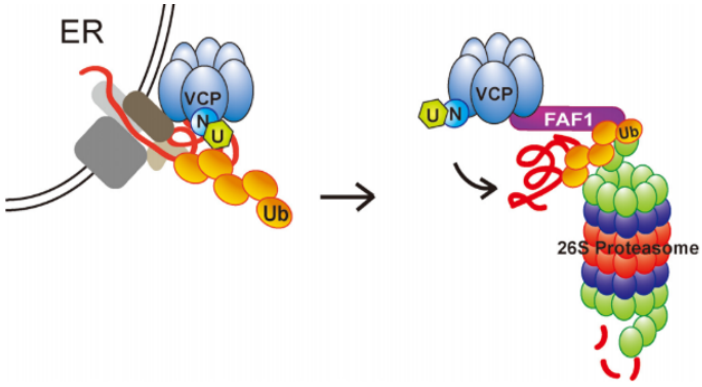

Figure 3: Faf1 acts as an adaptor for p97 mediated proteasomal degradation. Misfolded proteins are selectively ubiquitinated by the VCP-Npl4-Ufd1 complex. Faf1 scaffolds with the complex, binding to VCP through UBX domain and polyubiquitinated proteins through the UBA domain sequentially. Faf1 then aids in the translocation of the ubiquitinated targets to the proteasome where these products are partially or completely degraded in a substrate dependent fashion. Figure adapted from Lee, Jae-jin, et. al. 2003.

Ubiquitin Proteasomal machinery: Ubiquitin mediated proteasomal degradation is one of the two major bulk protein degradation pathways present in eukaryotes (Shin, Seung-Wook, et al. 2013) the other being the autophagy mediated lysosomal protein degradation. The 20S catalytic core and a 19S regulatory particle comprises the eukaryotic ubiquitin proteasomal machinery. The proteasomal machinery is very selective in proteolysis owing to the prerequisite of needing the substrates to be tagged with ubiquitin in specific lysine residues such as lysine 48 or lysine 29. Proteasomal assembly chaperones (PACs) help in the assembly of four heteroheptameric rings to form the 20S subunit. The expression of ubiquitin proteasomal system (UPS) is auto regulatory, wherein one of the substrates for UPS, Ubiquitin mediated proteolysis 1 (Ump1) induces the production and assembly of UPS. Inhibition of UPS by MG132 has shown to result in elevated levels of Ump1 and a subsequent de-novo synthesis of the precursor subunits of the proteasome.

An interesting study has shown that proteasomal machinery can partially or completely degrade ubiquitinated proteins by detecting the differences of the polyubiquitin linkage signatures. The Gli family of transcriptional repressors are processed differentially in response to hedgehog signalling to activate hedgehog targets (Zhang, Zhao, et al. 2013). Cubitus interruptus (Ci), a Gli family transcriptional repressor in *Drosophila* act a key player in hedgehog signalling. In the absence of hedgehog ligand, patched inhibits the phosphorylation and activation of smoothened. In this scenario, Ci is sequentially phosphorylated by Protein KinaseA (PKA) Glycogen Synthase Kinase3 (GSK3) and Casein Kinase1 (CK1) which leads to lysine-11 linked polyubiquitination of Ci mediated by Cullin1 (Cul1)-Supernumerary limbs (slimb) E3 ligase complex. K11 ubiquitin linkage then targets Ci for partial degradation to release an N-terminal repressor domain Ci75. In the presence of hedgehog, Ci does not get phosphorylated causing its accumulation and subsequent translocation into the nucleus. This full-length Ci (Ci155) then activates hedgehog target genes. Roadkill (rdx) which is one of the downstream activated genes act as a negative regulator of

hedgehog signalling. Cul3-Rdx E3 ligase adds K43 linked polyubiquitin chains to Ci155 resulting in a complete subsequent degradation of Ci by the proteasome.

The proteasomal machinery plays a major role in the maternal to zygotic transition (MZT) as it is essential to degrade maternal proteins before the zygotic genome can start transcribing to elaborate its developmental program. Previous studies using mouse models have shown that Faf1 is essential in early development with Faf1 being a lethal mutant. Homozygous mutants for Faf1 fails to develop beyond the two-cell stage of early embryonic development (Adham, Ibrahim M., et al. 2008). It could be the maternal transcripts that rescue the development till two cell stage, it then becomes interesting to ask why such a stark lethal mutation phenotype is not seen in *Drosophila*.

Casp and immunity: In *Drosophila*, Casp has been shown to be a negative regulator of antibacterial immunity (Kim, Myungjin, et al. 2006). Innate immunity in *Drosophila* is broadly mediated by two different sets of signalling cascades: The toll signalling mediated anti-fungal and anti-gram-positive bacterial immunity and the immune deficient (IMD) mediated anti-gram-negative bacterial immunity.

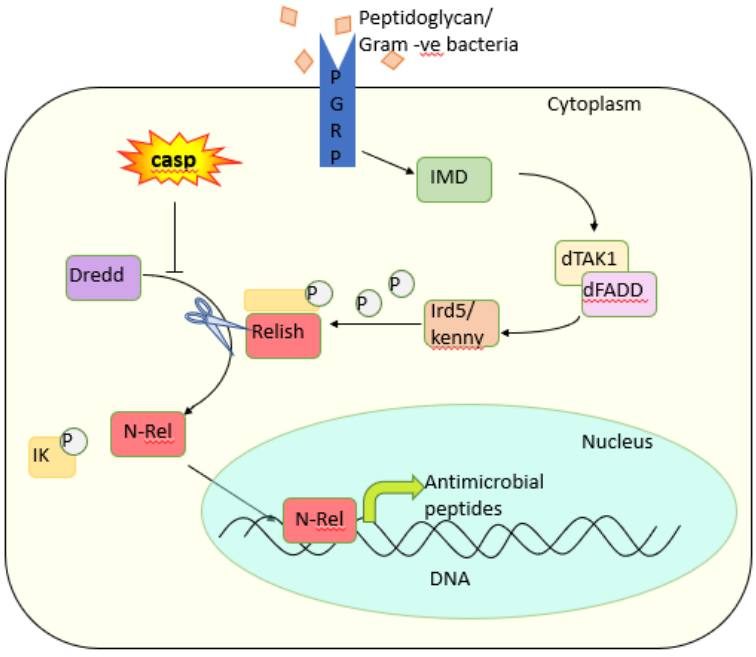

Figure 4: Casp is a negative regulator of IMD mediated innate immune response in *Drosophila*. *Drosophila* innate immune response towards gram positive bacterium is mediated through the IMD arm of innate immunity. Unlike the toll receptor pathway, there are no specific receptor clusters for IMD signalling. PGRPs activate IMD in response to a peptidoglycan load. Through a series of subsequent activation of downstream proteins, Relish

is phosphorylated and cleaved to release the N-Rel homology domain transcription factor which then translocates to the nucleus and activates downstream target genes such as diptericin. The cleavage of phosphorylated Relish is mediated by Dredd. Casp acts as a suppressor of Dredd mediated cleavage of Relish.

In the IMD arm of immunity, peptidoglycan recognition proteins (PGRPs) on recognising peptidoglycan, activates IMD through *Drosophila* TNF receptor associated factor 2 (dTRAF2) which then stimulates *Drosophila* fas associated death domain protein (dFADD) and *Drosophila* TGFβ activated kinase 1 (dTAK1) to activate the *Drosophila* inhibitory kappa kinase (DmIκK) Ird5/Kenny which then phosphorylates the C-terminal IκB domain of Relish. This results in the cleavage of Relish into REL68, containing the DNA binding domain and C-terminal IκB domain. Rel68 then translocates into the nucleus and induces the production of antimicrobial peptides like diptericin. Casp inhibits this immune signalling by suppressing the Dredd mediated cleavage of relish (Fig. 4).

Casp as a maternal effect gene: Early embryonic development is a very intricate and well-orchestrated event. All multicellular organisms start from a single cellular fertilized egg, which then undergoes repeated and tightly regulated cell divisions. Cell migration and patterning events decide the relative positions of each cell in a growing embryo which then determines the developmental fate of each cell, transitioning it from a pluripotent cell to differentiated progenitor cells. A seemingly homogenous egg cell has very well-defined molecular gradients set up across it defining the major developmental axes. In *Drosophila* embryo, the anterior-posterior, dorso-ventral and terminal patterning determinants define the A-P, and D-V axes. The mononucleated embryo does not transcribe all the gene products required for regulating the polarity of the embryo and its early development, rather these gene products are deposited into the developing oocyte by the nurse cells of the egg chamber during oogenesis. These include bicoid, oskar and gurken that define the anterior posterior and dorsal poles of the embryo respectively (Nusslein-Volhard, et al. 1987) and many more such as pipe, nudel, snake, spatzle, gastrulation defective, nanos etc. Tailless and torso are two of the maternally deposited transcripts that are essential for terminal patterning (Lu, X. I. A. N. G. Y. I., et. al. 1993). Since these maternally deposited proteins are crucial for the early developmental program, mutations of these genes in the maternal germline causes deposition of aberrantly functioning transcripts into the egg and this

causes defects in the developmental program irrespective of the genotype of the zygote itself (Morgan & Claypool Life Sciences; 2010). These genes are categorized under the umbrella term ‘maternal effect genes.’

In a recent study conducted in our lab, Casp has been identified as a maternal effect gene (Neel Wagh, MS thesis, 2019). Casp mRNA is deposited into the oocyte by the nurse cells and is translated to the Casp protein in very early stages of the embryo. By using a 5’-UTR pBac insertion loss of function allele for Casp (referred to as $Casp^{lof}$), it was shown that Casp plays a critical maternal role in early development of *Drosophila* embryos. Around 75% of the embryos are non-viable when the female is homozygous for the $Casp^{lof}$ allele. This phenotype was not rescued by a paternally derived zygotic copy of wildtype Casp gene, confirming that the observed phenotype is indeed due to maternal effect of Casp. Even though embryos from a Casp null female proceeds to gastrulation, they fail to develop beyond stage 10-15 and as a result, these embryos fail to deposit a cuticle. It is hypothesized that the nonviability of the embryos might be because of the lack of degradation of maternal proteins. This assumption is made on the basis that, Faf1 has been reported to be involved in ubiquitin mediated protein degradation and also that an effective degradation of maternally deposited proteins is essential to facilitate maternal to zygotic transition and a successful activation of the zygotic developmental program. It has been shown in mouse models that Faf1 is essential for zygotic development and Faf1 null embryos fails to develop beyond the two-cell stage (Adham, Ibrahim M., et al. 2008), it thus becomes interesting as to why do we not see such lethality in *Drosophila*. In the mouse system it is possible that the development proceeds till two cell stage due to the presence of maternal transcripts and further development stalls as there is no zygotic expression of Faf1.

Faf2 another member of the Faf family: Fas associated factor 2 (Faf2) earlier known as ubiquitin regulatory X domain-containing protein 8 (Ubxd8) is another member of the Faf family. Faf2 conserves the UBA, UAS domain and UBX domain similar to Faf1 but lacks a major fraction of the linker between the UBA and UAS domains (Fig. 5).

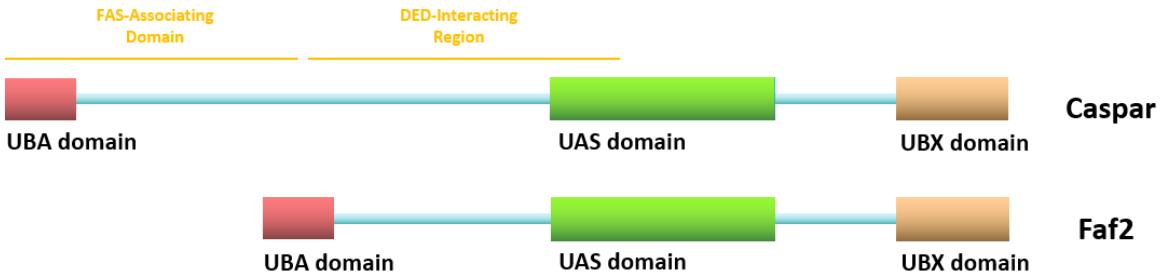

Figure 5: Faf2, like Casp, contains the UAS and UBX domains. Faf2 shows 46% sequence conservation with Casp with 24% identity. Like Casp, Faf2 retains the UBA, UAS and UBX domains. The linker region between the UBA and UAS domain is highly truncated in Faf2 as opposed to Casp.

Faf2 has been shown to act as a major sensor for the levels of long chain poly-unsaturated fatty acids (LCPUFA) through its UAS domain (Kim, Hyeonwoo, et al. 2013). Faf2 plays a major role in regulating fatty acid synthesis in cells. The highly positive surface patch on UAS domain contains six lysine and arginine residues that are essential for the detection of levels of LCPUFA. The negatively charged carboxy terminal of fatty acids interacts with the UAS domain helping it to multimerize. In low levels of fatty acid (FA), Faf2 promotes the proteasomal degradation of Insig-1. In the absence of Insig-1, Sterol regulatory element binding protein (SREBP)-1 is proteolytically activated and its N-terminal domain act as a transcription factor for activating the genes required for FA synthesis. High levels of LCPUFA disrupts the interaction between Faf2 and Insig-1, stabilizing Insig-1 which then prevents proteolytic activation of SREBPs.

Faf2, like Casp, acts as an adaptor for ubiquitin mediated protein degradation. Interestingly, Faf2 also primes P97 proteasome for ubiquitinated protein unfolding and remodelling. Other than regulating FA levels, it was shown that Faf2 plays a major role in regulating mRNA stability (Zhou, Hua-Lin, et al. 2013). HuR is an RNA binding protein that stabilizes mRNAs and facilitates the ribonucleoprotein assembly to facilitate RNA translation. Faf2 promotes the segregase activity of P97 and the Faf2-P97 complex remodels lysine-29 linked polyubiquitinated HuR and dissociates it from mRNAs causing a destabilization of the mRNAs. Faf2 has also been implicated in pathogenesis of Amyotrophic lateral sclerosis (ALS). ALS associated mutation in Ubiquilin 2 (UBQLN-2). The interaction between UBQLN-2 and Faf2 was shown to be disrupted in the UBQLN-2 P497H mutants (Xia, Yuxing, et al. 2014). These mutants show accumulation of null Hong Kong variant of α-1-antitrypsin (NHK) which is a

defective protein that usually is degraded by the proteasome. Interestingly, any alterations in the levels of Faf2 or UBQLN-2 showed this NHK accumulation. These observations suggest that Faf2 plays a major role in the ERAD pathway in maintaining protein homeostasis.

Paternal effect genes: Much like the maternal effect genes, a few genes have been identified to show paternal effects during embryogenesis. Paternal effect genes are genes, the gene products of which are supplied to the embryo by the sperm. In case of paternal effect genes, mutant males cause abnormal embryonic development post fertilization or are sterile males that produce motile sperms that can successfully inseminate eggs (Fitch, Karen R., et al. 1997). In *C. elegans* Spermatocyte protein spe-11 (spe-11) was identified as a strictly paternal effect gene. Spe-11 mutant sperm fertilizing a wild type egg results in abnormal embryonic development whereas the reciprocal cross yields viable offspring. Eggs fertilized by mutant sperms prevents polyspermy and also forms the pronuclei but fails to complete meiosis. Another example from the vertebrate system is the Axolotl ts-1 gene. The ts-1 mutant sperms are effective in fertilizing the eggs and the embryogenesis progresses till gastrulation after which the development gets arrested.

Four paternal effect genes have been previously identified in *Drosophila*. Sneaky (snky), Male sterile-3-K81 (K81), Paternal loss (pal) and Horka ($lds^{Hor\text{-}D}$). In snky mutants, the sperm successfully inseminates the oocyte but the sperm nuclei do not decondense. The plasma membrane around the sperm head fails to dissolve to release the nuclear material (Wilson, Kathleen L., et al. 2006.). Oocyte completes meiosis but no development happens further. The organization of the sperm tail within the egg is abnormal and might cause abnormal placement of the sperm pronuclei in the egg resulting in the observed abnormality. In K81 mutants, the gonomeric spindles are incorporated into the paternal chromosomes resulting in chromosome bridges and chromosomal breaks during early development (Fuyama, Y. et. al. 1986). In this mutant, 10 percent embryos were shown to survive till just before hatching but these 10 percent are haploid individuals that do not incorporate the paternal pronuclei into its genome. Pal mutant males are fertile, but the progeny of mutant males shows loss of paternal chromosomes in the first three cleavage cycles. Y chromosome and chromosome 4 show the highest rate of loss, producing null-exceptional progeny or mosaics (Baker, Bruce S. 1975). Unlike the previous three mutations Horka is a gain

of function mutation. These mutants show loss of paternal chromosomes like in Pal but in contrast Horka mutants does not show a loss of Y chromosome (Szabad, Janos. et. al. 1995).

Objectives: The mechanism by which Faf1 elicits a maternal phenotype is not known. Given that the Faf1 UBA domain can stabilize ubiquitinated proteins and prevent their degradation, while the UBX domain promotes VCP mediated proteasomal degradation of ubiquitinated target proteins, it needs to be determined how Casp influences the stability of its targets. It is not known whether the interacting partners of Casp modulate its pro and anti-protein degradation activity. Whether there is any tissue specificity in the activity of Casp and whether these changes, if there, are mediated by different interacting partners.

Faf2 being another UBX domain containing proteasomal adaptor, is quite similar to Casp in its domain structure. Whether Faf2 also has a maternal role in development needs to be verified. Does Faf2 and Casp share a common interactome is an interesting question. If there are unique targets for Casp and Faf2, the significance of such a diversification will be interesting to study in an evolutionary context. Faf2 hasn't been reported in an immunity context previously, but since Faf2 acts as a sensor for LCPUFA levels, Faf2 might be involved in NfκB activation. Direct cross talk between Faf2, like Casp, with the innate immunity regulators are not reported. A complete Faf2 interactome will provide more insights in this direction.

For my MS research project, I have two main goals. First is a domain analysis of Faf1/Casp by deleting different functional domains and evaluating the resulting effect on maternal Faf1 function. Second is an analysis of knock down effects of Faf2, another UBX containing proteasome adaptor, in comparison with the available data for Faf1 loss of function in maternal context. In the next few chapters, I describe the protocols and methods used in my research (Chapter 2), results (Chapter 3) and finally Discussion and future plans (Chapter 4) of my research project.

Chapter 2

Materials and methods

Summary: In this Chapter I have listed the large number of techniques that I have learnt during my MS project. The techniques include executing *Drosophila* genetics, performing CRISPR screens and utilising the UAS Gal4 system for modulating gene function. CRISPR/Cas9 genome editing as a technique is very new and has merited a more detailed introduction, which has been provided as part of this Chapter.

***Drosophila* husbandry:** Flies were maintained on standard yeast-cornmeal media. Experimental crosses were set up at 25 degrees while the stocks were maintained at room temperature varying between 19 to 25 degrees. flies were phenotypically characterized by observing under a standard light microscope and carbon dioxide was used for anaesthesia. Virgin flies for experimental crosses were collected using standard blackspot virgin collection procedure. Fly strains were procured from BDSC or generated in our lab.

Table 1: *Drosophila* stocks used for experiments.

Sl. No:	Genotype	Short name	Source
1	$\frac{w-}{w-}\,;\,\frac{casp^{lof}}{cyo/casp^{lof}}\,;\,\frac{+}{+}$	$casp^{lof}$	BL11373
2	$\frac{+}{+}\,;\,\frac{casp^{df}}{cyo}\,;\,\frac{+}{+}$	$casp^{df}$	BL8915
3	$\frac{w-}{w-}\,;\,\frac{gla}{cyo}\,;\,\frac{TubPBacTransposae}{mkrs}$	Transposase 3C	
4	$\frac{w-}{w-}\,;\,\frac{+}{+}\,;\,\frac{+}{+}$	W^{1118}	
5	$\frac{w-}{w-}\,;\,\frac{tft}{cyo}\,;\,\frac{+}{+}$	Tft/Cyo	
6	$\frac{nos-cas9}{nos-cas9}\,;\,\frac{+}{+}\,;\,\frac{+\{attP\}}{+\{attP\}}$	nos-Cas9	BL54591
7	$\frac{w-}{w-}\,;\,\frac{faf2i}{cyo/faf2i}\,;\,\frac{+}{+}$	faf2-RNAi	BL43224
8	$\frac{w-}{w-}\,;\,\frac{+}{+}\,;\,\frac{nos-gal4}{TM3/nos-gal4}$	Nanos-Gal4	BL4937

9	$\frac{w-}{w-}$; $\frac{13.4\ mat\ Gal4}{13.4\ mat\ Gal4}$; $\frac{13.4\ mat\ Gal4}{13.4\ mat\ Gal4}$	13.4 mat Gal4	Generated in lab
10	$\frac{w-}{w-}$; $\frac{if}{cyo-YFP}$; $\frac{mkrs}{ser-GFP}$	2nd 3rd balancer	

Table 2: Primers designed for various experiments.

Name	Sequence	Use
null_5'_fp	*tatataggaaagatatccgggtgaacttcggcattacctgaaaactggtcagttttagagctagaaatagcaag*	Primer for cloning the protospacer of 5' binding gRNA for complete gene deletion
UBx_5'_fp	*tatataggaaagatatccgggtgaacttcggttcggacggctcctgaggtagttttagagctagaaatagcaag*	Primer for cloning the protospacer of 5' binding gRNA for Ubx domain deletion
UAS-UBx_5'_fp	*tatataggaaagatatccgggtgaacttcggtcatccgtatcgtttggtacgttttagagctagaaatagcaag*	Primer for cloning the protospacer of 5' binding gRNA for deletion of both UBA and Ubx domains
null_3'_rp	*attttaacttgctatttctagctctaaaaccaggaaacggtcatcctggaccgacgttaaattgaaaataggtc*	Common primer for cloning the protospacer of 3' binding gRNA for the deletions
pCFD4_RP	*ccggatatctttcctatatatactgtact*	Forward primer for amplifying pCFD4 backbone
pCFD4_FP	*ttagagctagaaatagcaagttaaaataagg*	Reverse primer for amplifying pCFD4 backbone
null_5'screen_FP	*cggcattacctgaaaactggtcag*	Colony screening for proper recombinants of null deletion construct
UBx_5'_screen_FP	*ttcggacggctcctgaggt*	Colony screening for proper recombinants of Ubx deletion construct
DualKOscreen_FP	*cggtcatccgtatcgtttggtac*	Colony screening for recombinants of UBA_Ubx deletion construct
M13R	*agcggataacaatttcacacagg*	Common reverse primer for recombinant plasmid screening
null_3'screen_RP	*caggaaacggtcatcctggacc*	Primers for sequencing plasmids for validation
M13R	*agcggataacaatttcacacagg*	M13 reverse screening primer
pBAC_Excision_F	*ttctgatgtggcggcggcaa*	Forward primer binding 5' to *piggy*Bac insertion site
pBAC_Excision_R	*gcccgtaatgctctgcggat*	Reverse primer binding 3' to *piggy*Bac insertion site

Casp_null_F	*gtgccgttagcagcagtagc*	Primer for screening Casp^{null} mutants
Casp_null_F 2	*caactggtcacactgactagcc*	Primer for screening Casp^{null} mutants
Casp_UAS_ Ubx_F	*ggacagtgagagctcgacagat*	Primer for screening domain deletion mutants
Casp_Ubx_F	*aaggcagagcaggacatggc*	Primer for screening Casp$^{\Delta Ubx}$ mutants
Casp_null_R	*ccaatcgaacgaaacggcc*	Reverse primer for sequencing mutants
Casp_null_F 3	*gcgcataaatcgcttactctcaactg*	Primer for screening Casp^{null} mutants
Casp_null_R 2	*accggtagtatctggtgctg*	Primer for screening Casp^{null} mutants
Casp_null_R 3	*actttctttctcttctttgctgctatgctc*	Primer for screening Casp^{null} mutants
cmPUASPatt B	*ataggccactagtggatctgatgtaccc atacgatgttccagattacgctggcggc*	Primer for adding the pUASPattB 5' homology arm to inserts
pUASCasp_ F	*tgttccagattacgctggcggc*	Primer for amplifying the UAS_Casp inserts
pUASCasp_ R	*accatgggtttaggtataatgttatcaag ctcc*	Primer for amplifying the UAS_Casp inserts
pUASddR	*ttaggtataatgttatcaagctcctcacgt ggagccacttatctcatcatccg*	Reverse primer for amplifying the UAS_Casp_ΔUAS_ΔUbx insert
pUASdUAS_ F2	*cggatgatgagataagtggctccacgg aaacatgcgaaatgtttgaggagcag*	Forward primer for amplifying the fragment downstream of UAS domain
pUASdUAS_ R1	*cgtggagccacttatctcatcatccg*	Reverse primer for amplifying the fragment upstream of UAS domain
pUASdUBA_ F	*tgttccagattacgctggcggcccccat cctatcctggtgcc*	Forward primer for amplifying the UAS_Casp_ΔUBA insert
pUASdUbx_ R	*ttaggtataatgttatcaagctcctcattc ggacggctcctgaggtag*	Reverse primer for amplifying the UAS_Casp_ΔUbx insert

Competent cells: High efficiency competent PPY cells were made using iGEM recommended CCMB80 mediated competent cell preparation protocol. CCMB80 (10mM KOAc, 80mM $CaCl_2$, 20mM $MnCl_2$, 10mM $MgCl_2$, 10% glycerol and set pH to 6.4 using HCl) was freshly prepared, filter sterilized and stored at 4 degrees. 5mL LB containing Chloramphenicol and Streptomycin was inoculated with PPY cells and cultured overnight at 37 degrees, 180 rpm. A 100mL LB-Chloramphenicol-Streptomycin was inoculated with 100uL of the primary culture and was incubated at

37 degrees, 180 rpm till the OD reached 0.4. The culture was chilled on ice and pelleted at 6000rcf, 4 degrees. Supernatant was discarded and the pellet was resuspended in CCMB80 and incubated on ice for 20 minutes. Cells were again pelleted at 6000rcf, 4 degrees and were then resuspended in CCMB80 to a final OD of 1.5. Cell suspension was then aliquoted of volumes 50uL in fresh sterile Eppendorf. Aliquots were chilled on ice, flash frozen with liquid nitrogen and stored at -80 degrees.

***E. coli* transformation:** 50uL single use PPY competent cell aliquots were used for individual transformations. Aliquot were thawed on ice. To an aliquot of competent cells, a maximum of 1.2uL DNA template was added for transformation. DNA was mixed well by gently tapping the Eppendorf. Incubated on ice for 20 minutes and was given a 42-degree heat shock for 45 seconds. After the heat shock, the cells were chilled on ice for 20 minutes. 1mL fresh LB was added to the vial and was incubated at 37degrees 180 rpm for 45 minutes. For plasmid transformations, 100uL of the sample was plated on a LB-Agarose plate. In case of fragment recombination, the cells were pelleted, the pellet was then resuspended in 100uL LB and all of it was plated on a LB-Agarose plate. The plate was incubated at 37degrees overnight for colony growth and the transformant colonies were screened for required constructs.

Mini-prep and Midi-prep: Qiagen mini-prep/midi-plus kits were used for plasmid isolation and purification (Qiagen.com/resources). The standard protocol issued in the manual was followed. For mini-prep 1ml and for midi 50ml of bacterial culture grown in Luria-Bertini broth for 12 hours at 37°C and 180 rpm were used respectively. The culture was pelleted at 6000g, 4°C, for 15 minutes. Pellet was then resuspended in buffer P1 and was lysed with buffer P2 for 4 minutes. For mini-prep the resulting solution was neutralized with buffer N3 and was then spun down at 17900rcf the same speed was used for all the subsequent steps. Supernatant was transferred to the DNA binding column and spun down and the flow through was discarded. The column was washed with PE buffer, the flow through was discarded and then DNA was eluted in distilled nuclease free water. For the midi-prep the bacterial lysate was neutralized with buffer S3 and then spun down at 17900rcf. The supernatant was transferred to a fresh falcon and buffer BB was added and then was passed through the DNA binding column. Column was washed with ETR buffer followed by buffer PE. DNA was then eluted in 200ul nuclease free water. Product concentration was estimated by nanodrop analyser and size was verified on agarose gel.

Agarose gel electrophoresis: 0.8, 1 and 1.2% agarose gels were made as per requirement and Ethidium bromide was added to a final concentration of 0.2ug/ml. DNA separation was performed at 120 volts generating essentially a 6V/cm gradient in 1X TAE buffer. Running time varied between 20 to 40 minutes depending on the product size to be analysed. A standard DNA ladder was used for verifying the size of the sample fragments. Post resolving, the gel was visualized with the help of Gel-doc (Syngene G-box – Chemi 16 Bio Imaging System).

DNA gel elution: Qiagen gel extraction kit was used for gel purifications. Desired DNA fragments were resolved on a gel and size verified. DNA fragments were visualized in the gel with the help of an UV transilluminator. Desired gel fragment was cut out from the gel using a clean blade and the gel piece was transferred to a clean Eppendorf. To the Eppendorf, QG buffer equivalent to 3 times the volume of the gel was added and incubated at 50 degrees to dissolve the gel piece. Slightly invert the tube to mix the gel fragment well and properly dissolve it. To this mix, add isopropanol, equivalent to the volume of the gel fragment. Mix well and transfer the solution into a gel extraction column. Spin the column at max speed on a table top centrifuge (13900rpm) and discard the flow-through. Add 500uL QG buffer to the column and spin it down. Discard the flow through and wash the column with 700uL PE buffer. Spin and discard the flow through. Spin the column again to remove any residual buffer and transfer the column to a clean labelled Eppendorf. Let the column dry. Add 20-50uL nuclease free water to the column, incubate at room temperature for 5 minutes and Spin to elute the purified DNA fragment.

Colony Screening PCR: Transformant colonies were screened to identify recombinants by performing colony PCR. A 10uL reaction was set up per colony to be screened in the following composition: 1uL 10X Taq buffer with 25mM $MgCl_2$, 0.6uL dNTP mix (25mM of each), 0.1uL Taq polymerase, 0.5uL each of the 10M respective forward and reverse primers. The final volume was made up to 10uL using nuclease free water. Individual colonies were picked up with a sterile pipette tip and mixed well into the reaction mix. A polymerase specific denaturing temperature of 95degrees and extension temperature of 72degrees were used. The extension time and annealing temperature were decided based on the amplicon size and the primer pair being used (fig. 6).

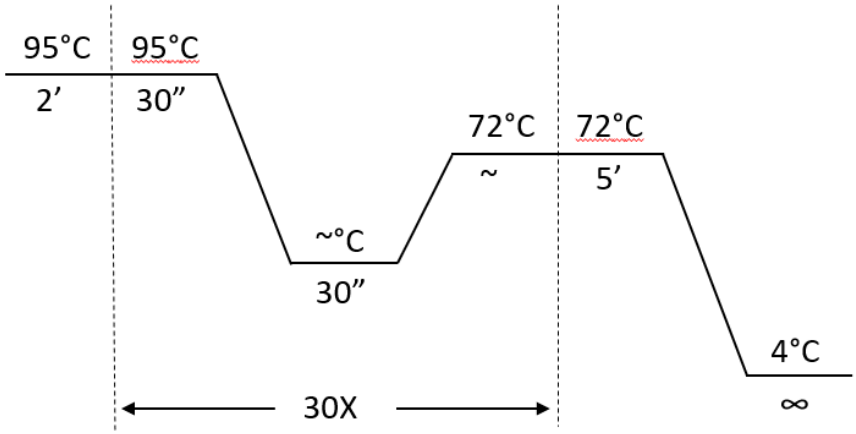

Figure 6: PCR program used for colony screenings. The shown program was used as the general reaction settings for colony screening PCRs. An initial denaturation of the DNA was done at 95degrees for two minutes. Following this a 30 cycle amplification is performed, giving a 30 seconds denaturation at 95degrees, 30seconds annealing at the primers suitable annealing temperature (usually 2-3degrees lower than the primer melting temperature) and an extension at the taq optimal 72degrees giving enough extension time based on the product size (normal taq amplifies around 1000bp/minute). At the end of the amplification cycles, an extended 5 minutes extension time was given for 5 minutes following which the reaction setup was then held at 4degrees indefinitely.

Gradient PCR: In order to identify the proper annealing temperature for various primer pairs, an annealing temperature gradient PCR was setup using Eppendorf mastercycler. Usually a gradient of T_m-7 to T_m+4 was used as the gradient range where T_m is the higher value of the melting temperatures of the primers in the pair being used. Products were resolved on an agarose gel and a suitable annealing temperature for the set of primers were identified based on which of the lanes show a high intensity single product of interest.

Genomic DNA isolation: In order to screen for mutants, single homozygous flies were collected from the stable lines. From lines that were not homozygozing, Cyo balanced flies were taken. Genomic DNA as isolated by crushing the flies in squishing buffer (10mM Tris-Cl pH 8, 1mM EDTA, 25mM NaCl, 200ug/mL freshly added proteinase K). The lysate was incubated at 37 degrees for 30 minutes and heat inactivated at 85 degrees for 5 minutes. The lysate was then shortly spun to settle the debris and stored at 4 degrees.

Genomic PCR: CRISPR mutants were screened by amplifying the genomic region around the targeted area. Primers were designed to bind around 150 to 300 base pairs upstream of the 5' gRNA target site and 150 to 300 base pairs downstream of the 3'

gRNA binding site. A 10uL PCR reaction was setup with the following composition. 1uL 10X taq buffer with 25mM $MgCl_2$, 0.6uL dNTP mix (25mM each), 0.5uL each of the 10M screening primer pairs, 0.1uL taq polymerase (5 units/uL) and 1.5uL of isolated genomic DNA as template. The final volume was made up to 10 uL using nuclease free water. Listed below are the different PCR programs used for the various screening (Fig. 7).

Program: Casp null screening

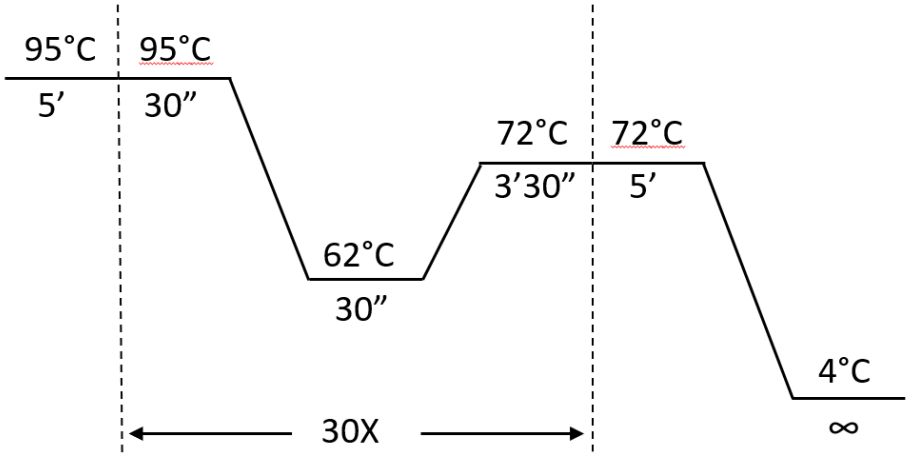

Program: Casp domain screening

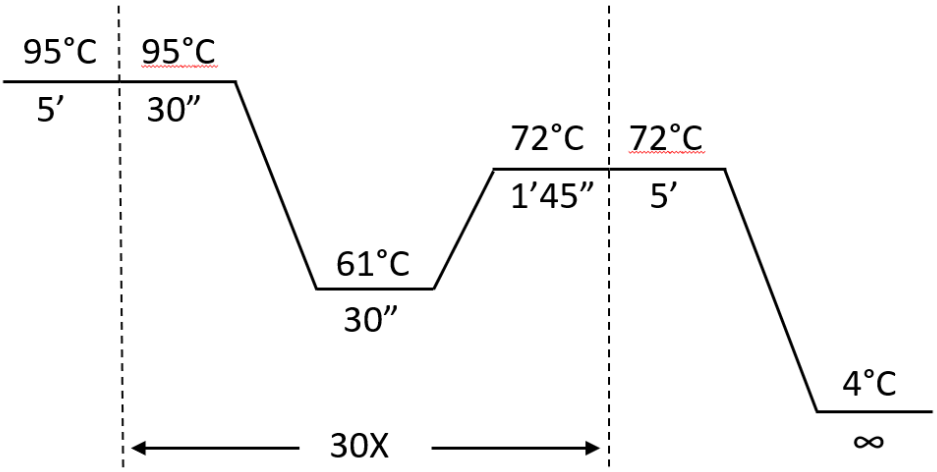

Figure 7: CRISPR screening PCRs. The PCR conditions shown above were used for screening the CRISPR lines. For the null screen, an annealing temperature of 62 degrees was used to avoid non-specific products and an extension time of 3 minutes 30 seconds since the product is around 3.2Kb. In case of the domain deleted mutants, the primer pair was behaving best at 61degree annealing and a 1 minute 45 seconds extension time was sufficient.

Embryo viability assay: Embryo lethality was used to identify genes that are essential for early embryonic development. Maternal effect genes can also be studied by looking at defects in development in embryos when these embryos are collected from a homozygous mutant mother. Maternal effects are independent of the paternal genotype. For Embryo lethality assay, fly cages were setup using 5-6 days old flies. Respective crosses were setup in vials containing normal yeast cornmeal media. 10 males and 30 females were used per replicate. Flies were transferred to the cages on the 5th day. Flies in the cages were fed freshly prepared yeast for proper oogenesis and enhanced egg lay. 3% sugar agar plates were used for collecting eggs. Eggs were harvested at 12-hour intervals and 200 eggs from each cross were plated onto a fresh sugar agar plate and incubated at 25 degrees. Number of embryos that hatched were manually estimated at 24 hours post spotting and 48 hours post spotting. This data was used to calculate lethality

Cuticle preparation: Medium cages were setup with sugar agar plates and freshly prepared yeast. Flies of the desired genotype were allowed to mate and feed on normal cornmeal media. On day 3, the flies were transferred to the cages and were allowed acclimatise for a day. On day 5, 0-2hr embryos were collected and were incubated at 25 degrees for 22 hours allowing them to develop and deposit cuticle. Embryos were then transferred onto a sieve using a clean brush and washed thoroughly in running tap water to remove all yeast. Embryos were dechorionated by placing them in 100% bleach for 2 minutes. Wash thoroughly to remove any residual bleach and transfer the embryos to a vial containing 2mL 100% ethanol. Swirl the embryos once and remove the ethanol. Give a wash with 100% methanol. Remove the methanol and add fresh equi-volume mix of methanol and heptane. Shake vigorously to devitellinise the embryo. Remove the heptane layer and wash the devitellenised embryos twice in fresh methanol. Place the embryos on a slide and air dry them. Add enough volume of 85% lactic acid to cover the embryos and put a coverslip. Keep the slides in a slide warmer overnight at 55 degrees for lactic acid to digest the tissues. In case of fly lines that deposit cuticle, it is fine to devitellinise the embryos. But if the particular mutant does not deposit cuticle, devitellinising the embryo will result in complete dissolution of the embryo in the subsequent digestion. In such cases, retaining the vitelline membrane is advised.

Embryo DAPI Staining: Cell division in early embryos was visualized by performing DAPI staining (1:1000 dilution of DAPI in 2% BSA in 1X PBS 0.3%Triton). Desired genotype flies were acclimatized in cages and embryos were collected in 2-hour intervals. These embryos were then aged to let them develop into the stage of interest. Transfer the embryos into a sieve using a clean brush. Wash thoroughly in tap water to remove all yeast. Dechorionated the embryos by placing them in 100% bleach for 2 minutes. Wash thoroughly to remove all bleach. Transfer the embryos into a scintillation vial containing 2mL n-Heptane and 2mL freshly prepared 4%PFA in PBS. Place the vial in the nutator for 20 minutes at room temperature for fixing the embryos. Remove the PFA bottom layer and let the embryos rest in n-heptane for 20 minutes. Add 2mL of chilled methanol to the vial and shake vigorously to devitellinise. Devitellinized embryos fall into the bottom methanol layer. Remove heptane and non-devitellinized embryos then remove methanol and add 2mL fresh methanol. Embryos can be stored in methanol at -20 degrees. Rehydrate the embryos using 0.3% PBS-Triton. Give four washes with PBS-T for 15 minutes each. Transfer the embryos to a 600uL Eppendorf and add 500uL 2% BSA in PBS-T. Block the embryos for 15 minutes. Add DAPI (1:1000) in 2% BSA PBS-T, 200uL per vial and incubate on a rocker at room temperature for 15 minutes. Wash the embryos twice with 0.3% PBS-T for 15 minutes each and mount the embryos on a slide. Using a clean tissue wipe, blot out all of PBS-T and add enough antifade mounting media to the embryos. Put a coverslip and seal it using clear nail polish.

Image acquisition: Embryos were imaged using Zeiss multiphoton (Zeiss Inverted LSM 780 multiphoton) at 10X magnification. A 405nM excitation laser was used and the images were acquired at 1.7X zoom. Laser power was set to 5 and gain was adjusted to get maximum dynamic range. Z-stack images were captured at scan speed 9.

SDS page: Protein separation and resolving was done using a standard SDS page. An acrylamide gel of 1.5mm thickness was casted in a casket with a 5% stacking phase of pH 6.8 and a 10% resolving phase of pH 8.8. Fly lysates were prepared by crushing 5 flies in 100ul RIPA. 5X SDS loading dye was added and samples were heated for 20 minutes at 95 degrees at 750rpm. Tissue debris was spun down at 13000rpm and the supernatant was used for loading. 40uL of the lysate was loaded per well. 3uL BlueEye pre-stained protein marker (PS-104) was used as the reference

standard. 1X SDS-glycine running buffer was used. The samples were stacked at 90 volts for 20minutes till they reached the margin between the stacking and the resolving gels. Proteins were then separated in the resolving gel at 120volts.

Western blotting: Casp was visualized by performing western blotting using Casp specific polyclonal antibody (1:10000 dilution) generated from rabbits. Separated proteins were transferred onto a preactivated PVDF membrane (Immobilin-E) using a standard blotting apparatus. 1X Towbin transfer buffer was used. Transfer was performed at 90volts for 120minutes. Post transfer the PVDF membrane was blocked on 5% skimmed milk in 1X TBS-0.1% Tween 20 in-order to prevent nonspecific binding of antibodies to the membrane for an hour at room temperature. Blot was transferred to rabbit α-casp antibody (1:10000 in 5% skimmed milk in 1X TBS-0.1% Tween 20) and incubated overnight at 4degrees. Blot was washed in 1X TBS-Tween thrice for 15 minutes each. α-rabbit HRP was used as the secondary antibody. Blot was incubated in secondary (1:10000 in 5% skimmed milk in 1X TBS-0.1% Tween 20) for an hour at room temperature. Three washes were given in 1X TBS-Tween thrice for 15 minutes each. Blots were developed using Luminata classico HRP luminol substrate and imaged using gel-doc (Syngene GBox-chemi-XX6).

pBac Excision experiments: pBac excisions are precise in nature leaving no scar on excision, but it has been shown that a very small fraction of the excisions are imprecise causing frameshift mutations (Kim, Heuijong, et al., 2012). In order to generate an alternate $Casp^{null}$ allele, transposase mediated excision of the pBac element was performed in the $Casp^{lof}$ line. $Casp^{lof}$ flies were crossed with transposase 3C flies and the subsequent progeny having both the $Casp^{lof}$ and transposase were chosen and crossed back to transposase 3C. Flies having a complete excision of the pBac element were identified by scoring for eye color as the pBac element contains a mini-white gene. Each founder was expanded using Tft/Cyo and a stable population was established with a floating Cyo balancer. Single fly crosses were setup to score for egg viability and lines showing increased embryonic lethality were complemented with $Casp^{lof}$ allele to choose desirable mutants (fig. 8)

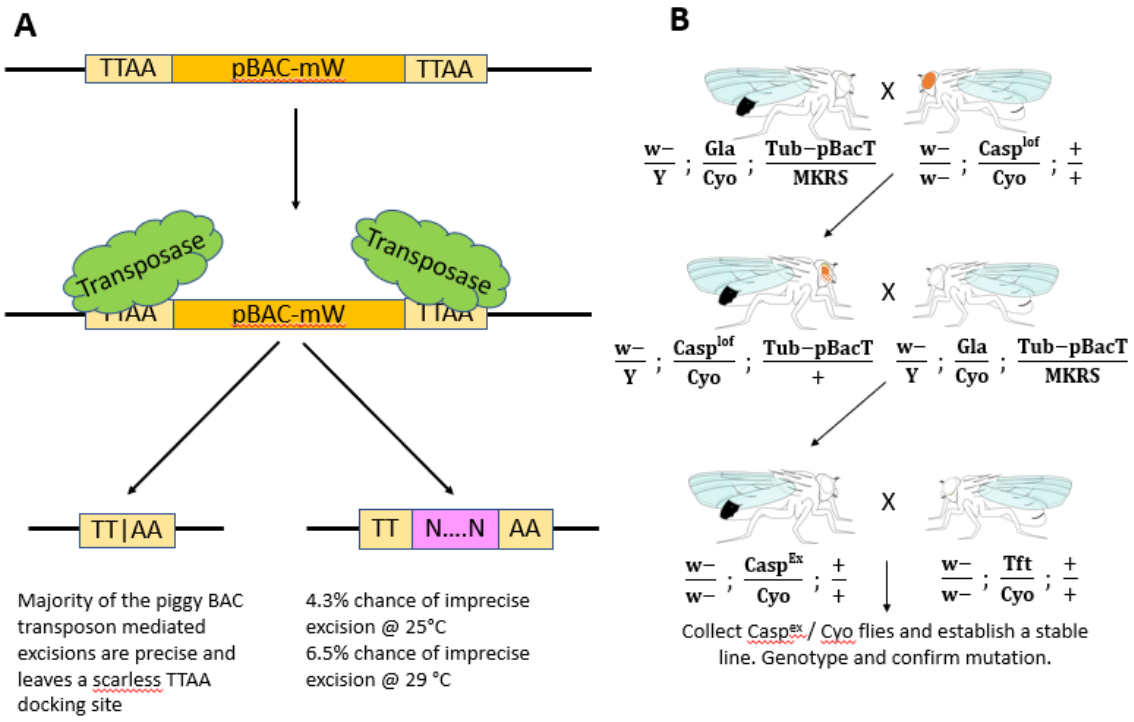

Figure 8: Generation of an alternate frameshift Casp^{null} By imprecise pBac excision. A) Schematic showing generation of frameshift mutations by transposase mediated excision of pBac element. A very small fraction of the excisions might lead to a frameshift. The probability of which has been shown to increase with increase in temperature. B) Strategy for crossing and generating the desirable frameshift mutant. Casp^{lof} flies were crossed with a 3rd chromosome transposase line. From the next generation non-tufted non-MKRS flies were chosen, many of which showed mosaicism in their eyes indicating the occurrence of possible excisions. These were crossed to the transposase line again till flies with single genomic excisions were obtained, indicated by complete white eyes. These flies were then crossed to a 2nd chromosome balancer line to expand the population of the particular allele and from the progeny, single virgin flies with a Cyo balancer were chosen to establish a stable population. As a primary screen, egg viability was tested. Lines showing increased lethality were complemented with Casp^{lof} to confirm it is a Casp mutant.

Generating Casp mutants through CRISPR Cas9 genome editing: CRISPR (Clustered Regularly Interspaced Short Palindromic Repeats) Cas system (CRISPR Associated) is a quite popular and routinely used genome editing tool. CRISPR was initially identified as a locus containing regularly spaced palindromic sequences as the name suggests and few associated genes in *E. coli* (Ishino, et, al. 1987). Later, identification of such loci in other bacterium led to the characterization of CRISPR as an adaptive immune system in various bacteria and several archaea. This defence utilizes an RNA mediated sequence dependent cleavage of invasive DNA molecules (Barrangou, Rudolphe, et, al. 2015). The main components of a CRISPR system are

a CRISPR RNA (crRNA), a trans activating CRISPR RNA (tracrRNA) and the target processing Cas proteins.

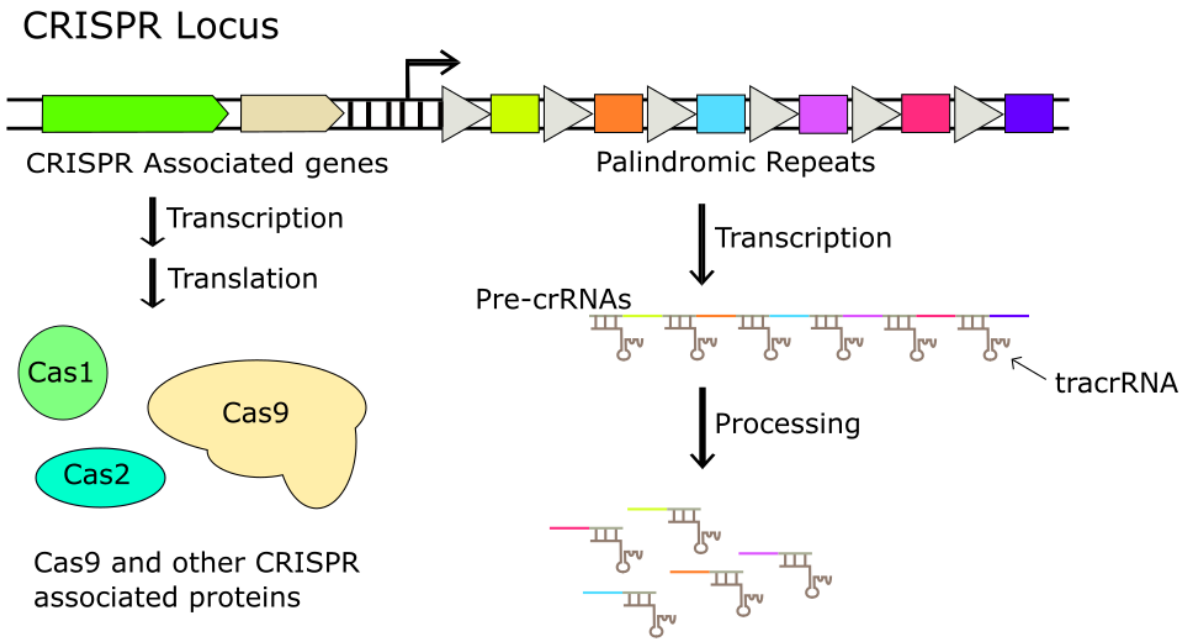

Figure 9: Schematic representation of type-II CRISPR Cas9 locus. CRISPR locus contains the regularly spaced CRISPR repeats and the CRISPR associated genes. In a type II CRISPR system, the endonuclease is Cas9. Cas1 and Cas2 help in identification and incorporation of foreign DNA specific spacers into the CRISPR locus. The long CRISPR locus transcript is cleaved to release separate crRNAs with the help of tracrRNA. These crRNAs along with tracrRNA act as gRNAs.

The CRISPR mediated immune response happens in three steps, Adaptation, crRNA biogenesis and targeting. During adaptation, Cas1 and Cas2 identifies a protospacer motif from the foreign DNA fragment and incorporates it as a spacer into the CRISPR locus (Yosef, et, al. 2012). Protospacer sequences are usually detected based on the presence of a downstream constant tri-nucleotide sequence known as the protospacer adjacent motif (PAM). The first eight nucleotides right upstream of the PAM sequence is called the seed sequence. Complete sequence complementarity between the seed and the target as well as the presence of the PAM sequence in the target are essential for the Cas9 mediated binding and cleavage of the target (Yosef, et, al. 2012). There are three major classes of CRISPR Cas systems namely type I, type II and type III with twelve further sub-classes (KS, Makarova, et, al. 2011). The defining feature of each of these are the Cas protein involved in processing of the downstream target. These are Cas3, Cas9 and Cas10 in type I, II and III systems respectively (KS, Makarova, et, al. 2011). In case of the Type II Cas9 system, the PAM

sequence is NGG. Twenty nucleotides upstream of this PAM sequence are used as a spacer by the CRISPR locus. Across systems, the protospacer sizes vary from 21 to 72 nucleotides long (Barrangou, Rudolphe, et, al. 2015). Post adaptation, crRNA biogenesis takes place. crRNA transcript contains the spacer sequence followed by the CRISPR repeat sequence. During crRNA biogenesis, the CRISPR locus undergoes transcription and a long RNA containing the spacers and the CRISPR repeats is synthesised. CRISPR repeats can bind to the tracrRNA because of sequence complementarity. This then triggers the cleavage of the long RNA between the 3' end of a repeat and the 5' end of a spacer causing the release of individual target specific guideRNAs (gRNA) comprising of the crRNA and tracrRNA (Barrangou, Rudolphe, et, al. 2015) (Fig. 9). Binding of gRNA to Cas9 brings in conformational changes to Cas and activates their nuclease domains (Jinek, Martin, et, al. 2014). The endonuclease Cas proteins can now identify and cleave its targets with the help of this gRNA and this process is called targeting. This allows the bacterium to target bacteriophage and plasmid DNA and provides immunity towards these invasive nucleic acids. The requirement of the presence of PAM sequence for the cleavage of the target DNA protects the host DNA from being targeted by the Cas enzymes (Yosef, Ido, et, al. 2012). However how does the protospacer acquisition enzymes differentiate between the host DNA and the invasive DNA are not well known.

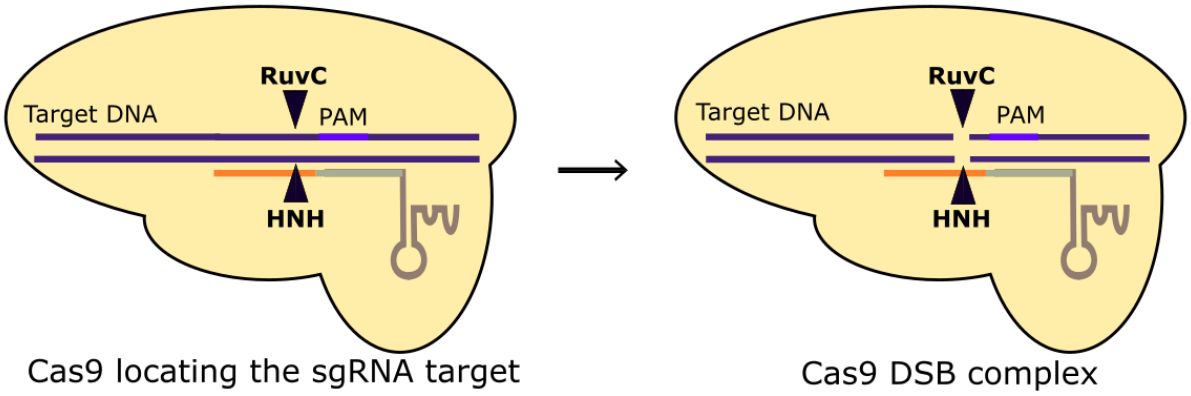

Figure 10: Cas9-sgRNA mediated genome editing. A single guide RNA (sgRNA) can be used instead of the crRNA-tracrRNA complex along with Cas9 to locate and cleave DNA targets. Binding of sgRNA-Cas9 to the target DNA followed by recognition of PAM sequence in the target by Cas9 activates its HNH and RuvC nuclease domains to cleave the target three nucleotides upstream of the PAM sequence. Post cleavage, Cas9 remains in the target DNA as a Cas9 DSB complex.

Type II CRISPR Cas9 system from *Streptococcus pyogenes* is the most widely used for site directed genome editing. Binding of gRNA is required for the activation of Cas9. For ease of usage, a single guide RNA (sgRNA) that can mimic the gRNA in binding to and activating Cas9 was engineereded, of which the first twenty nucleotides could be changed in order to target any DNA of interest (Jinek, Martin, et, al. 2014). Independent studies have looked at the role of position specific nucleotides in the protospacer sequences in deciding the efficiency of various gRNAs in Cas9 mediated DNA cleavage. A guanosine in the 20^{th} position is shown to cause very high efficiency where as a thymine in the same position of the gRNA causes a comparatively low rate of mutagenesis (Gagnon, James A., et al. 2014, Chari, Raj, et, al. 2015). It takes around 6 hours for a single Cas9 gRNA complex to locate its target and once bound, the complex is stabilized. Complete complementarity of the seed sequence with the target and PAM sequence will lead to cleaving of the target. A few mismatches outside the seed sequence is often tolerated and leads to off target mutations (Fu, Yanfang, et, al. 2013). Once the Cas9-sgRNA complex binds to the target, the HNH and RuvC nuclease domains of Cas9 cleaves the target on the gRNA complementary and gRNA non-complementary strands respectively (Richardson, et, al. 2016). The cleavage site is three nucleotides upstream of the PAM sequence (Jinek, Martin, et, al. 2012) (Fig. 10). Post cleavage, the Cas9-sgRNA complex stays bound to the double strand break (DSB) forming a Cas9-DSB complex which when disrupted exposes the DSB to cellular repair machinery. Repair can happen either through non-homologous end Joining causing indels or through homology directed repair which can be utilized to make specific mutations by a donor sequence containing a mutation and homologous arms that binds to either side of the target location (Barrangou, Rudolphe, et, al. 2015).

In order to study the role of various domains of Casp we used CRISPR mediated genome editing of the Casp locus. To make deletions of chunks of DNA, a dual gRNA mediated approach is utilized. The dual gRNA targets regions upstream and downstream of the desired domain region, and this could result in the exclusion of the in-between DNA sequences during repair mediated by NHEJ pathway. The advantage of introducing mutations into the native gene is that it preserves the expression pattern and levels of the target gene while expressing the mutated variant. We used pCFD4 vector since it can express dual gRNAs (Port, Fillip, et al. 2014).

Cloning pCFD4-gRNA constructs: Cloning was performed as previously suggested in fly-CRISPR manual (pCFD4 cloning), slightly modifying it to suit our convenience. Long primers containing the target specific guide RNA sequences flanked by homology arms with the pCFD4 backbone and complementary primers for amplifying the backbone were designed (table. 2). A 600bp insert was amplified using PCFD4 as the template using these primers. Backbone of size 6.4Kb was amplified such that it has 20bp overlap with the insert. The PCR reaction using platinum superfi-taq was performed under conditions as shown (fig.11). Backbone amplification yields two products since the forward primer binds to the gRNA loop which is present twice in the backbone. Thus, the smaller product was purified and gel eluted to exclude the presence of any non-specific gRNA expression.

A

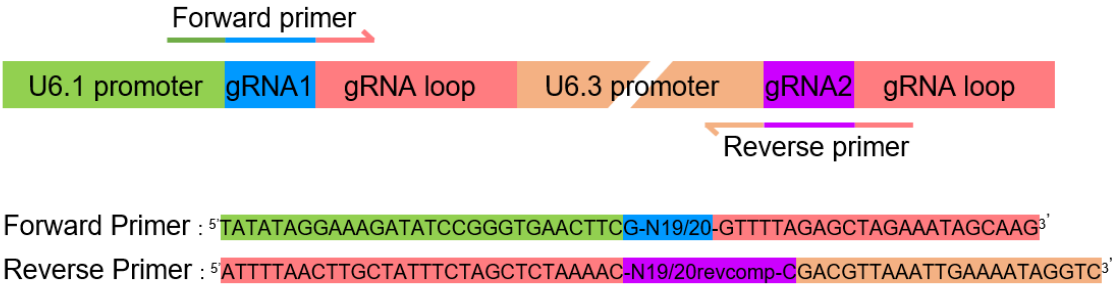

B

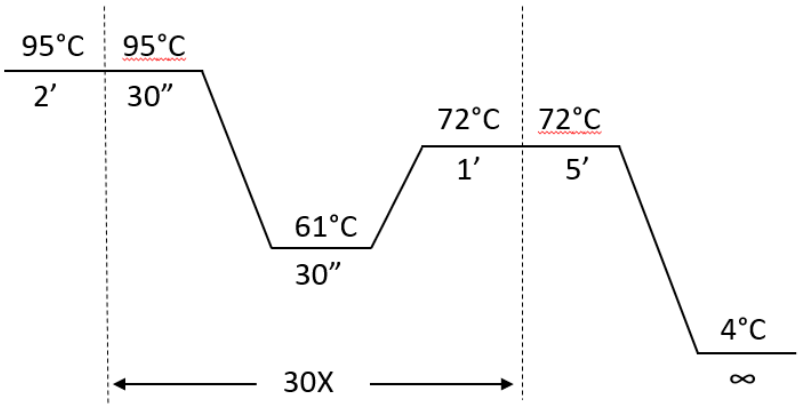

C

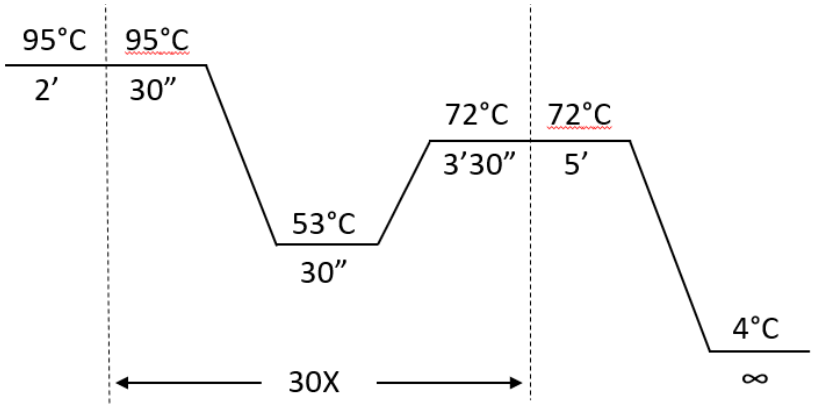

Figure 11: pCFD4-gRNA cloning. The specific gRNA sequences were cloned into the pCFD4 backbone using over extension PCR. A) Diagram of the long primer design adapted from FLyCRISPR. Over extension primers having sequence homology to the plasmid backbone and containing the required gRNA sequence were designed as shown. These primers amplify a 600bp long product containing sequence complementarity to 3' end of U6.1 promoter, the first guide RNA, entire U6.3 promoter, second gRNA followed by a sequence complementarity with the hairpin loop. B) Insert amplification PCR: Insert was amplified using the shown PCR program. For the long primers, irrespective of their T_m , a constant 61degrees annealing temperature was used. C) Backbone amplification PCR: the 6.4kb backbone was amplified using the shown program. Primer annealing were done at 53degrees. An extension time of 3 minute 30 seconds was used since Platinum superfi-taq polymerizes DNA at around 1kb per 30 seconds rate.

Amplified products were run on an 8% agarose gel at 120volts for 30 minutes and the size was verified. Fragments were then gel eluted and used for transformations. *E.coli*_PPY cells (DH10B expressing optimised λ prophage Red recombinase) were used to prepare chemically competent cells. These cells were transformed using both amplified fragments. Colonies were selected on ampicillin plates and proper recombinants were identified by screening using primers specific to the gRNA sequences (table. 2). colonies that gave an amplification were then min-prepped and sequenced. Sequencing was done using the 3' gRNA sequence binding reverse primer to screen the 5' gRNA sequence and an M13R to sequence the 3'gRNA sequence. Positive clones with desired sequence were then midi-prepped and 70ug of the purified DNA was lyophilized and sent to NCBS microinjection facility for injections.

Generating stable CRISPR lines: pCFD4 vector expressing desired guide RNA were sent to NCBS for microinjections. Injected embryos were shipped to IISER. These

embryos were allowed to develop at room temperature between 19 to 22 degrees. Injecting the gRNA vector in the posterior pole of a Cas9 expressing fly will cause a variety of mutations in the germline of the animal. Resulting in each of its progeny to be a potential founder for a mutation. In order to get these mutations preserved onto a stable population, the flies emerging from the injected embryos were crossed to the Tft/Cyo second chromosome balancer line. Each of the progeny inherits only one copy of the second chromosome from the injected fly. This ensures that each of these flies could be the potential founders for a mutation. Since Cyo balancer prevents recombination and dilution of the mutation, Cyo balanced male flies were chosen from the progeny as founders and were crossed with the Tft/Cyo line to expand the population. From the progeny, single Cyo balanced flies were selected and crossed to setup a stable population (fig. 12). Homozygous flies were taken from these individual populations and were screened through PCR to identify mutants.

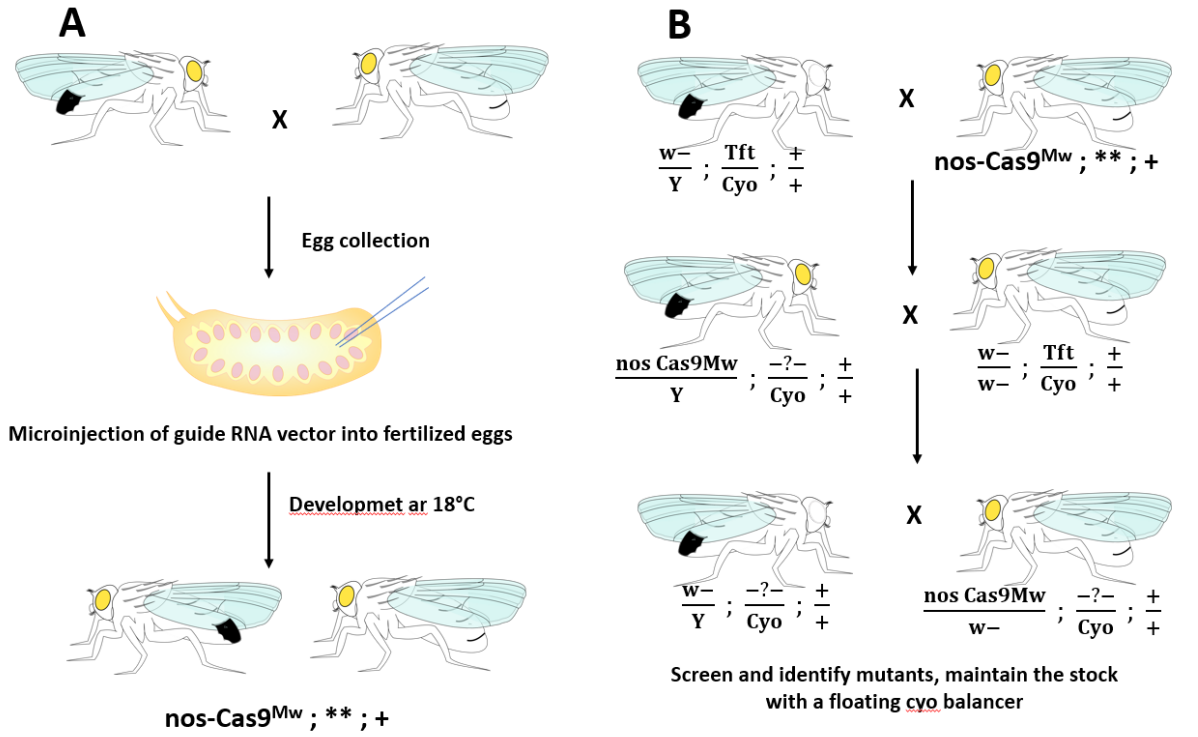

Figure 12: Generartion of Casp mutants through CRISPR Cas9 mediated genome editing A) pCFD4 vector cloned with gRNAs targeting Casp locus was injected into the pole plasm of a 3rd stage embryo that expresses cas9 under a nanos promoter. Injected animals were allowed to develop at low temperatures aiding them to develop under reduced stress. B) Each of the injected animals were crossed with the 2nd chromosome balancer line and from the progeny of each, 3 individual Cyo balanced males were chosen as founders. Founders were crossed with Tft/Cyo to expand the population. Single Cyo balanced flies were selected to establish a stable population. The nos-Cas9 is associated with the X-chromosome and can be tracked due to the presence of an associated mini-white marker.

pUASPattB Casp cloning to perform rescue experiments: UAS Gal4 system is one of the most versatile tools in the genetic tool box of *Drosophila melanogaster.* Gal4 is an 881 amino acid protein that binds to four sets of 17 nucleotide long binding sites called the Upstream Activating Sequences (UAS) which acts like the multicellular eukaryotic enhancers to enable the translation of the downstream target genes (Gininger, Edward, et al. 1985). This UAS-Gal4 technique acts as a bimodular system consisting of a driver and a responder. The driver is the Gal4 whose expression can be regulated spatiotemporally by the use of enhancer traps that imitate the natural gene expression patterns, giving rise to very specific expression patterns for the Gal4 (Duffy, Joseph B. 2002). Responder recapitulates the expression pattern of Gal4 and so can be regulated spatio-temporally in its expression. The responder is the gene of interest cloned under tandemly arranged pentamer of optimized UAS sites. The promoter sequence that is downstream of these UAS sites will be inactive in the absence of Gal4, making it possible to maintain lines that could express detrimental peptides, without having to compromise the viability of the organism. Gal4 being temperature sensitive makes it possible to regulate its activity by modulating surrounding temperature (Duffy, Joseph B. 2002).

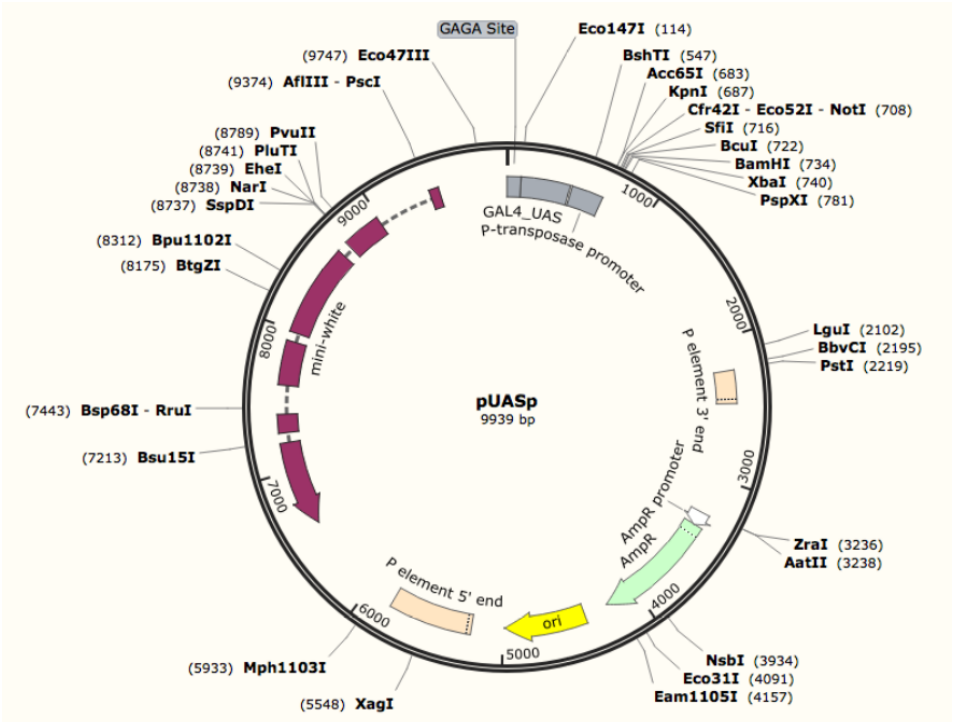

Figure 13: pUASP Vector map. pUASP vector was designed to enable the expression of genes of interest in the germline as well as the soma. This is enabled by the p-Transposase promoter element cloned under the UAS response sites.

pUAST and pUASP are two major vectors used for cloning the responder construct into *Drosophila.* pUAST encodes an hsp70 promoter downstream of the UAS element. pUAST though efficient in driving expression in the soma, is not efficient in expression in the female germline due to inactivity of the hsp70 promoter. pUASP circumvents this problem with the use of a P-transposase promoter in place of the hsp70 promoter (Fig. 13). pUASP is efficient in driving genes of interest both in the germline as well as in the soma. Also, pUASP along with maternal Gal4 drivers can be used for maternal loading of responder transcripts.

Various domain deleted constructs of Casp were cloned in pUASPattB vectors in order to perform Casp null rescue. HA-tagged Casp-wt cloned by Dr. Bhagyashree Khaduskar was used as template for these clonings. Primers were designed to amplify only the required parts of the gene (table. 2) to be cloned into the backbone. A common primer cmPUASPattB was used to add the 5' homology arm to these amplified fragments. Since Superfi Platinum taq can be used with a common annealing temperature of 60degrees irrespective of the primer T_m and can precisely amplify the fragments of interest as long as there is more than required time of extension available for the fragment to amplify, a common PCR reaction named Casp_pUASP_frags was used for amplifying all of the inserts. For the ΔUAS mutant, the region upstream of the UAS domain and downstream of the UAS domain were amplified separately with a 22 base pair overhang for stitching and later was tried to stitch together through overlap extension PCR. Since it did not work, we repeated the stitching by a two-step strategy where the fragments were stitched together first without any end primers and then would be resolved on a gel and the annealed product would be purified and later be amplified using the end specific primers. But our stitching reaction did not yield any stitched product. These 2 fragments with the backbone were then simultaneously transformed into PPY cells and recombinant colonies were screened for proper recombinants. Colony screenings were done using pUASPattB screening primers. The same were used for sequencing the positive recombinants. Clones having proper recombined sequences were then sent to NCBS for transgenic fly generation.

Generating and Characterizing Casplof/Caspdf line: Since $Casp^{lof}$ allele was shown to have some leaky expression, the line was not behaving consistently. This necessitated us to use an alternate model system. For this we decided to use BL8915 fly line which is a deletion mutant that lacks Casp and 24 other genes. This deficiency

line is haplo-insufficient and is maintained over a Cyo balancer. $Casp^{lof}/Casp^{df}$ line can be generated by crossing individuals from the respective genotypes. Since this line lacks one entire copy of Casp and the $Casp^{lof}$ allele has reduced expression levels, we expect to see a drastic phenotype in this line.

Germline Faf2 knockdowns using RNAi method: RNA interference (RNAi) is gene knockdown method used to selectively degrade mRNAs of target genes by utilizing small 21-23 nucleotide long double stranded RNAs (Zamore, Phillip D., et al. 2000). The phenomenon of gene silencing by double stranded RNA (dsRNA) was first discovered in *Caenorhabditis elegans* by Andrew fire and Craig mellow. A few dsRNA was sufficient to knockdown the expression of genes that are homologous to the dsRNA (Fire, Andrew, et al. 1998). The long double stranded RNA is chopped by DICER- RNA interference deficient 1 (Rde1) complex to release short interference RNA (siRNA) which are characteristically 21 nucleotides long with a 19 nucleotides complementarity and 2 nucleotide overhangs on 3' end of both strands (Tabara, Hiroaki, et al. 1999). siRNA is unwound by the DICER helicase in an ATP dependent manner to release the antisense oligo which then binds to the homologous target mRNA and causes its cleavage and degradation by the RNAi silencing complex (Fig. 14) (Zamore, Phillip D., et al. 2000).

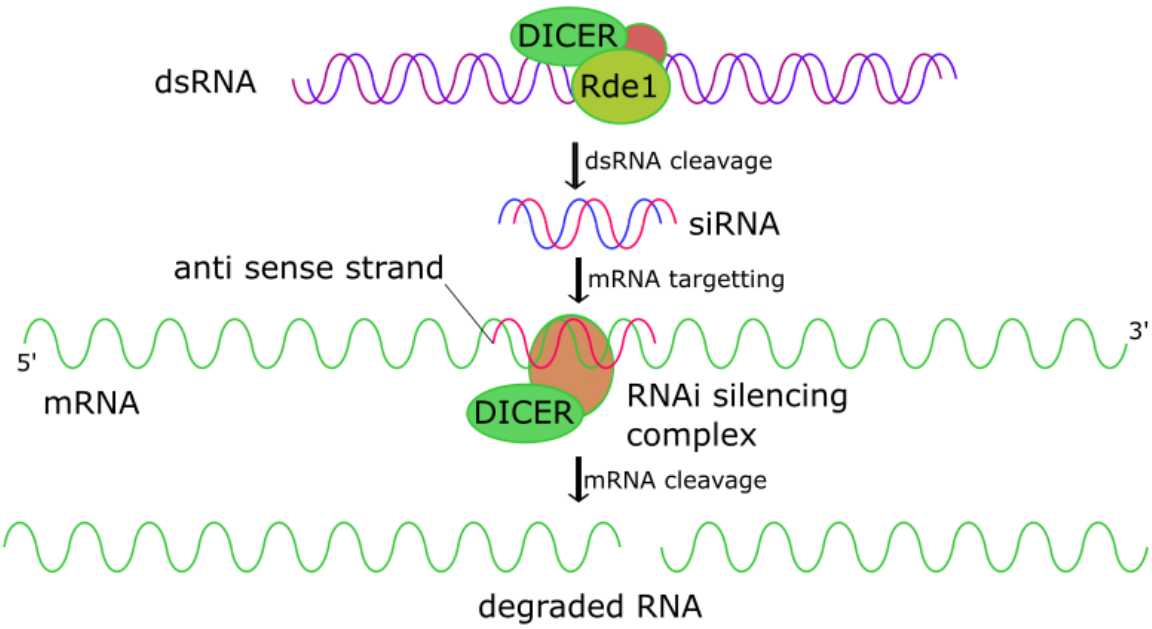

Figure 14: Schematic representation of RNAi. The double stranded RNA is processed by DICER Rde1 complex to release siRNAs. siRNA usually consists of two 21 nucleotides long RNAs with 19 base pairs duplex. The helicase unwinds the siRNA duplex in an ATP dependent

manner. The anti-sense strand is then used by the RNA silencing complex to target and cleave the mRNA. Figure modified from McManus, Michael T. 2002.

Further studies have shown that 70 to 80 nucleotides long, short hairpin RNAs containing these short homology dsRNA stem is also processed by the DICER complex to release the siRNA, the anti-sense strand of which can then target the mRNA from its homologous gene leading to suppression of gene expression (Paddison, Patrick J., et al. 2002). RNAi is proposed to be a naturally existing mechanism to supress transposon translocation in the germline. Mutations in RNAi proteins such as Rde-2, Rde-3, mut-2, mut-7 causes inactivity of RNAi and increases transposon mobilization (Tabara, Hiroaki, et al. 1999).

Valium (Vermilion-AttB-Loxp-Intron-UAS-MCS) vectors are used for expressing RNAi constructs in *Drosophila* (Ni, Jian-Quan, et al. 2008). Second generation Valium vectors (valium20, 21 and 22) uses shRNA driven RNAi. The RNAi constructs are cloned under Gal4 responsive elements. Valium 20 use an hsp70 basal promoter that can efficiently drive the construct expression in somatic and germline cells. Whereas Valium 21 and Valium 22 uses a P-transposase core promoter that's mainly active in the germline as opposed to somatic cells (Ni, Jian-Quan, et al. 2010). Here we used a Valium 22 based Faf2 RNAi line to knockdown Faf2 in the parental germline. In order to study the role of Faf2 in early embryonic development.

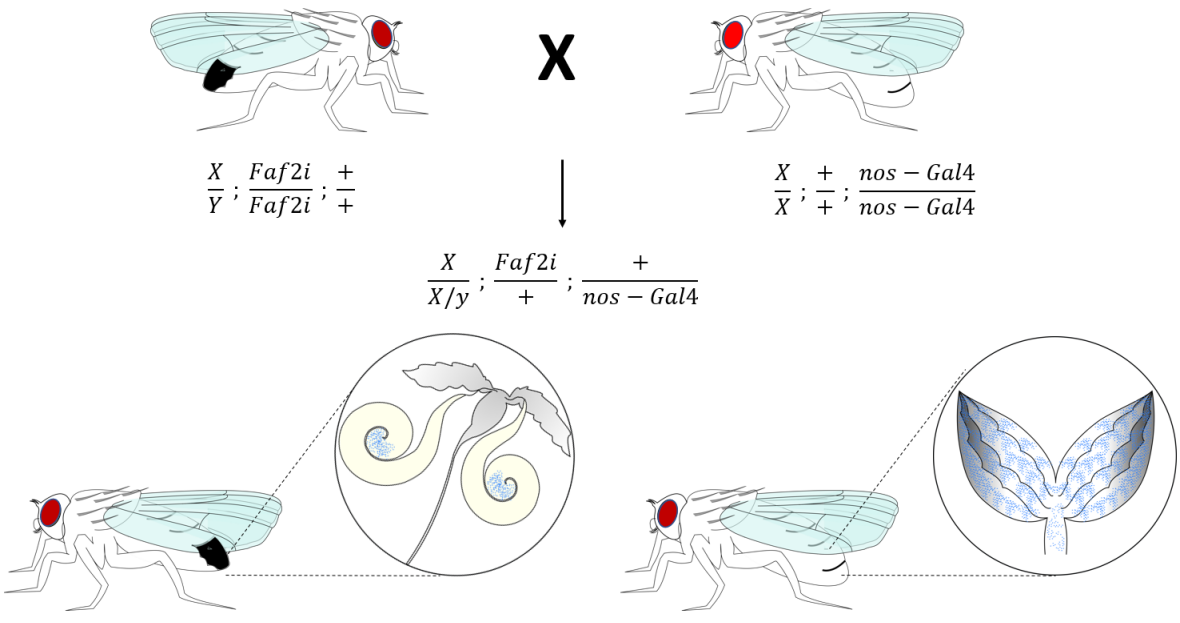

Figure 15: Generating germline Faf2 RNAi knockdown flies. Knockdown of Faf2 in the germline of adult flies was done by crossing a homozygous second chromosome Faf2i line with a third chromosome nanos-Gal4. In the germline of the F1 progeny, gal4 drives the expression of the Faf2-RNAi construct leading to a knockdown in Faf2 levels. Blue shaded region indicates nanos driven gal4 expression. Nanos expresses all over the ovary during oogenesis whereas in the testes, nanos expression is limited to the male germline stem-cell and spermatogonium. Presence of gal4 drives the expression of RNAi construct in these tissues.

Faf2 valium22 RNAi line was obtained from Bloomington stock center (BL43224). Germline knockdown of Faf2 was performed by crossing these lines to different germline specific Gal4 lines such as 13.4MAT Gal4 and Nanos Gal4 (fig. 15). Since Nanos Gal4 was giving a stronger phenotype, further experiments were done using Nanos Gal4. Homozygous Faf2 RNAi flies were crossed to homozygous Gal4 flies and the F1 generation was used to study parental effects on embryo viability. Embryos collected from the F1 flies were also used for cuticle preparation and various embryonic stages were collected and stained using DAPI to study their development.

Chapter 3

Results

Summary: This Chapter describe results of my experiments. I have attempted to generate Casp variants with deletions in different domains. The technology used for deletions at the genomic locus was CRISPR/Cas9 based genome editing. This was a massive effort, especially at the level of screening the flies for domain deletions. The screen unfortunately failed for every deletion attempted. This has led me to an alternative null:rescue approach and I have generated transgenic UASp-Casp variants with the same domain deletions. These deletions will be used to dissect out functional roles for Casp domains in the near future. Further, I examined roles for the Casp/Faf1 homolog Faf2 in early *Drosophila* development using a loss-of-function approach.

Guide RNAs targeting Casp were identified and cloned into pCFD4 vector: Casp extended gene sequence was obtained from fly base (Flybase.org) and was used as the reference sequence. CRISPR Cas9 based genome editing targets the DNA region upstream of an NGG PAM site. The twenty base pair long guide RNA was designed in such a way that there are no off targets in the genome. Multiple online gRNA identification tools like FlyCRISPR, Benchling and CHOPCHOP which use particular algorithms to find out gRNA sequences and check for their off targets in the genome, were used to identify suitable gRNA sequences. The following guide RNAs were chosen based on their binding sites in the gene region (Fig. 16). Different 5' gRNA was used based on the extent of gene region that needed to be deleted and a common 3' gRNA was used as all the planned deletions included the common 3' region (Table. 3).

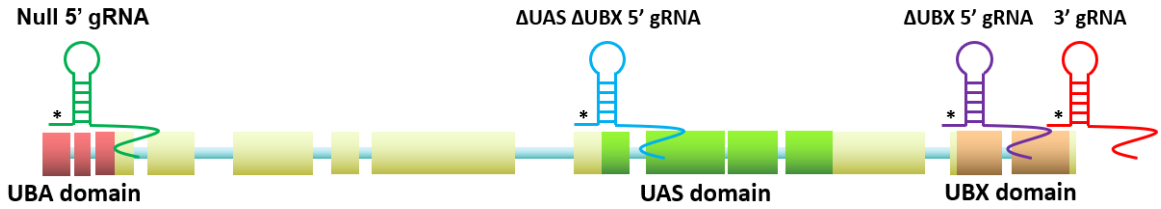

Figure 16: Diagramatic representation of gRNA binding sites on Casp gene region. Identified four different guide RNAs bind to the respective regions shown in figure. The 5' gRNA for null generation binds to the first exon that codes for a part of the UBA domain. ΔUAS

ΔUBX 5' gRNA binds in the exon prior to the UAS region. Similarly, ΔUBX 5' binds to the exon containing the UBX domain, prior to the domain sequence. Asterics indicate the protospacer sequence that anneals to the target region. All gRNAs were designed such that they bind to the coding strand of the gene (complementary to the coding strand). Each square box depicts the exons in the gene. Exons with dual color indicate that they code for parts of different domains of the protein.

Table 3: List of gRNAs selected for mutagenesis. gRNA protospacers were chosen based on their scores predicted by various algorithms and also ensuring that they don't have off targets.

gRNA name	Sequence
Null 5' gRNA	*gcattacctgaaaactggtca*
ΔUAS ΔUBX 5' gRNA	*gtcatccgtatcgtttggtac*
ΔUBX 5' gRNA	*gttcggacggctcctgaggta*
Common 3' gRNA	*gtccaggatgaccgtttcctg*

Sixty nucleotide long primers containing the guide RNA sequences flanked by homology arms with the pCFD4 vector were designed as previously described in the pCFD4 cloning protocol. Using these primers and backbone specific primers, 600bp insert containing the gRNA sequences and a 6.4kb backbone were successfully amplified. pCFD4 vector was used as template in these reactions (Fig. 17A). The size of these fragments was verified on a 0.8% agarose gel and were then gel eluted for transformation. PPY cells were transformed with these fragments and selected on LA-Ampicillin plates. PPY cells expressing λ prophage recombinase can successfully recombine more than 15 nucleotide homology arms. From the transformants, proper recombinants were identified through PCR based colony screening using primers that were specific to the insert (Fig. 17B). These colonies were used for miniprep and were sent for sequencing. Through sequencing, it was confirmed that some of these colonies had the correct sequences of the gRNA sequence incorporated in them (Fig. 17C-F). These colonies were then used for midi-preps and the lyophilised plasmids were sent for micro injections. These midi-prepped products were later sequenced to ensure the sequences are correct. Rather than generating transgenic lines expressing the gRNAs, we chose to perform direct injection into embryos of cas9 expressing flies due to the shortage of time.

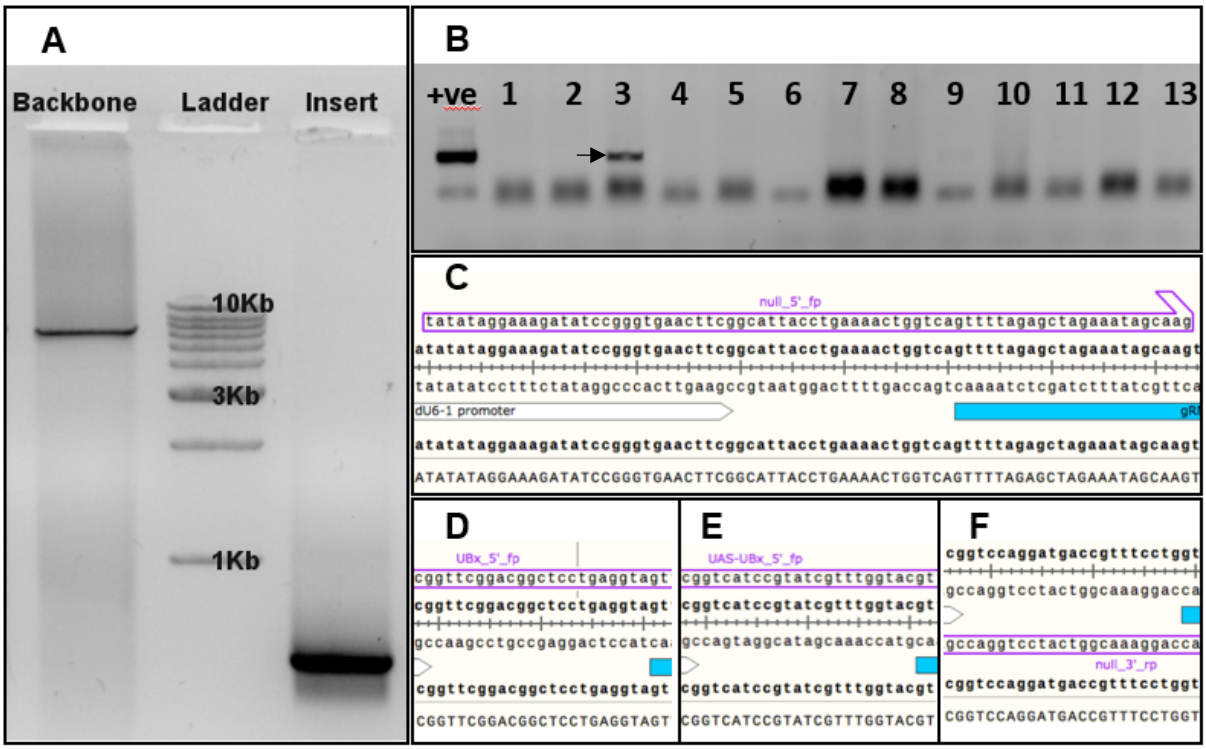

Figure 17: Cloning of gRNA constructs into pCFD4 vector. A) representative image showing successful amplification of pCFD4 backbone (6.4kb) and the insert (600bp) containing the required gRNA sequence. Insert shown is the one used for cloning the gRNAs required for the null mutant generation. Marker used is Gen-i 1kb step up DNA ladder. B) Representative image showing one of the colony screening reactions. The amplified insert was used as the positive control. Primers specific to the required protospacer was used for screening. Lane 3 indicates a positive recombinant. C-F) sequencing results showing successful incorporation of desired protospacer sequences into the backbone.

Stable lines were generated from injected embryos: The gRNA constructs were injected into the pole plasm of X-nosCas9 embryos at the NCBS fly micro-injection facility [BL: 54591 y[1] M{w[+mC]=nos-Cas9.P}ZH-2A w[*]] and these injected embryos were sent back to IISER. Embryos were maintained at room temperature between 19-22°C in order to facilitate slow development enabling low stress for the embryos. Injection in the pole plasm will result in mosaicism in the germline of these embryos since they contain both the cas9 and the guide RNAs. As a result, the progeny of these flies won't be clonal. Some of the progeny might inherit the mutated Casp gene if the injections successfully result in mutagenesis. These flies were collected as virgins post eclosion and were crossed with $\frac{w-}{w-}$; $\frac{Tft}{CyO}$; $\frac{+}{+}$ flies.

Since the injections are done on the posterior pole, in some cases this damages the germline of the fly causing them to be sterile. These sterile flies won't generate any progeny and will be discarded after the first round of crosses. The rest produces progeny that have inherited one of the second chromosome from the injected fly and

the other chromosome it inherits would be either a tufted (Tft) marker or a CyO (Curly of Oster) balancer from the other parent making it feasible to track the putative mutant chromosome. Balancer chromosomes have multiple inversions in them which prevents the it from recombining with the homologous chromosome and so can be used to stably maintain mutations in chromosomes. These inversions usually also result in gene disruptions making them mostly homozygous lethal and also have altered phenotypes characteristic to them. Marker chromosomes also have visible phenotypes associated with them and can be homozygous lethal but will not prevent recombination and thus cannot be used for stabilizing mutations. Balancing of the second chromosome over a CyO balancer stabilizes mutations that might have occurred through CRISPR directed mutagenesis.

From the progeny of these first round of crosses, 3 males each having a CyO balancer were selected as founders, as each of them will inherit only one type of putative mutated chromosome from the injected flies, and crossed to $\frac{w-}{w-}$; $\frac{Tft}{CyO}$; $\frac{+}{+}$ to expand the population. In the subsequent generation single fly crosses were setup using CyO, nontufted virgins { $\frac{w-}{w-}$; $\frac{**}{CyO}$; $\frac{+}{+}$ }, to establish a stable population with a floating CyO balancer. CyO being homozygous lethal will dilute out eventually so long as the induced mutation in the other chromosome is not lethal. The results of these experiments are tabulated in the following table (Table 4)

Table 4: CRISPR_Cas9 stable line generation.

		Casp (Δ)	**Casp (ΔUBX)**	**Casp (ΔUAS-ΔUBX)**
I.Molecular Biology	gRNA vectror	pCFD4	pCFD4	pCFD4
	Sequenced	yes	yes	Yes
II. Injections	#Embryos injected	360	325	350
	#Embryos hatched	170	288	299
III. Screening	#Sterile	19	99	65
	#Fertile	151	189	234
IV. Balancing	#Lethal lines	101	109	127
	#Non-lethal lines	405	458	473

Screening of fly lines for Caspar mutants did not identify any desired mutants: Homozygous { $\frac{w-}{w-}$; $\frac{**}{**}$; $\frac{+}{+}$ } flies were collected from each of these stable populations and were then used for genomic screening. Genomic screening was done by PCR based method as there are no prominently visible phenotypes known to be associated with the mutations in Casp. Casp null mutants are expected to show ectopic melanisation (kim, myungjin, et. al. 2006) due to the hyperactive immune system but this might not be the case for the domain deletion mutants. Thus, primers flanking the whole gene were designed to screen the null mutant and primers flanking the UAS-UBX region to screen the domain deletion mutants.

For the null mutant screening the primer pair Casp_null_F and Casp_null_R was used which amplifies a 3144bp band from the wild type genome where as a successful mutant should generate a 251bp band thus the mutants could be identified based on the size of the PCR amplified band. Since the primer pair was generating nonspecific amplifications and was resulting in multiple bands during the screening (Fig. 18A), another forward primer, Casp_null_F2, was then designed for the screening (3075bp product size). Multiple bands were amplified in the new reactions thus a gradient PCR was setup to identify suitable annealing temperature that prevents nonspecific amplifications (Fig. 18B). 62 degrees was chosen as the annealing temperature for screening based on the results of this gradient PCR.

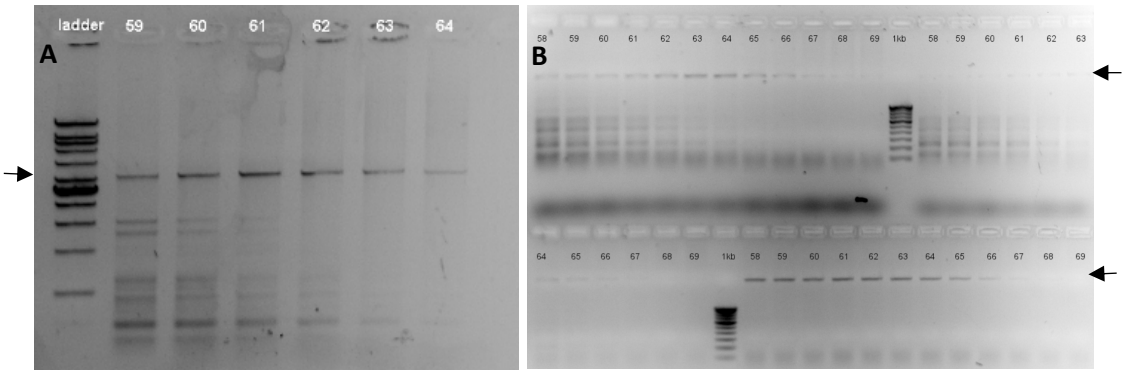

Figure 18: Gradient PCR for primer characterization. Gradient PCR for primer pairs Casp_null_F : Casp_null_R and Casp_null_F2 : Casp_null_R. A) Gradient was setup for Casp_null_F : Casp_null_R using 0.5uL genomic DNA per 10uL reaction. The temperature gradient was from 59 degrees to 64 degrees. B) Gradient was setup for Casp_null_F : Casp_null_R using 1uL and 1.5uL genomic DNA and Casp_null_F2 : Casp_null_R with 1.5uL gDNA per 10uL reaction. The temperature gradient was from 58 degrees to 69 degrees. Since Casp_null_F2 paired with Casp_null_R amplified single band at 62 degrees for 1.5uL gDNA, this primer pair was used for further screening using an annealing temperature of 62 degrees.

Single flies were crushed in 50ul squishing buffer containing freshly prepared proteinase K. Lysate was then incubated at 37 degrees for 30 minutes and the proteinase K was inactivated at 85 degrees for 5 minutes. 1.5ul of the template was used as template for the screening PCR. Out of the 480 independent lines only 108 lines produced a clear amplificon (supplementary figures). All these amplicons were of the same size as the wild type bands. None of the Screening reactions produced a smaller product indicating a possible deletion of the gene. On repeating the PCR reactions on the remaining samples, there were inconsistencies in the amplification of the product whereas when the same genomic DNA was used for a PCR reaction using previously characterized Dorsal primers (dorsal_F and dorsal_R) a consistent amplification was obtained across different samples thus, it was concluded that there might be a problem with the primer pair that was being used for the screens (Fig. 19A). Thus three more primers were designed (Casp_null_F3, Casp_null_R2 and Casp_null_R3) and these pairs were blasted using primer-blast3 against the *Drosophila* genome to ensure they are specific to the casp gene and the pairs Casp_null_F2 : Casp_null_R2, Casp_null_F2 : Casp_null_R3, Casp_null_F3 : Casp_null_R2, Casp_null_F3 : Casp_null_R3 were shown to produce only single amplicons from the fly genome in silico. These pairs along with Casp_null_F3 : Casp_null_R1 pair, which is predicted to produce 3 different amplicons, were used to setup a single PCRs to identify suitable screening primer pairs (Fig. 19B). The primer pair Casp_null_F2 : Casp_null_R2 did not amplify any product. Single amplified bands were seen in the remaining reactions.

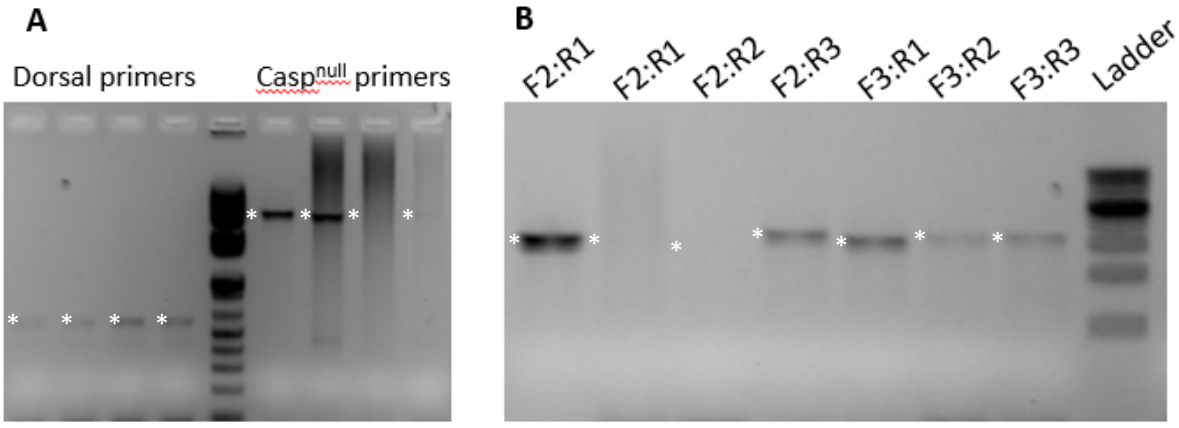

Figure 19: Characterization of Casp^{null} screening primers. A) Characterizing the efficiency of the null screening primer pair in PCR genotyping. PCR reactions were setup using a previously characterized primer pair (DorsalF and DorsalR) and the null screening primers (Casp_null_F2 and Casp_null_R) for the same set of genomic DNA. B) Characterizing various

primer combinations to test the feasibility of using them for screening null mutants. PCR program Casp null screening. Asterisks marks expected product size.

The primer pair UAS_UBX_F and Casp_null_R was used for screening the domain deletion mutants. This primer pair should produce a band of size 1507bp in case of wild type. Deletion of the UBX domain should result in the product to run at 1215bp and the deletion of both UAS and UBX domains will result in a product size of 231bp. Gradient PCR was setup with different DNA concentrations to identify suitable PCR conditions (Fig. 20). Based on the results of this experiment we proceeded using a template volume of 1.5 ul and annealing temperature of 60 degrees. Single band amplifications were obtained in the genomic screen. 375 lines were screened in case of ΔUASΔUBX deletion and 351 lines in case of ΔUBX deletion. None of these lines showed a band that was migrating at the expected lower size (supplementary figures).

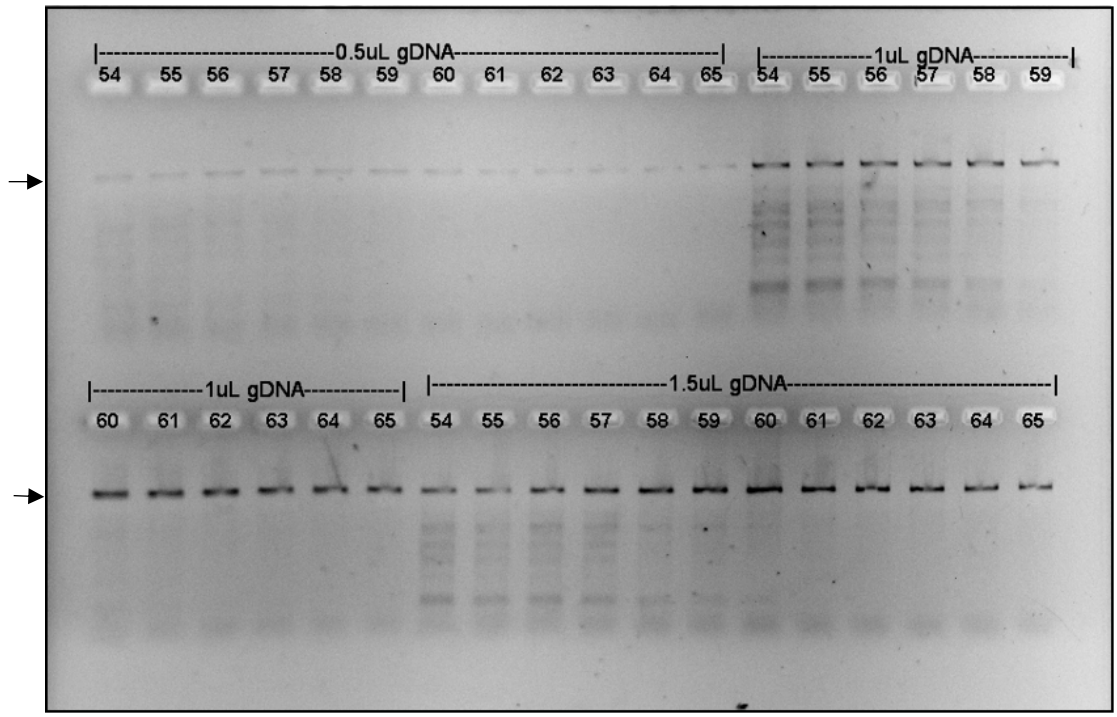

Figure 20: Gradient PCR for domain mutant screening primers. A gradient PCR ranging from 54 degrees to 65 degrees was set up. Different volumes of template for a 10uL reaction. As seen, single prominent amplification was seen at 1.5uL template volume at an annealing temperature of 61 degrees.

pUASPattb HA Casp constructs were successfully cloned: Due to difficulties in generating a Casp mutants through CRISPR mutagenesis, it was decided to perform a phenotype rescue for Casp^{lof} line using UAS-Gal4 system. Five desired constructs

of Casp was cloned into the pUASPattB vector along with an N-terminal HA tag for this (Fig. 21). These were namely ΔUBA which lacks the N terminal UBA domain, ΔUAS which lacks the internal UAS domain, ΔUBX lacking the C terminal UBX domain, ΔUASΔUBX lacking both the UAS and the UBX domains and an HA tagged wild type Casp to be used as control in these experiments.

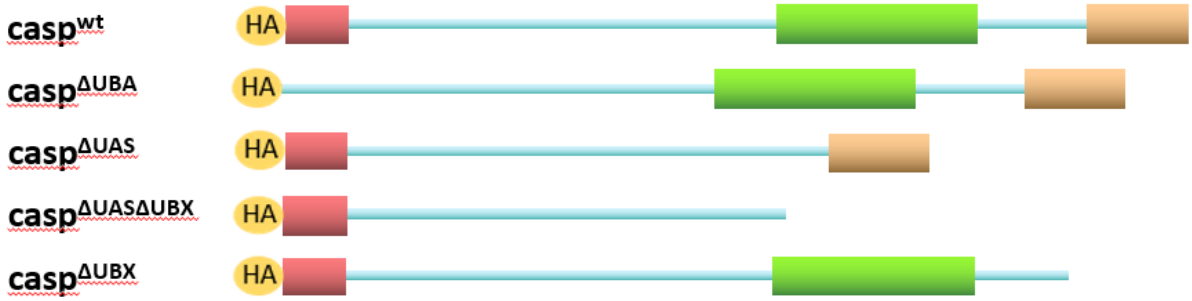

Figure 21: HA tagged domain truncated variants of Casp. Digrammatic representation of various domain truncated versions of Casp cloned into pUASPattB vector. For detection and pull down, an N-terminal HA tag was added to the constructs.

For the cloning, a previously generated pUASPattB HA-Casp_wt (Bhagyashree Khaduskar, Thesis, 2018) construct was used as template. This construct lacked a start codon in the beginning of the tag. As a result, a two-step cloning strategy was adapted. In the first step, a functional HA tag sequence was added to the 5' region and the second step introduced a twenty-nucleotide homology arm to the pUASPattB backbone using a common forward primer (cmPUASPattB). For the wild type Casp construct, a 2153bp long fragment containing a part of the HA tag and the entire Casp coding sequence and a twenty-nucleotide homology with the pUASP backbone was amplified using the primer pair pUASCaspF and pUASCaspR. This fragment was verified on an agarose gel (Fig. 22D) and purified by gel elution. The 5' homology with the pUASPattB was added to this fragment by reamplifying the fragment with primers cmPASPattB and pUASCaspR. The pUASPattB backbone was midiprepped and digested overnight with BamH1and given a CIP treatment for an hour. The enzymes were then inactivated at 80 degrees. The digested mix had a final concentration of 100ng/ul. PPY competent cells were transformed with a 1:1 volume mix of the backbone and the reamplified insert. The transformed colonies were then screened using pUASP screening primers pUASP_F and pUASP_R. Positive recombinants were then sent for sequencing. Sequencing was done using primers pUASP_R and Casp_UBA_3'R. Proper recombinant colony with the correct sequence was then

midiprepped and the lyophilized plasmid DNA was sent to NCBS for injection (supplementary figures).

For the ΔUBA construct, pUASdUBA_F was used as the forward primer. This primer contained part of the HA tag and Casp CDS after the UBA domain in the reading frame. A 1989bp long fragment was amplified using this forward primer and pUASCasp_R. The PCR product was then resolved on a 0.8% agarose gel (Fig. 22A). The 1.9Kb fragment was gel eluted and reamplified by using cmPUASPattB and pUASCasp_R. Reamplification yielded a single band at the desired size (Fig. 22C) which was then used for transformation in a 1:1 volume ratio with the digested backbone using PPY competent cells. One of the colonies were identified positive and was sent for sequencing but it turned out to have one of the C terminal glutamate residues replaced by a phenylalanine. The cloning was repeated and a new set of positive clones were sent for sequencing and the ones with the correct sequence was then midiprepped and sent to NCBS for transgenic generation (supplementary figures).

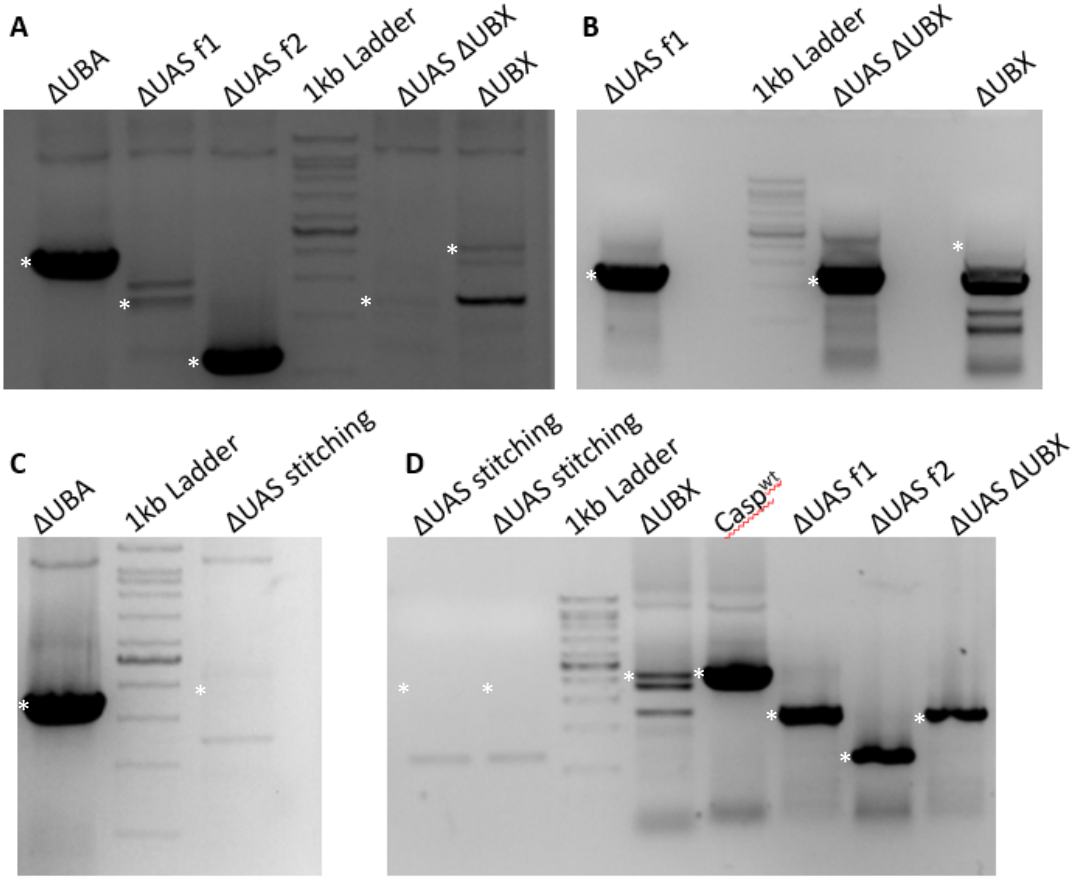

Figure 22: Fragment amplification for pUASP cloning. Various insert fragments for cloning the pUASP constructs were successfully synthesised through PCR. A) amplification of different fragments using their respective primers. Asterisk indicate the fragment of interest B) Reamplification of various fragments with cmpUASPattB C) Reamplification of ΔUBA and one step stitching reaction for ΔUAS D) two step stitching reactions and reamplification of inserts with cmpUASPattB forward primer. Asterisks mark the expected product size.

Next in line was for us to generate a ΔUAS line which needed amplifying the region upstream of and downstream of the UAS domain separately and stitching them together. The specific primers designed for these were pUASdUAS_R1 and pUASdUAS_F2. The upstream fragment of size 1147bp was amplified using pUASCasp_F and pUASdUAS_R1. Which was then verified on an agarose gel. On resolving the product, rather than a single 1.2kb band, it contained two more bands migrating at 0.6kb and 1.4kb (Fig. 22A). The 1.2kb band was cut out and purified by gel elution. This band was then reamplified using cmPUASPattB and pUASdUAS_R1 primers (Fig. 22B). The downstream fragment of size 585bp was successfully amplified with the primer pair pUASdUAS_F2 and pUASCasp_R. It was size verified by running on a 0.8% agarose gel (Fig. 22A) and gel eluted for purity. It was reamplified using the same primer pair. A stitching reaction was performed by taking 2ul and 1ul each of reamplified fragments one and two respectively as template and setup a 50ul PCR reaction using the cmPUASPattB and pUASCasp_R. This stitching reaction failed to yield a product. We then repeated the tried to anneal the products by a two-step reaction where 20ul of fragment 1 and 10ul fragment 2 were used in a 50ul reaction without any primers for stitching and was split into two pots, 25 ul each. The end primers were added to these reaction pots and the reaction volumes were made up to 50ul each. This reaction also did not yield any amplified product. Since the fragments have a 20bp homology arm between them and they have homology with the backbone, it was reasonable to assume that the PPY cells will be able to recombine these fragments with directional specificity. Thus, we tried to perform a three-fragment transformation. A DNA mix was made by taking 2ul of 100ng/ul digested pUASPattB backbone and 1.25ul of reamplified fragment 1 along with 0.75ul of reamplified fragment 2. Four vials each of 50ul PPY competent cells were transformed using 1ul each of the fragment mix. Transformed colonies were screened and one of them showed a recombinant fragment of desired size of 1.8kb. This colony was sent for sequencing and was verified to have the proper sequence. The midiprep of this construct was sent for transgenic generation (supplementary figures).

The dual UAS-UBX (ΔUASΔUBX) deletion construct was designed by using pUASCasp_F and pUASdd_R primers. A 1147bp long fragment was amplified using these primers. There were mutltiple bands amplified in this reaction which were visualized in a 0.8% agarose gel. We then gel eluted the fragment of the desired size and reamplified it with the cmPUASPattB primer and pUASdd_R primer. By using PPY competent cells, these fragments were recombined and recombinants were identified by colony PCR (Fig. 22A,B). Positive constructs were sent for sequencing. Post sequencing, the colony having desired plasmid sequence was midiprepped and sent for microinjection (supplementary figures).

For the ΔUBX, the fragment was amplified using primer pair pUASCasp_F and pUASdUBX_R. This primer pair yielded multiple bands on amplification, two of which were migrating very close by around 1.9 to 2kb. Since the desired fragment was about 1890bp long, we isolated the lower band and reamplified it using cmPUASPattB and pUASdUBX_R primers. This reamplification also yielded multiple bands (Fig. 22A,B,D) making it difficult to use this for further processing. Later it was noticed that the reverse primer and the forward primer adds the overhangs to the construct making it 1950bp long rather than 1890bp and so we isolated the higher migrating band which then was successfully reamplified using the reamplification primers. It was later used in a 1:1 ratio with the digested backbone to transform PPY cells. Antibiotic resistant colonies were then screened with screening primers for positive recombinants. The identified positive recombinants were sequenced and the ones with proper sequence was midiprepped and sent for injection (supplementary figures). Cloning and transgenics data are summarized in the table below (Table. 5).

Table 5: Generation of pUASP Casp transgenics. The table summarizes the results of the pUASP-HA tagged Casp transgenics generation experiment. All the constructs were cloned and stable transgenics were successfully generated

Construct	Cloning Status	Transgenic Status
pUASP-HA-Casp^{wt}	Cloned	Generated (2 lines, Chr. III)
pUASP-HA-Casp$^{\Delta UBA}$	Cloned	Generated (2 lines, Chr. III)
pUASP-HA-Casp$^{\Delta UAS}$	Cloned	Generated (2 lines, Chr. III)
pUASP-HA-Casp$^{\Delta UAS\Delta UBX}$	Cloned	Generated (2 lines, Chr. III)
pUASP-HA-Casp$^{\Delta UBX}$	Cloned	Generated (2 lines, Chr. III)

Casplof pBac Excision did not generate any null alleles: In order to generate an alternate null allele, we performed the pBac element excision from the $Casp^{lof}$ allele. The $Casp^{lof}$ has a piggyBac element inserted in the 5'UTR region causing it to be a near null allele. We tried to excise out this pBac element using the piggyBac transposase. PiggyBac is a precise transposase element such that when it is excised out from the genome it does not produce any scars in the genome. But it was previously reported that there is a 2-6% chance of imprecise excision that occurs causing minor additions or deletions of DNA bases (Kim, Heuijong, et al. 2012). We generated 17 excision lines out of which only one showed embryonic lethality as in case of the $Casp^{lof}$ allele. But this line complemented $Casp^{lof}$ allele indicating that the observed embryonic lethality is due to some other off target effect (Table. 6).

Table 6: Generation of a frameshift mutant. Table summarizes the piggyBac excision experiments

Number of crosses setup	150
Number of mosaics collected and crossed	150
Number of complete excisions obtained	17
Number of lines showing embryo lethality	1
Number of lines failing to complement $Casp^{lof}$	0

After 3 rounds of repeated crossing with the transposase line, we succeeded in generating 17 independent excision lines (selected based on the lack of pigmentation in the eye indicating a lack of miniwhite gene). Of these only one line showed ~70% embryonic lethality. But this line successfully complemented the $Casp^{lof}$ allele.

In order to verify that the Casp expression is unaffected in the excision line with increased lethality, western blotting was done. The polyclonal rabbit α-Casp antibody does not show any difference in the expression levels of the main Casp band but interestingly the other bands that showed which could be cleaved Casp products or non-specific targets showed changes in the banding pattern (Fig. 23). These results suggest that the excision line in question is not a Casp null.

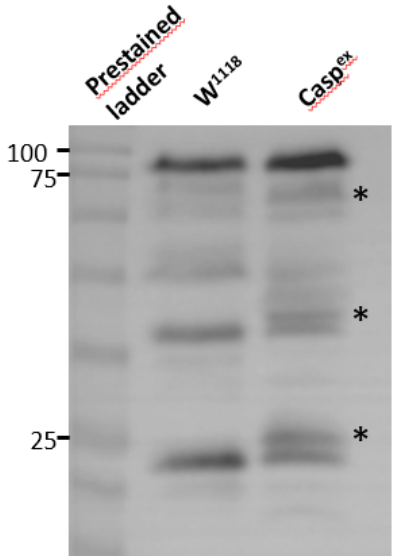

Figure 23: Casp^{ex} line expresses Casp. Fly lysate from five adult females were resolved on an SDS page and blotted onto PVDF membrane. Blot was probed with rabbit polyclonal anti-Casp antibody to visualize Casp and its cleaved products. Casp^{ex} line shows the presence of Casp (78.44KDa) suggesting that the respective excision did not cause any frameshift and as a reason the allele is not a null. It is interesting to note that there are variations in the cleaved products in Casp^{ex} in comparison with wild type. Casp^{ex} shows few additional bands (asterisks) as compared to the wild type pattern.

Casplof/Caspdf (Casplof/df) flies show increased lethality of its progeny: Casp$^{lof/df}$ flies were generated by crossing homozygous Casp^{lof} males to Casp^{df}/Cyo virgin females. Non Cyo female flies were selected to set-up cages. These were pre-mated females. A cross was setup with Cas$^{lof/df}$ males in a small size cage. A significantly high lethality of 83.5 percent with a standard deviation of 11.75 was observed. Compared to a 7.5 percent lethality in wild type with a 1.25 standard deviation (Fig. 24). Previous study in the lab has shown that homozygous Casp^{lof} females shows causes 75% embryonic lethality due to maternal effect (Neel Wagh, Thesis, 2019). Here this higher lethality suggests that Cas$^{lof/df}$ results in a slightly severe phenotype as compared to Casp^{lof} homozygotes.

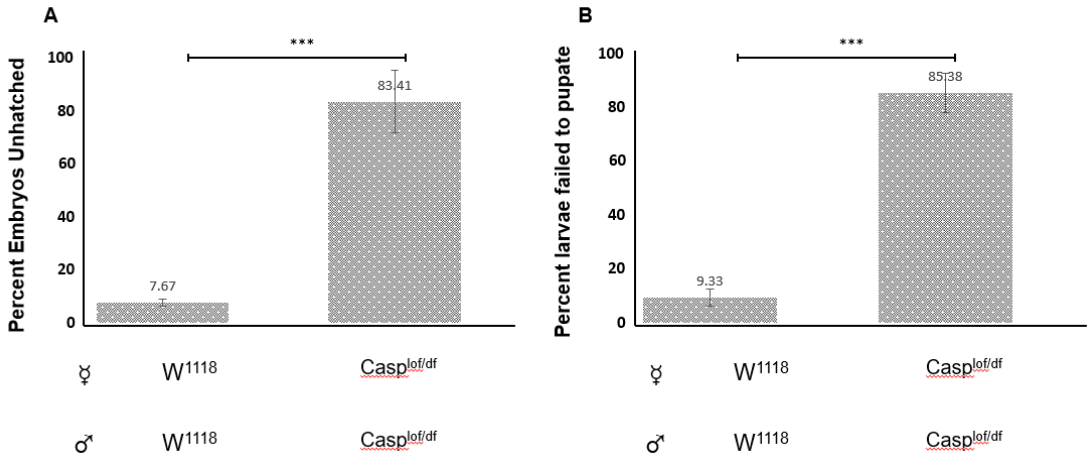

Figure 24: Progeny of Casp$^{lof/df}$ shows significantly high lethality. A) Graph showing embryonic lethality in case of Casp$^{lof/df}$ embryo development. As opposed to an ~7.5% lethality

in wild type (W^{1118}), $Casp^{lof/df}$ flies show a significantly higher lethality of ~83.5%. For each replicate (N=3) 15 females were used to set up a cage and 200 embryos were screened. B) Graph depicting lethality during larval development. Progeny of $Casp^{lof/df}$ mothers show around 85% lethality as opposed to ~9.5% in case of wild type. All the larvae that hatched were transferred onto 6% media for lethality analysis in case of $Casp^{lof/df}$ where as in case of wild type, 100 larvae were taken per trial (N=3). Significance was calculated using t-test: two samples assuming equal variance. *** indicate a P<0.001.

Progeny of $Casp^{lof/df}$ flies showed significantly higher lethality during larval development. As opposed to an ~9.5% lethality in wild type the progeny of $Casp^{lof/df}$ showed an ~85% lethality with a standard deviation of 7.5%. By the end of each round of the experiment, hardly 5 to 6 larvae pupated. Of these few that pupated, none showed any pupal lethality.

Progeny of Casplof/df flies undergo gastrulation: DAPI staining of the 2 to 4 hour old embryos showed proper gastrulation in the majority of the progeny of $Casp^{lof/df}$ flies (Fig. 25). This suggests that the observed lethality is not a result of male sterility nor defects in fertilization. Early development in these embryos seems almost unaffected.

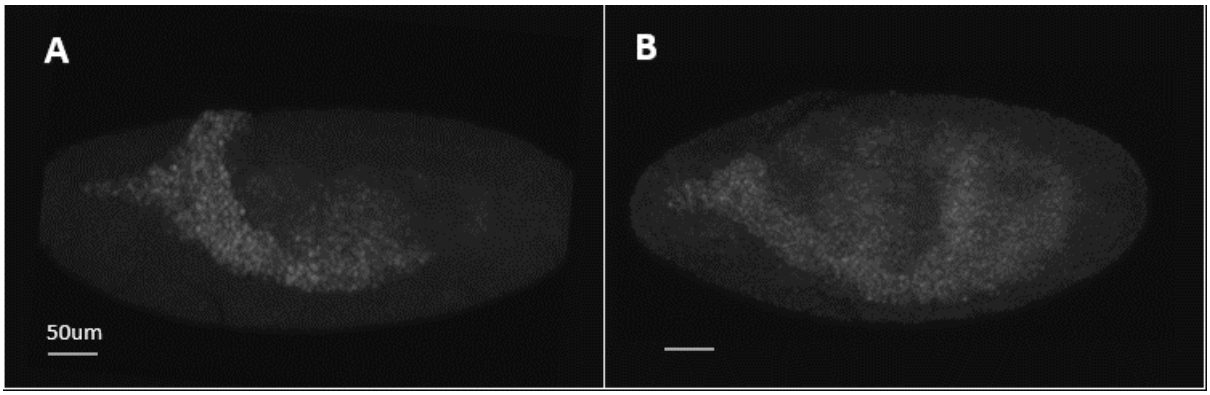

Figure 25: Progeny of $Casp^{lof/df}$ flies undergoes gastrulation. A) W^{1118} embryo in gastrulation B) Progeny from $Casp^{lof/df}$ undergoing gastrulation. Staining was done with DAPI for visualization (1:1000). N=1 number of embryos=20. Both embryos shown are around stage 6.

Progeny of Casplof/df flies does not deposit cuticle: Embryos collected from $Casp^{lof/df}$ flies were aged for 24 hours and were digested with lactic acid to visualize the cuticle. The cuticle preps reveal that these progenies fail to deposit cuticles in comparison with the wild type embryos. Out of the 25 samples observed, only one showed deposition of cuticle (Fig. 26).

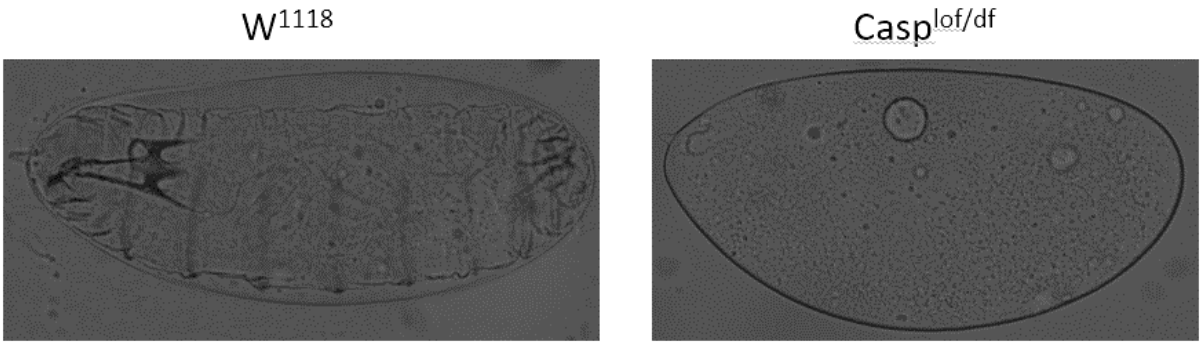

Figure 26: Cuticle prep for Casp$^{lof/df}$. Casp$^{lof/df}$ embryos fail to deposit cuticle 24 hrs post fertilization indicating developmental arrest before stage 16. N=1, number of embryos = 25.

Expression of Faf2 in the parental germline is required for embryonic development: Faf2 RNAi reagent flies were obtained from Bloomington *Drosophila* Stock center (BDSC). The available RNAi reagent BL43224 (complete genotype: y[1] sc[*] v[1] sev[21]; P{y[+t7.7] v[+t1.8]=TRiP.GL01569}attP40) is an insertion of a UAS regulated Faf2 RNAi dsRNA construct cloned in a Valium 22 vector into the attP40 docking site. Valium 22 constructs are efficient in driving RNAi constructs in the germline (Perkins, Lizabeth A., et al. 2015). This line will be referred to as Faf2i. This line is balanced over a Cyo balancer. Homozygous female flies were collected from the 13.4-Mat Gal4 line and were crossed to Cyo balanced males from the Faf2i line. From the progeny, non Cyo flies were selected as the parents driving Faf2 knockdown in their germline. Cyo flies were used as the Gal4 controls. Germ line knockdown of Faf2 resulted in elevated embryonic lethality (Fig. 27).

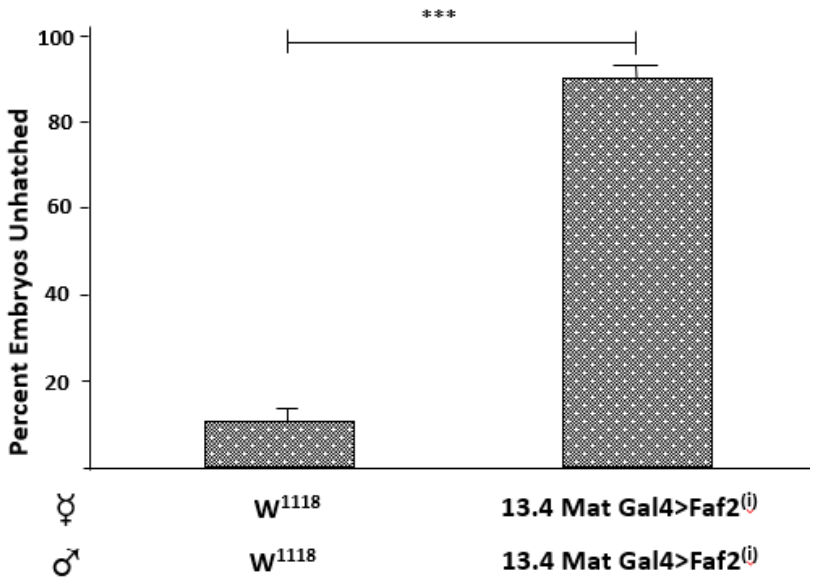

Figure 27: Knockdown of Faf2 in parental germline causes elevated embryonic lethality. Graph shows the embryonic lethality caused by the knockdown of Faf2 in the parental germline. As opposed to an 8.75% percentage lethality in case of wild type, the progeny of the flies with Faf2 knockdown in the germline shows an average lethality of 90% with a standard deviation of 3.15. For each replicate (N=3) thirty females were used to set up cages and 200 embryos were screened. Significance was calculated using t-test: two samples assuming equal variance. *** indicate a P<0.001.

It was observed that a germline knockdown of Faf2 in parents resulted in elevated lethality in the embryos. In contrast with the 8.75% wild type embryonic lethality in wild type, an elevated lethality of 90% was observed in case of embryos from flies with a germline knock down of Faf2.

Faf2 in paternal germline is essential for early development: Faf2 being another adaptor of the ubiquitin proteasomal machinery (Xu, Yue, et al. 2013), and belonging to the family as caspar (Fas associated factors), this observed lethality in the embryos because of a germline knockdown of Faf2 in their parents lead us to hypothesise that Faf2 also might be a maternal effect gene. Germline Faf2 Knockdown flies were generated by crossing Cyo balanced Faf2i male flies with 13.4 Mat gal4 homozygous females. Non Cyo flies were selected for setting up egg collection cages. Cyo flies were used as Gal4 controls to check whether Gal4 causes any effects in embryonic lethality.

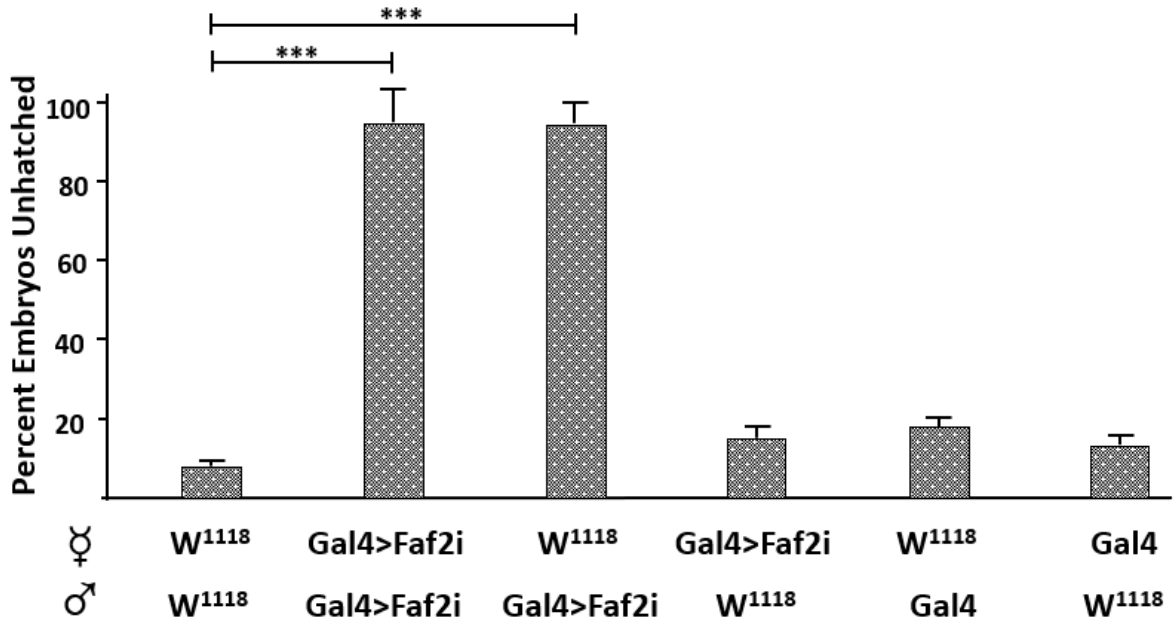

Figure 28: Faf2 knockdown in paternal germline causes increased embryonic lethality. Graph showing the paternal contribution Faf2 towards early embryonic development. Faf2 RNAi was driven using 13.4 Mat Gal4. As opposed to a baseline lethality in wild type of 7.5%,

knockdown of faf2 in the paternal germline resulted in ~88% lethality irrespective of whether the mother is wild type or also has Faf2 knocked down in the germline. Interestingly, knockdown of Faf2 in the maternal germline did not show any significant increase in embryonic lethality (14% percentage with a standard deviation of 3%). Similarly, the Gal4 control flies also showed only baseline lethality, indicating that there is no detrimental effect due to the presence of Gal4 alone in these embryos. All replicates (N=3) were generated by setting up cages containing 30 females and 15 males. 200 embryos were screened to observe lethality. T-test: two samples assuming equal variance were used to calculate significance in the observed change. *** indicate p<0.001.

To our surprise, it was observed that knockdown of Faf2 in the paternal germline but not the maternal germline that is causing the high embryonic lethality (Fig. 28). Importantly, knockdown of Faf2 in the female germline did not show any change in the embryo viability as opposed to wild type. This suggests that either Faf2 knockdown in the male germline causes male sterility or that Faf2 is a paternal effect gene. These results were reproduced using a nanos Gal4 driver (Fig. 29). In comparison with 13.4 Mat Gal4, nanos Gal4 resulted in an even stronger phenotype. Nanos driven knockdown of Faf2 in the paternal germline resulted in 98.5% embryonic lethality. Nos driven Faf2 RNAi in the maternal germline did not show any change in the embryonic lethality.

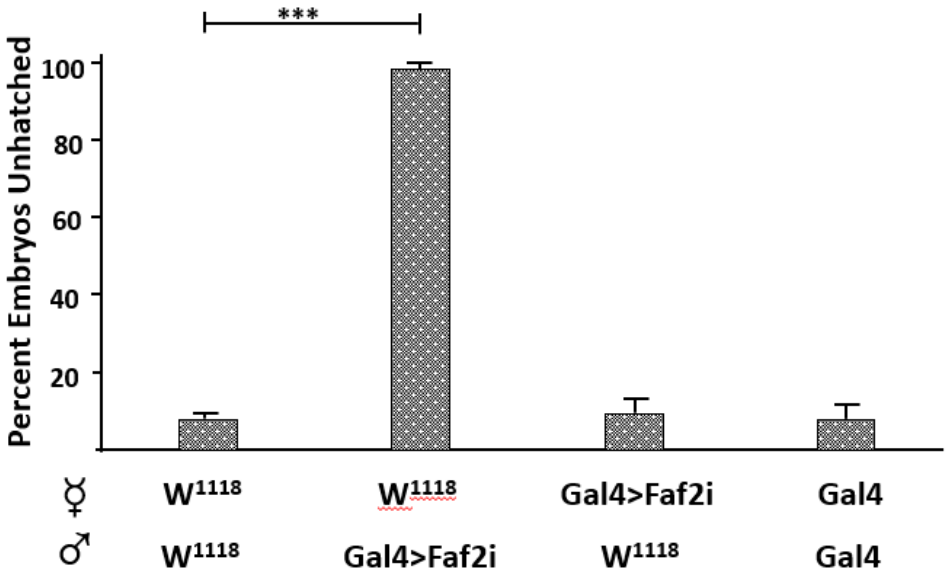

Figure 29: nos-Gal4 driven Faf2 RNAi shows a stronger phenotype. Graph showing embryonic lethality in case of nos Gal4 driven Faf2 knockdown in male germline. Nanos driven Faf2 knockdown causes a 98.5% embryonic lethality with a standard deviation of 1.75%. Each of the replicates (N=3) were produced by setting up cages containing 30 females and 15 males. 200 embryos were screened to calculate the lethality per trial. Significance value *** indicate P<0.001. Calculated using t-test: two samples assuming equal variance.

Faf2 is a paternal effect gene: To distinguish whether Faf2 RNAi causes male sterility or is it a paternal effect gene, we checked whether the sperm from the germline Faf2 knockdown males were able to fertilize eggs from W^{1118} flies. DAPI staining of 2-4-hour embryos and 5-7-hour embryos suggest that Faf2 germline knock down does not cause male sterility. Sperm of these flies are able to penetrate and fertilize these embryos as evident from the occurrence of nuclear divisions (Fig. 30).

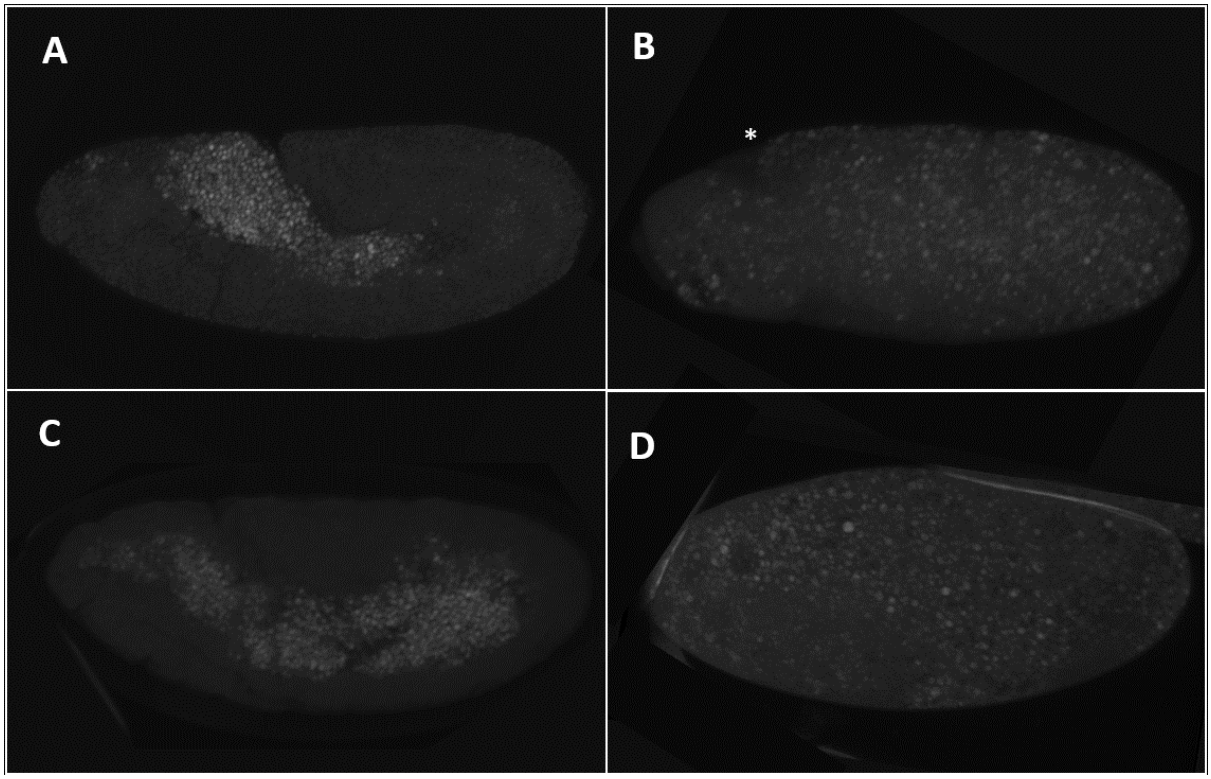

Figure 30: Faf2 paternal knockdown flies exhibit developmental defects. A) W^{1118} embryo in gastrulation (Stage 7). B) Paternal Faf2 knockdown embryo in developmental stages somewhere between 3 to 5. Asterisk marks the beginning of anterior mid-gut invagination. C) A W^{1118} embryo in stage 9 of development. D) Faf2 paternal knockdown embryo shows diffused staining and improper nuclear localization. Panels A and B are from 2-4-hour old embryos while C and D are from 5-7-hour embryos. Staining was done with DAPI (1:1000) N=1, number of embryos=10

Progeny of Faf2 RNAi flies does not deposit cuticle: Since paternal germline knockdown of Faf2 caused abnormalities in gastrulation, it was decided to check whether these embryos deposit cuticle or not. Observations suggest that these embryos do not deposit a cuticle suggesting embryonic lethality much before stage 16 since cuticle deposition occurs at stage 16 of development (Fig. 31).

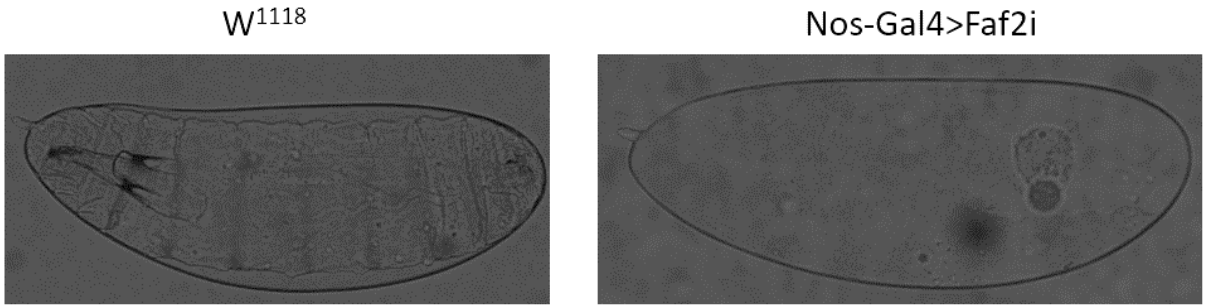

Figure 31: Paternal Faf2 RNAi embryos does not deposit cuticle. Embryos fathered by flies having a germline knock down of Faf2 driven by nanos Gal4 fail to deposit cuticle 24 hrs post fertilization indicating developmental arrest before stage 16. Embryos were not devitellinised and the vitelline membrane could be seen in the images. N=1, number of embryos = 197.

Out of 197 embryos, only 4 deposited cuticle. These results suggest that expression of Faf2 in the paternal germline is essential for embryonic development. Indicating paternal roles for Faf2 in development.

Chapter 4
Discussion and future plans

Summary: In this Chapter I discuss the way ahead, after the failure of the CRISPR/Cas9 genome editing experiments. The pUASp Casp domain deletions flies have already been generated and I need to validate these lines and express them in a Casp null background. The physiological roles for Faf2 that I have uncovered lead to a study of both Faf1 and Faf2 as genes that show functional sub-functionalization. Both genes, as discussed, probably have distinct roles in the Ubiquitin proteasomal pathway.

Failure of CRISPR screen: We were unsuccessful in generating the desired Casp mutants using CRISPR-Cas9 mediated genome editing. Partly owing to the difficulties associated with the PCR based screening to identify the desired mutants (Supplementary figures). Across the three different CRISPR mutagenesis sets, none of the 834 different lines that were successfully screened showed a desired smaller amplicon as was expected. This led us to suspect that the mutagenesis strategy that was designed might not be efficient.

Cas9 was shown to form a stable DNA binding complex with the target DNA, utilising the base pair complementarity with the protospacer sequence of the gRNA, that's stable unless disrupted by the DNA unwinding helicases during DNA replication in bacterial systems (Jones, Daniel Lawson, et al. 2017). Similar results were reported in eukaryotic systems. Cas9, irrespective of its catalytic activity, forms stable complexes with DNA and DSBs on the target lasting (Richardson, Christopher D., et al. 2016). Their reported off rate of the Cas9-DSB complex is ~5.0±0.3 X 10^{-5} S^{-1} indicating a lifetime of 5.5 hours. Owing to this Cas9-DSB stability, it takes up to 15 hours for the exponentially growing human cells to repair 90% of the CRISPR induced DSBs as opposed to just an hour to repair 90% DSBs induced by ionising radiations (Kim, Sojung, et al. 2014). It was shown that the PAM distal non-target strand is released quite easily from the Cas9-DSB complex and is not a major component of the Cas9-DSB complex, as a result an asymmetric ssDNA fragment complementary to the non-target strand destabilizes the Cas9-DSB complex and results in an HDR

repair rate of up to 57±5% (Richardson, Christopher D., et al. 2016). The optimum design for this ssDNA is a 36bp overlap with the PAM distal and 91bp with the PAM proximal non target strand across the Cas9 cleavage site. An ssDNA donor binding the non-target strand increases the homology directed repair frequencies by 4 folds as opposed to a dsDNA and up to 2.6 folds in comparison to a ssDNA binding to the target strand (Richardson, Christopher D., et al. 2016). These observations suggest that destabilization of the Cas9-DSB complex is essential for effective CRISPR mediated mutagenesis.

Two independent studies have shown that transcriptional state of the target genes influence the efficiency of mutagenesis. A library screen of various gRNAs targeting a wide range of target genes has shown a positive correlation between H3K4 trimethylation of genes, an epigenetic mark associated with transcriptionally active genes, with their susceptibility towards CRISPR mediated mutagenesis (Chari, Raj, et al. 2015). It was shown that in transcriptionally active genes, RNA polymerase displaces the Cas9 from the DSB in a directional manner, exposing the DSBs to the cellular repair machinery (Clarke, Ryan, et al. 2018). The efficiency of various gRNAs to induce double strand breaks across various target genes shows a bimodal distribution where the gRNAs targeting the template strand of a transcriptionally active gene has an efficiency of greater than 30% as opposed to greater than 1.5% percent in case of gRNAs targeting the coding strand of a transcriptionally active gene (Clarke, Ryan, et al. 2018). They have reported that sgRNAs targeting the template strand cause 2.9 to 7.6 times increase in levels of H2AX phosphorylation, a mark of active DNA repair as opposed to sgRNAs targeting coding DNA strand. Template targeting gRNA also resulted in enhanced binding of DSB binding NHEJ recruiters Ku70/80 on the target DNA fragments. Transcriptional state of the gene also determines the mutation efficiency where a 2-4-fold increase was observed when a gene was transcriptionally active as opposed to its off state (Clarke, Ryan, et al. 2018). These observations indicate that an RNA polymerase can displace Cas9 from the Cas9-DSB complex to expose the DSB and result in the subsequent repair and mutagenesis only if it is approaching the Cas9-DSB complex from the PAM distal site and not from the PAM proximal region. In other words, RNA polymerase enhances CRISPR mediated mutagenesis in transcriptionally active genes when the gRNA targets the template strand.

Another factor that affects the ability of Cas9 to cleave target DNA is the levels of nucleosome occupancy of the target sequence. Nucleosome hinders the Cas9 from accessing the target DNA (Gilbert, Luke, et al, 2016). This study suggests that ability of Cas9 to cleave the target DNA has a negative correlation with the nucleosome occupancy of the target. Regions with low nucleosome density shows enhanced chances of indels when targeted with gRNAs. But chromatin remodelling events enhances the DNA accessibility for Cas9 (Gilbert, Luke, et al, 2016). These findings are summarized in the following figure (Fig. 32).

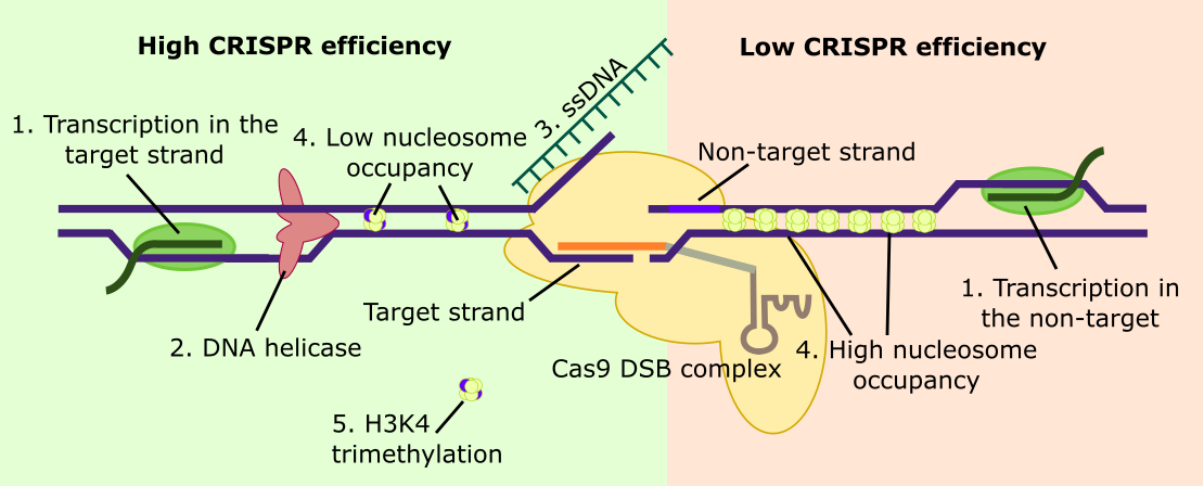

Figure 32: Factors influencing CRISPR mutagenesis frequency. 1) Transcriptional state of the target gene influences mutagenesis efficiency. Transcription in the target strand destabilizes the Cas9-DSB complex, possibly by disrupting gRNA and target strand interaction, and increases the indel frequency. RNA polymerase transcribing in the non-target gene cannot displace Cas9. 2) DNA unwinding helicases can displace Cas9 from the DSB. 3) ssDNA annealing to the non-target strand displaces Cas9, exposing the DSB for efficient HDR repair. 4) nucleosome occupancy influences mutation frequency since nucleosomes cause physical hindrance to Cas9 and prevents its binding to the target. Low nucleosome occupancy favours Cas9 binding to the target. Since chromatin remodelling enzymes displaces nucleosomes, chromatin remodelling aids in CRISPR mediated mutagenesis. 5) H3K4 trimethylation mark is associated with enhanced CRISPR mediated mutation frequencies. H3K4 trimethylation flags transcriptionally active state of genes.

Our CRISPR designs used gRNAs targeting the coding sequence of Casp. This suggests that each of our gRNAs have a low probability of targeting and causing a mutation in the target site. Our PCR fragment size-based screening strategy will detect a mutant only when there has been a simultaneous DSB and repair in both the gRNA targets. In case of gRNAs theoretically having a low ability to produce a free DSB for repair, an event of simultaneous generation of DSBs at both the target sites has a very low chance of occurrence. Suggesting that our screen might have had indel mutants at either of the target sites but not necessarily a domain deletion mutant. modENCODE

data (Celniker, Susan E., et al. 2009) shows high levels of Casp expression in *Drosophila* embryos suggesting that Casp is transcriptionally active in the embryo and so transcriptional inactivity is not the reason for failure of our CRISPR screening. Another reason might be the chromatin structure of Casp. High nucleosome occupancy in the gRNA target regions might be a reason why it was difficult to generate a Casp mutant through the CRISPR mediated mutagenesis.

Since we think that the gRNA design was the reason for the failure of the screen, we plan to repeat the screening to generate a $Casp^{null}$ by using another pair of gRNAs that target the template strand of Casp. We would also like to use ssDNA donor to enhance the rates of mutagenesis. The screening primer needs to be characterized and a different genomic DNA preparation method might be used in order to ensure efficient and consistent screening of the stable lines.

$Casp^{lof/df}$ is a suitable system to study Casp domain functions: Preliminary characterization of the $Casp^{lof/df}$ flies suggest that it is a suitable system for studying the domain functions of Casp. The progeny of these flies shows up to ~80% lethality. They develop proceed through gastrulation but fail to develop beyond stage 15-16 as they do not deposit cuticle. Faf1 being an adaptor for protein degradation, is needed for maintaining ER protein homeostasis. Faf1 promotes the proteasomal degradation of ER membrane associated misfolded proteins (Lee, Jae-jin, et. al. 2003).

ModEncode data for Casp shows that there is a high level of expression of Casp in the ovaries, salivary glands and in the digestive system. There are moderate high levels of Casp in the testes and fat bodies. And there is moderate expression of Casp in the male accessory glands. The oocyte contains considerably high amounts of Casp mRNA and protein. mRNA level fluctuates very much in the embryo but the protein levels remain almost the same throughout embryogenesis. The high levels of expression in the ovary might be an indicative of the importance of Casp in oogenesis as well as the embryonic development.

During embryonic development, initial developmental events are regulated by maternally deposited proteins (Tadros, Wael, et al. 2009). But as development proceeds the maternal deposits are degraded in two steps, the degradation of maternal mRNAs by maternally deposited proteins and degradation of maternal proteins by the proteins expressed from the embryonic genome (Tadros, Wael, et al.

2009). These events mediate the maternal to zygotic transition (MZT) of the developmental program. Since the initial development of $Casp^{lof/df}$ embryos are seemingly fine, we assume that observed defects are a result of irregular MZT. The lack of effective degradation of maternally deposited proteins might be resulting in elevated ER stress and subsequent cell death. Rescue experiments using the Casp variants cloned using the pUASP vector will be useful in providing further insight into the mechanistic roles played by Casp in regulating embryonic development.

Casp-pUASP transgenics were successfully generated: The cloning of the HA tagged variants of Casp were done successfully and we were able to generate the transgenic flies with the help of the NCBS fly transgenics facility. We have generated third chromosome balanced $Casp^{lof}$ and $Casp^{df}$ and second chromosome balanced Gal4 lines. We would be using these reagents to perform UAS rescue of the $Casp^{lof/df}$ line with the designed variants of Casp. The diagram below represents a road map for performing these rescue experiments (Fig. 33). The recue flies will be used to the role of various Casp domains towards the maternal phenotype. The UBA deficient line will be poor in its ability to stabilize ubiquitinated proteins. In comparison the Casp variant lacking the UBX domain will not be efficient in assisting proteasomal degradation of the ubiquitinated targets. This gives insight into whether Casp helps in degradation of maternal deposits or whether it stabilizes the maternally deposited proteins. This would provide more insight into the role of Casp in assisting the maternal to zygotic transition during embryonic development.

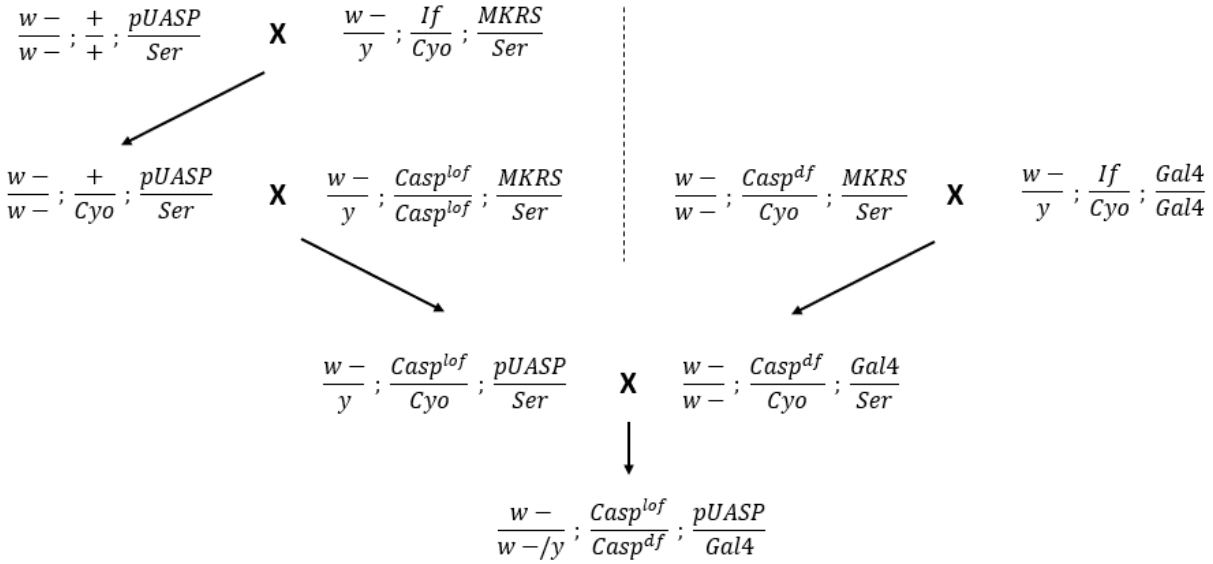

Figure 33: Roadmap for UAS-Gal4 driven Casp rescue: Contribution of various Casp domains towards its maternal effect and innate immune response will be studied using pUASP

mediated rescue of $Casp^{lof/df}$ line using various Casp variants. By using the second and third chromosome balancer line and the third chromosome balanced $Casp^{lof}$ line, a second chromosome $Casp^{lof}$ and third chromosome pUASP-HA-Casp variant line will be made. Similarly, with the use of the third chromosome balanced $Casp^{df}$ line and a second chromosome balanced third chromosome Gal4 line, a second chromosome $Casp^{df}$ third chromosome Gal4 line. These lines will act as the responder and the driver respectively. The non-Cyo flies from the progeny of this cross will be a Casp rescue animal which can then be used for further experimentation.

Similarly, these flies can be used to study the role of Casp domains in innate immunity. The UAS domain is known to act as a sensor for LCPUFA levels within the cell (Kim, Hyeonwoo, et al. 2013). Previous studies show that cells show activation of NfκB signalling in response to elevated levels of LCPUFA (Weigert, Cora, et al. 2004). The immune response elicited by the variant lacking the UAS domain will be interesting in studying the roles played by cellular LCPUFA levels in regulating the innate immune response. If the mutant is able to combat a gram-negative bacterial infection but is inefficient in eliciting a response towards a polyunsaturated fatty acid stress, it could be inferred that the inactivation of Casp by LCPUFA is the reason for the expression of NfκB response genes.

pBac excision did not generate a Casp null: Our transposase mediated piggyBac excision did not yield a frameshift null for Casp. Previous reports suggest that piggyBac is a precise transposon in its excision (Kim, Heuijong, et al., 2012). There is only a 4.3% chance for an excision to be imprecise causing an indel during its repair. Since we were able to generate only 17 independent excision lines, it is highly possible that none of these were an imprecise excision. The reason for such low numbers of excisions even after three rounds of crossing with the pBac transposase needs to be checked. In the meantime, since growing the flies at 29 degrees improves the chances of an imprecise excision to 6.5% (Kim, Heuijong, et al., 2012), it would be interesting to carry out these excision experiments again at 29 degrees.

One of the excised lines showed increased homozygous lethality. But it successfully complemented $Casp^{lof}$ allele. This suggests that the observed lethality is not due to a mutation in the Casp gene. A western analysis for Casp in these flies shows changes in the pattern of the cleaved products. This might be an experimental artefact which needs to be verified by repeating the western blot experiments. Further characterization of this line will be essential if the altered banding pattern is consistently seen across replicates.

Faf2 as a paternal effect gene: This study provides preliminary evidence that suggests Faf2 is a paternal effect gene. The germline Faf2 RNAi experiments show embryonic lethality ~88% with a 13.4 mat Gal4 driver which is elevated up to ~98.5% on using a nanos Gal4 driver. These embryos do not deposit any cuticle indicating the death of the embryos in early stages of development. DAPI staining of the embryos shows nuclear divisions indicating that Faf2 RNAi does not cause male sterility. The spermatocytes from these male flies are efficient in fertilizing oocytes and initiates nuclear divisions. DAPI staining reveals that progeny of the germline Faf2 knockdown males does not develop beyond early gastrulation (stage 3-5) as marked by the formation of the anterior midgut furrow. Staining of late stage embryos show nuclear mislocalization and morphological changes. There is a huge variation in the size of the nuclei with few giant nuclei visible randomly distributed across the embryo. This might be due to irregularities in nuclear divisions.

ModEncode data shows that there is a very high level of expression of Faf2 transcripts in the testes of an adult non-virgin male and there is high level of expression in the male's accessory glands and the female's ovaries. There are moderate levels of expression in other tissues of the animal. There is a very high level of maternally deposited Faf2 mRNA as well as protein in the embryo, the mRNA levels go down over time but the protein persists in high levels throughout the embryonic development. This suggest that Faf2 might be playing important roles during gametogenesis, especially in spermatogenesis, and embryonic development.

It is interesting to note that the nanos Gal4 driver does not express throughout the male germ line, rather its expression is limited to the male germline stem cells and the spermatogonia. Expression of nanos Gal4 in the late stages of spermatogenesis is not reported. Suggesting that the observed phenotype is not mediated by the physical presence of Faf2 in the spermatozoa. In support with this argument, the D*rosophila* sperm proteome (Wasbrough, Elizabeth R., et al. 2010) containing 1108 unique members does not report Faf2 as one of the proteins present in the mature spermatocyte. Thus, it is reasonable to speculate that Faf2 might be causing changes in the levels of certain other paternal effect proteins as Faf2 is shown to influence mRNA stability (Zhou, Hua-Lin, et al. 2013). Faf2 being an adaptor of proteasome for its segregase activity, might also be causing misfolding of its downstream targets causing the observed paternal effect phenotype (Zhou, Hua-Lin, et al. 2013).

During fertilization, the sperm head enters the oocyte to deliver the sperm pronuclei to the oocyte. The acrosome of the sperm contains the lytic enzymes required for the entry and release of the genetic material from the sperm. The major component given to the embryo by the sperm is the genetic material along with the associated DNA binding proteins. Of the previously reported paternal effect genes, Sneaky is a component of the acrosome (Wilson, Kathleen L., et al. 2006). Sneaky promotes exocytic disassociation of the sperm plasma membrane and aids in the delivery of the genetic material to the embryo. The two other paternal effect genes Pal and Horka ($lds^{Hor\text{-}D}$) encode proteins associated with the centromeres of paternally derived chromosomes. The mutants for these genes lose paternally derived chromosomes during embryo development. Pal mutants cause loss of chromosomes during somatic divisions resulting in the one of the daughters not receiving a copy of a chromosome while the others receive just one copy of the paternal chromosome (Baker, Bruce S. 1975). The Horka gain of function mutant also encodes a centromere associated protein that causes chromosomal nondisjunction during development and results in the loss of paternally derived chromosomes (Szabad, Janos, et al. 1995). Progeny of sneaky mutants fails to initiate nuclear divisions whereas the Pal and Horka mutants' embryos develop into mosaic adults.

In comparison, K81 mutants are reported to show a paternal phenotype much like what is observed in case of Faf2. K81 mutant sperms are able to fertilize the embryos but most of these embryos are arrested in the early nuclear cycles (Yasuda, Glenn K. et al. 1995). K81 is a duplication of the Hiphop gene that encodes a telomeric protein which is expressed exclusively in the male germ line (Gao, Guanjun, et al. 2011). K81 localises on the telomeres of the post mitotic cells. K81 is resistant to chromatin remodelling and is selectively retained in the paternal chromosomes from early stages of spermatogenesis and it acts as a protective cap on telomeres (Gao, Guanjun, et al. 2011). Embryos fathered by k81 null males fail to re-establish the protective cap in the paternally derived chromosomes during embryonic development. This causes telomeric instability and telomere fusion which hinders chromosome segregation and causes developmental arrest (Gao, Guanjun, et al. 2011).

Cytoplasmic incompatibility (CI) in drosophila caused by Wolbachia infection is an example of induced paternal effect (Schumann, Wolfgang. 1974). Wolbachia is an intracellular reproductive parasite that infects a wide range of arthropods. Being a

cytoplasmic parasite, the microbe is vertically transmitted from the mother to the progeny through the oocyte cytoplasm. The infected females have a selective advantage where their eggs can be fertilized by any fertile male but the sperm from an infected male fails to fertilize the eggs of an uninfected female (Lassy CW, Karr TL. 1996). This induced paternal effect is a resultant of the defective chromatin remodelling that happens in the male germline. Post fertilization, protamines are removed from the paternally derived chromosomes and H3.3 is incorporated to it followed by acetylated H4 and later H2A and H2B. Successful completion of these sequence of events activates DNA replication and possibly CDK1 signalling. In Wolbachia induced CI crosses, the paternally derived chromosomes are altered such that H3.3 and H4 incorporation is hindered and this also causes PCNA stalling leading to incomplete DNA replication and chromosome bridge formation during metaphase and subsequent developmental arrest (Riparbelli, Maria Giovanna, et al. 2012). It is interesting to note that during early stages of spermatogenesis, Wolbachia are removed from the sperm plasm along with other cytoplasmic contents (Bressac, Christophe. et al. 1993) indicating that modifications during early stages of spermatogenesis are sufficient to influence the subsequent chromatin remodelling. Wolbachia infection in the males alters the expression levels of zipper and lethal giant larvae (l[2]gl) proteins both of which are part of the cytoskeletal and trafficking machinery (Clark, Michael E., et al. 2006). Artificial disruption of the levels of which induces paternal effect phenotype.

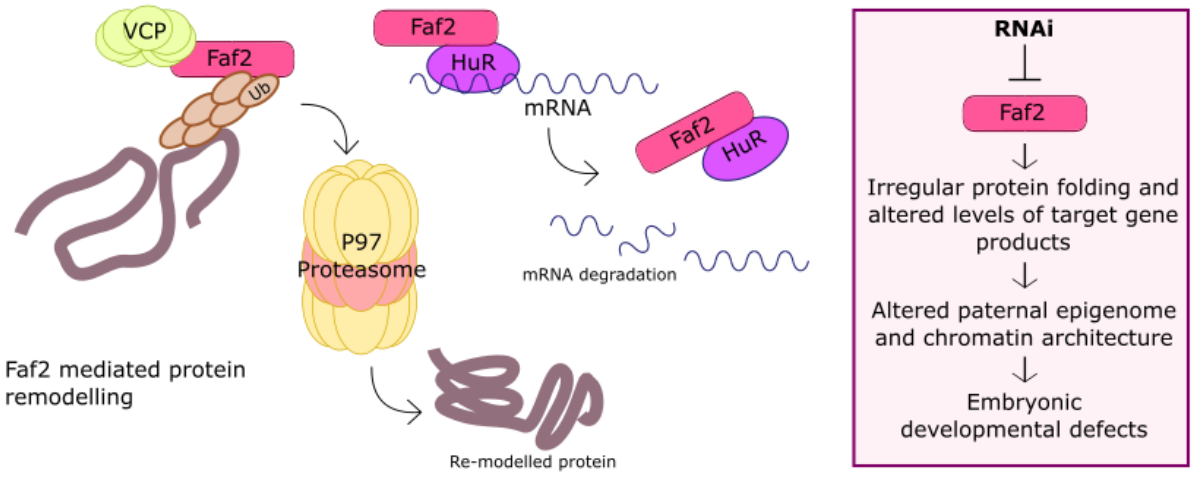

Figure 34: Paternal role of Faf2: A possible mechanism for the paternal role of Faf2. Faf2 aids in p97 mediated extraction and remodelling of K-29 linked polyubiquitinated proteins from

various protein complexes. Remodelling removes the ubiquitin tag from the target protein and alters its function. Faf2 has also been implicated in influencing mRNA stability by releasing the mRNA stabilizing protein HuR from mRNPs. Causing subsequent degradation of these mRNAs. This suggests that in case of germline knockdown of Faf2, there could be misfolding or changes in expression levels of chromatin associated genes altering the chromatin architecture of the paternal chromosomes. This might destabilize paternally derived chromosomes in the embryo during mitotic divisions.

From this available information, we hypothesise that the knockdown of Faf2 during early stages of spermatogenesis manifests in paternal effects by influencing the transcript levels or folded states of chromatin associated proteins that are passed on to the progeny (Fig. 34). Inhibition of faf2 in the paternal germline might interfere with the embryonic development in of the following ways; Faf2 knockdown can interfere with the telomere capping, resulting in telomeric instability and fusion of paternal chromosomes which then interferes with pronuclear migration and division leading to abnormal development. The other possibility is that Faf2 knockdown changes the epigenetic marks on the paternal chromosomes such that the histone-protamine exchange that occurs post fertilization is hindered. This can induce replication stalling, chromosomal breaks and chromosome loss etc, leading to developmental arrest. It is very well possible that K81, zipper or l[2]gl might be one of the downstream targets of Faf2. Further experimentation to identify the interacting partners of Faf2 in the male germline will be crucial in validating these claims. Simple staining for H3.3 and PCNA can be used to check whether the histone-protamine exchange is defective or not. Using anti-acetylated H4 antibody, paternal chromosomes can be stained and tracked to analyse the telomere stability. Using female transgenics that mark the nuclear envelope, a paternal knockdown cross can be setup and the nuclear divisions can be recorded to identify stages in embryonic development where Faf2 paternal knockdown induces the observed paternal effect phenotype. A proteomic study of Faf2 null sperm will provide more insights into whether Faf2 results in alteration in the expression of any other plausible paternal effect genes. We also plan on performing simultaneous knockdown of Casp and Faf2 to study the combinatorial effects of Faf proteins in early embryonic development.

Supplementary Data

1. pCFD4 cloning

Positive recombinant colonies were identified by colony screening PCR. Primers specific to incorporated gRNA were used for screening. A single 540bp band indicates a successful clone.

pCFD4 Casp^{null} colony screening:

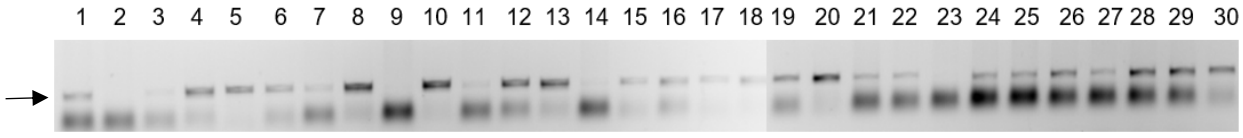

Screening for recombinant colonies identified colonies 8, 10, 12, 13 and 20 as positive recombinants since these colonies yielded a bright, single amplicon, non-shadow band

pCFD4 Casp$^{\Delta UAS\Delta UBX}$ colony screening:

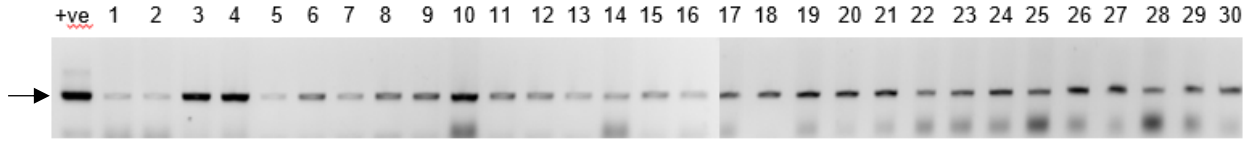

Screening for recombinant colonies identified colonies 3, 4, and 10 as positive recombinants since these colonies yielded a bright single amplicon band comparable to the positive control which was amplified from the 600bp insert

pCFD4 Casp$^{\Delta UBX}$ colony screening:

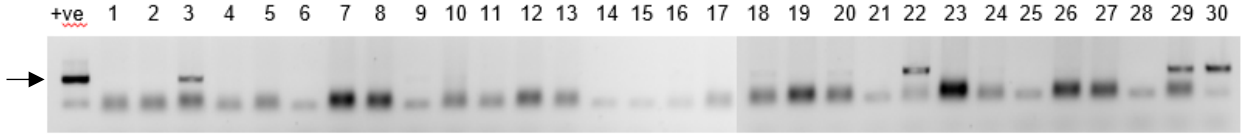

Screening for recombinants identified colony 3, 22, 29 and 30 to have the desired gRNAs incorporated in them. 22 and 30 were chosen for sequencing.

2. Caspar screening

Casp^{null} Screens: screenings were done using the primer pair Casp_null_F2 and Casp_null_R. A proper deetion should change the band size from 3144bp to 251bp. A 100bp ladder was used since the deletion product is small in size. 328

lines were subjected to screening of which 108 were successful and none of these indicated a desired mutant band.

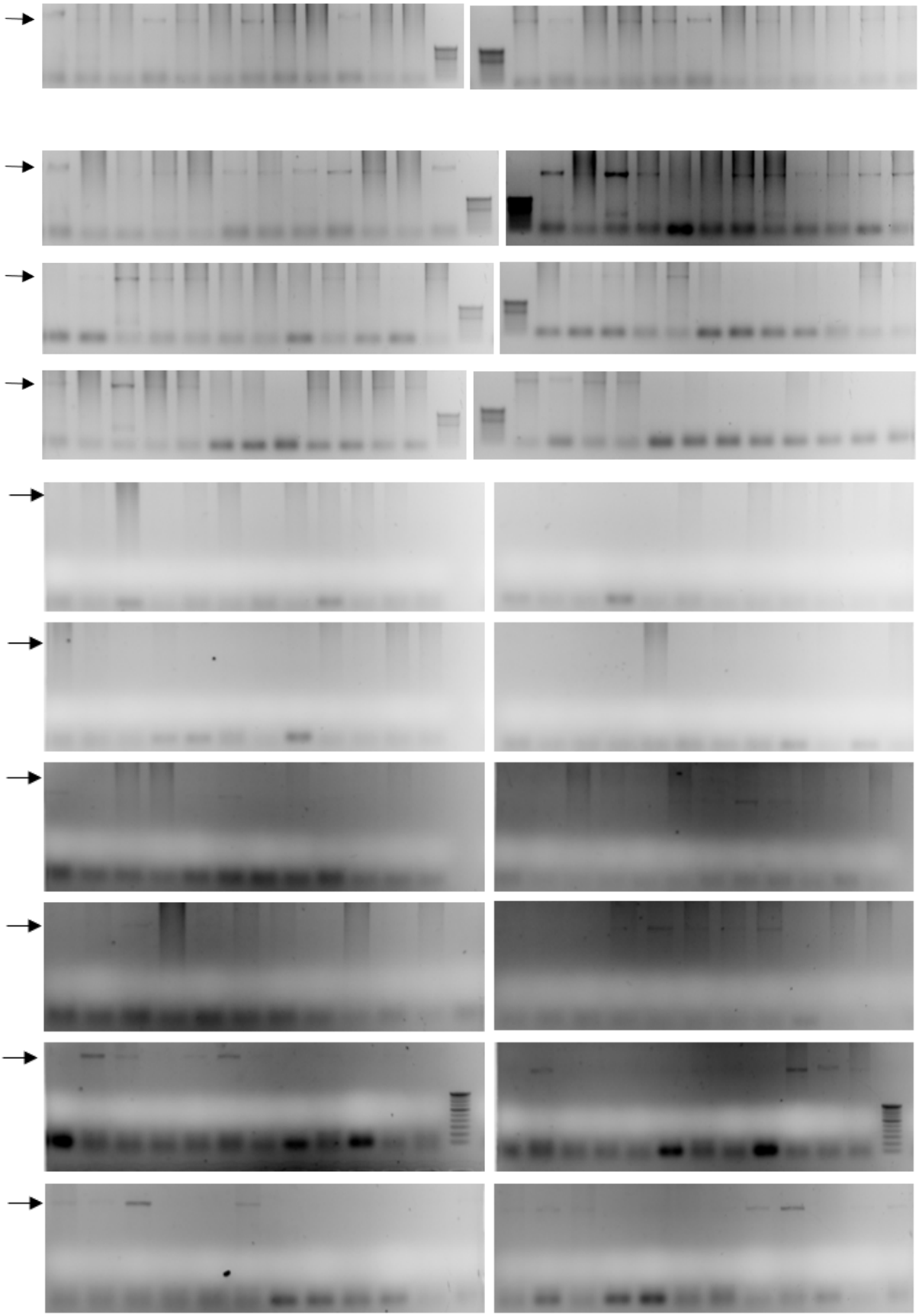

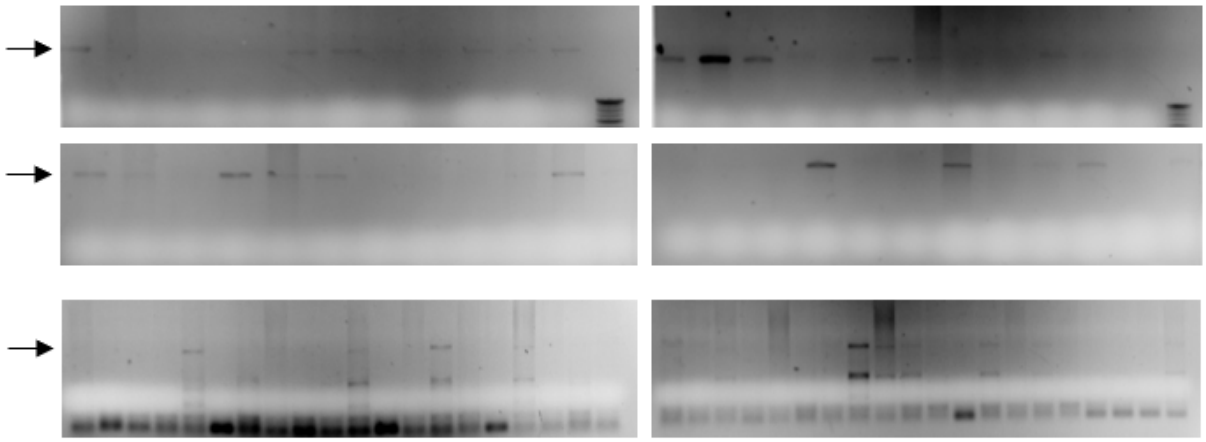

Shown in figure are the images of the screening gels for Casp^{null} stable lines. Orientation of the samples are from left to right in each row starting from top left and ending at bottom right, 328 colonies were subjected to screening of which only 108 lines produced an amplicon. The arrow mark indicates the expected running size of the Casp-wt amplicon. None of the lines showed the amplification of an expected deletion product of size 251bp. An additional 1.2kb band could be seen in many lanes along with the wildtype band these are non-specific amplifications since most of these flies were homozygous.

Casp$^{\Delta UBX}$ screening: primer pair Casp_UAS_Ubx_F and Casp_null_R were used for screening. A successful deletion should result in a 1215bp product as opposed to the 1507bp wildtype band. 1kb stepup ladder was used. None of the amplified products shown a desired smaller band.

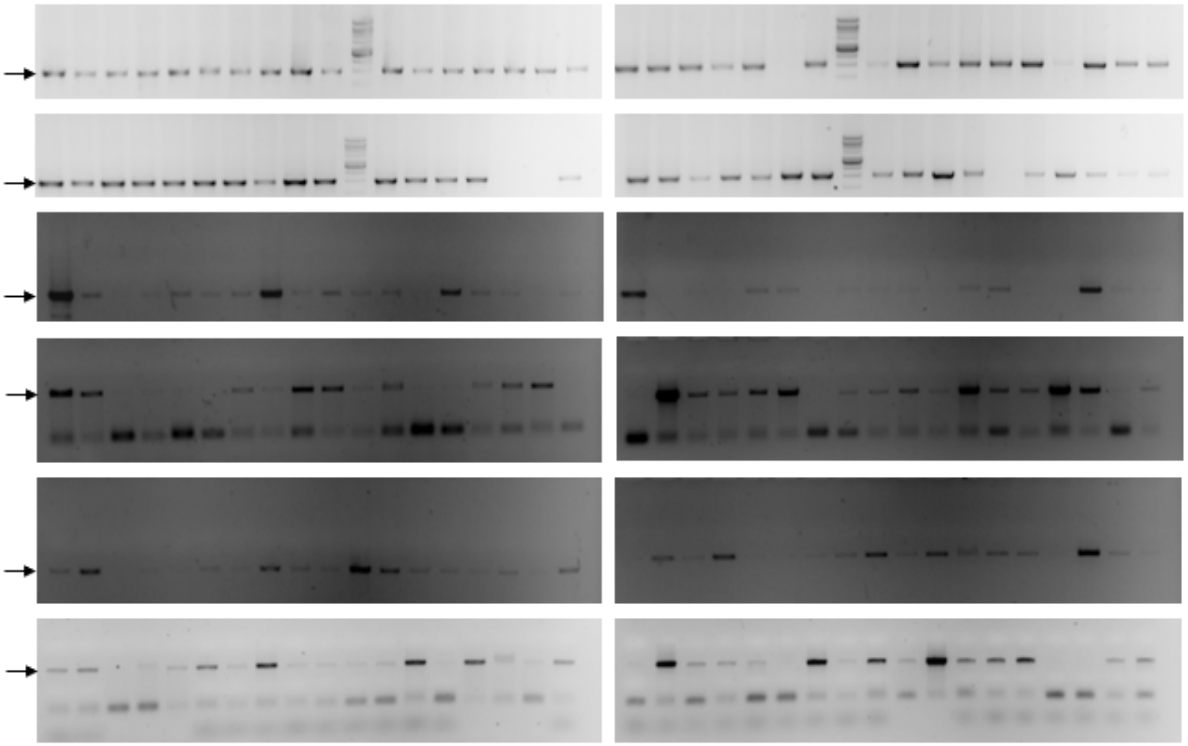

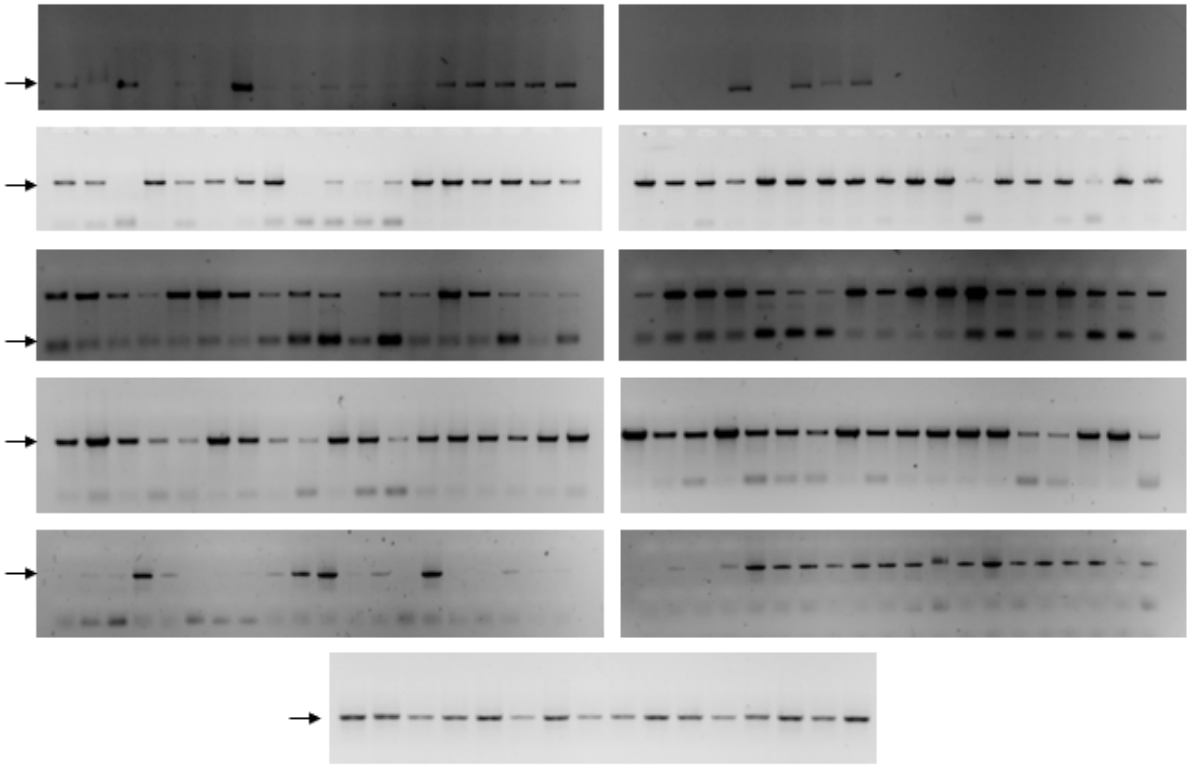

Shown are the gel images for the screening of Casp$^{\Delta UBX}$ line. Out of 419 stable lines screened, 348 lines produced clear amplification though none of the amplified product showed the desired lower migrating 1215bp band. Arrowheads indicate the position of the expected Casp wild type band.

Casp$^{\Delta UAS\Delta UBX}$ line: primer pair Casp_UAS_Ubx_F and Casp_null_R were used for screening and 1kb ladder was used for size comparison. A proper deletion should produce a 231bp product. None of the screened lines amplified 231bp product.

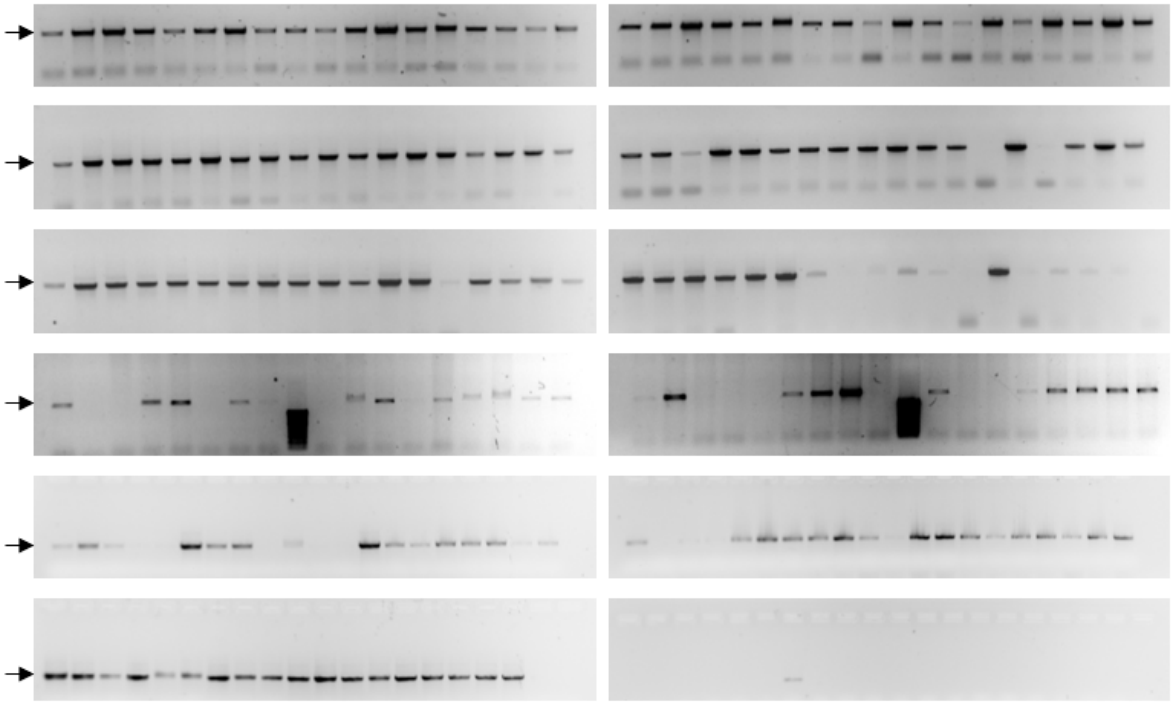

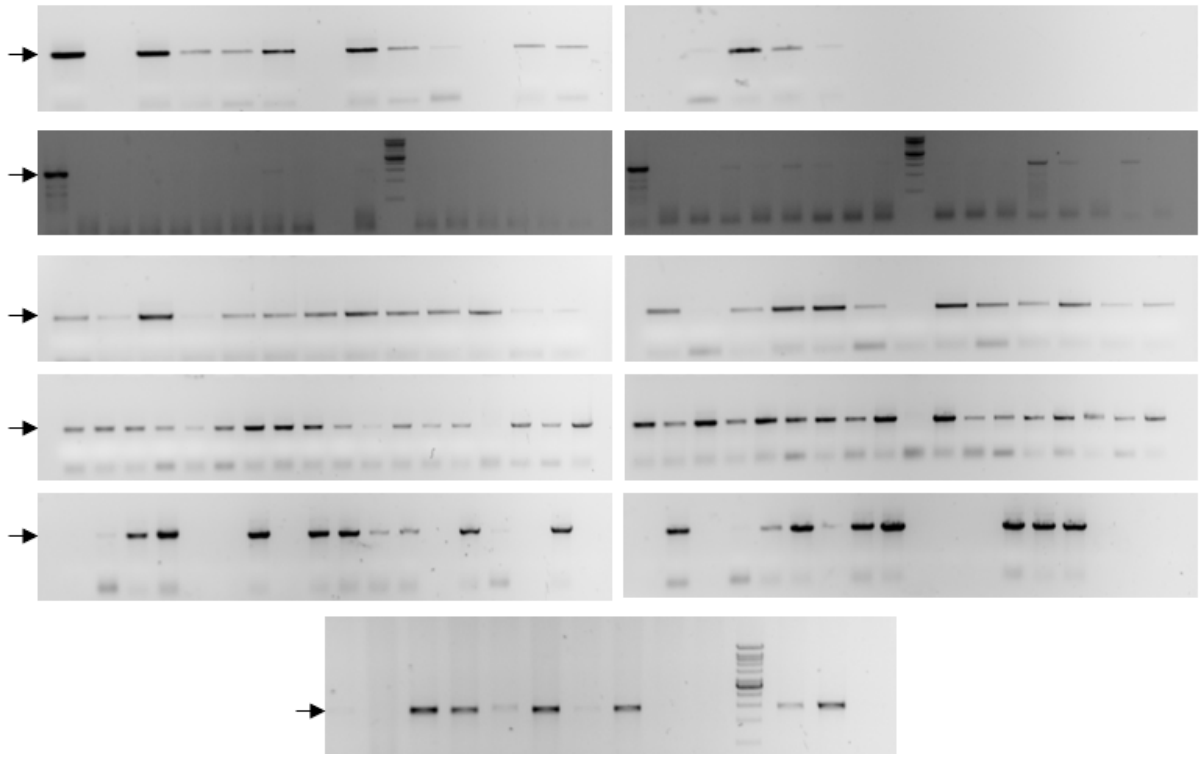

Out of all the stable lines that were screened, 362 generated amplification bands. None of these amplicons showed a lower migrating band that can be visualized at a 231bp size. The products were resolved alongside a 1Kb DNA ladder. Arrows indicate the expected migration size for a Casp-wt gene region amplicon.

3. pUASP Constructs

Vector maps:

1. pUASP-HA-Casp^{wt}

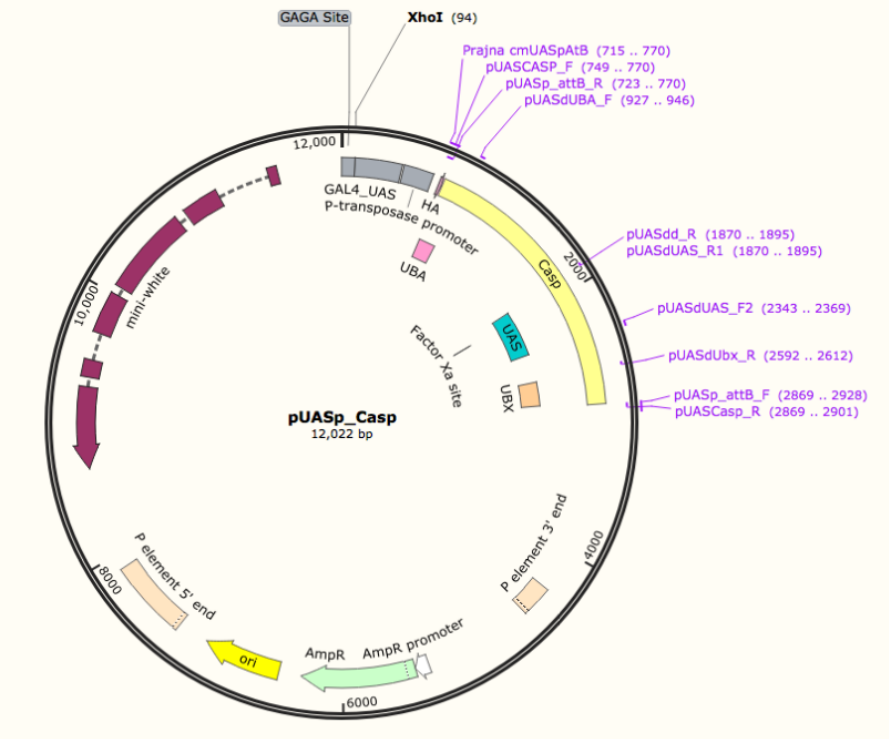

pUASP-HA-Casp^{wt}: Casp CDS along with an N-terminal HA tag was cloned in to pUASP to be used as control in the UAS-Gal4 rescue experiments.

HA-Casp^{wt} was cloned into the BamH1 and Xba1 restriction site. This construct was used as a template for amplifying inserts required for cloning rest of the pUASP_Casp constructs

2. pUASP-HA-Casp$^{\Delta UBA}$

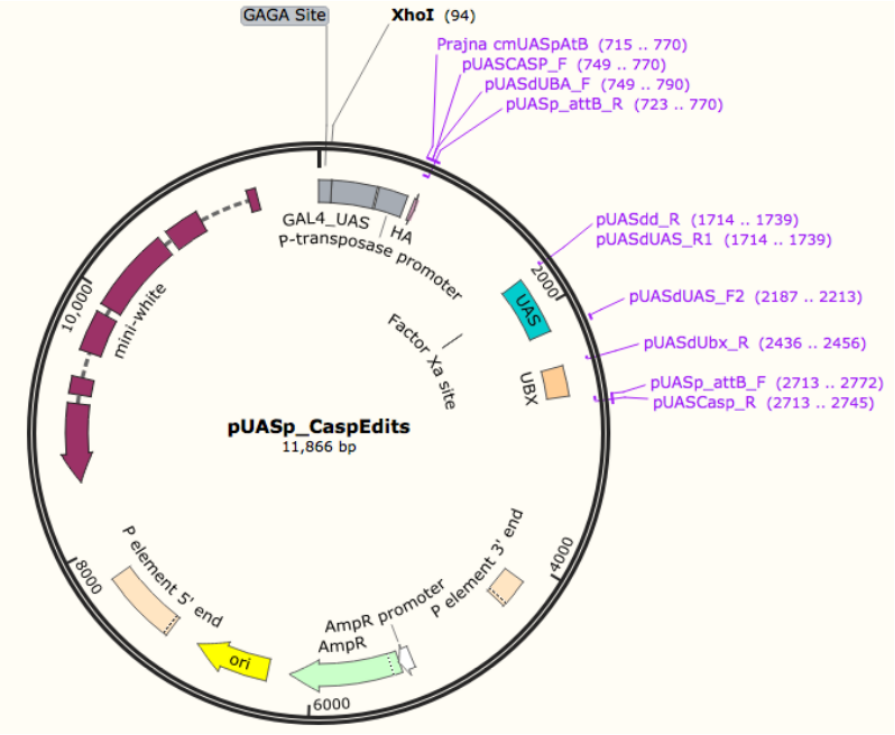

pUASP-HA-Casp$^{\Delta UBA}$: this construct was made to study the effect of the protein stabilization function of Casp in the observed maternal effect.

The insert was amplified from the pUASP-HA-Casp^{wt} vector using the primer pair pUASdUBA_F and pUAS-Casp_R. Insert was cloned into the BamH1 cloning site by recombination.

3. pUASP-HA-Casp$^{\Delta UAS}$

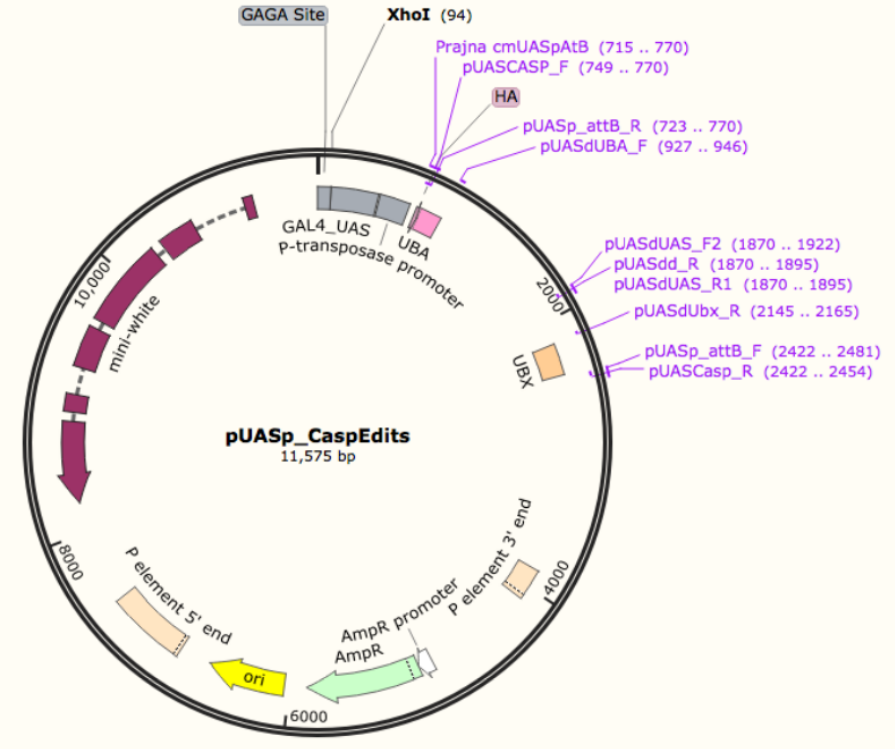

pUASP-HA-Casp$^{\Delta UAS}$: Role of UAS domain in LCPUFA mediated immune response can be studied using this construct given that it is able to perform rest of the biological functions.

The insert was amplified from the pUASP-HA-Casp^{wt} vector as two fragments using the primer pairs pUASCasp_F : pUASdUAS-R1 and pUASdUAS-F2 : pUASCasp_R. Fragments were directionally cloned into the BamH1 site by recombination.

4. pUASP-HA-Casp$^{\Delta UBX}$

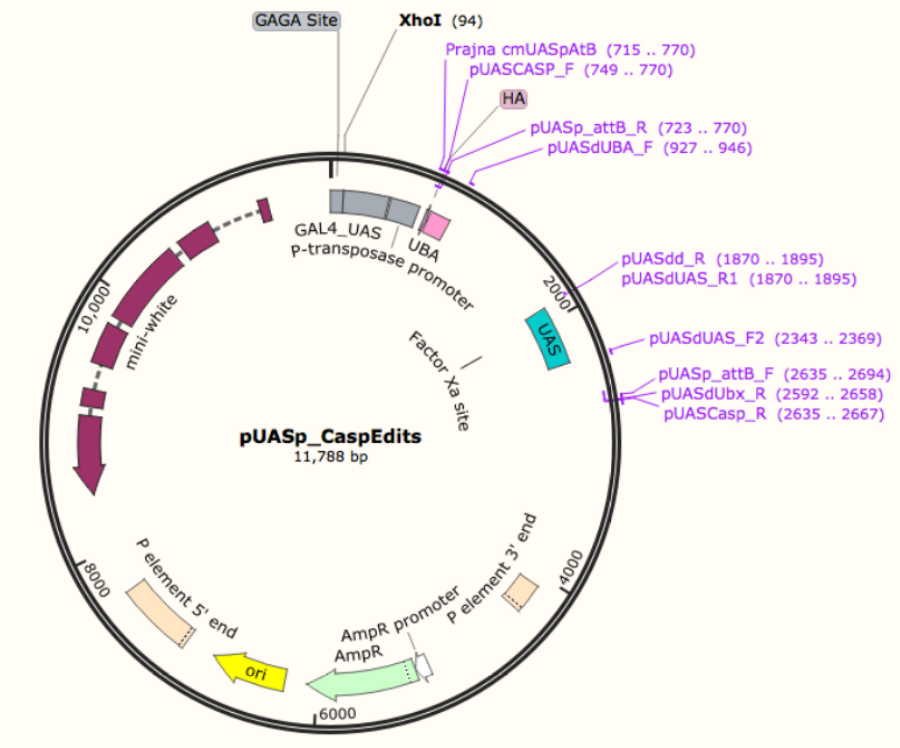

pUASP-HA-Casp$^{\Delta UBX}$: UBX aids in protein degradation. This construct should tell us the importance of Casp mediated protein degradation in the observed Casp associated phenotypes.

The insert was amplified from the pUASP-HA-Casp^{wt} vector using the primer pair pUASCasp_F and pUASdUBX_R. Insert was cloned into the BamH1 cloning site by recombination.

5. pUASP-HA-Casp$^{\Delta UAS\Delta UBX}$

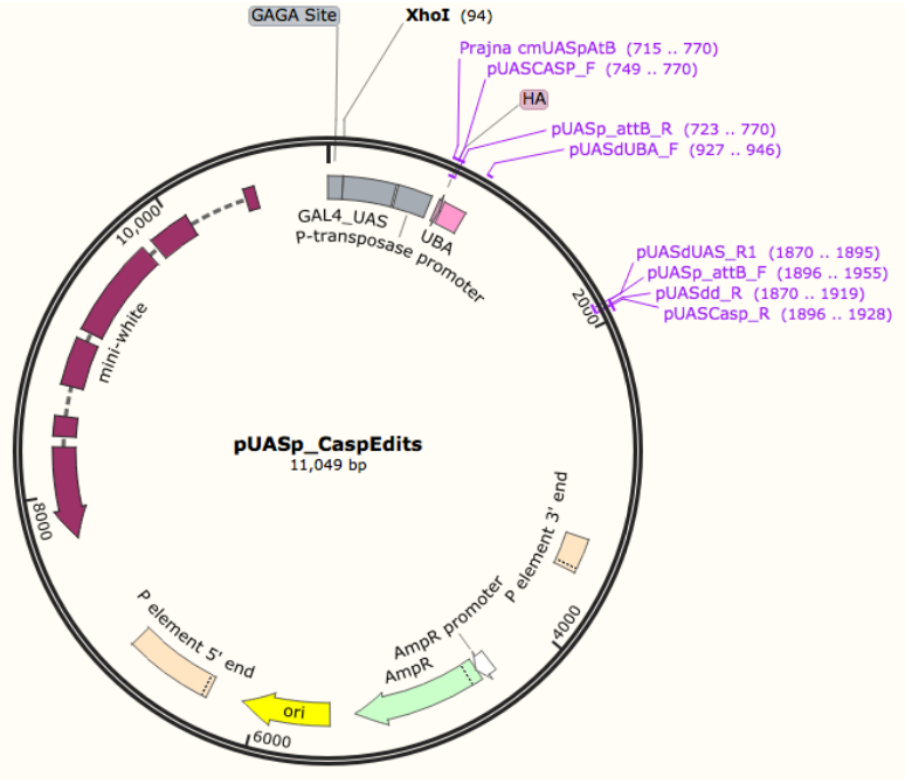

pUASP-HA-Casp$^{\Delta UAS\Delta UBX}$: The dual domain deletion construct is to study the combinatorial effects of the Casp domains in immunity and maternal effect.

The insert was amplified from the pUASP-HA-Casp^{wt} vector using the primer pair pUASCasp_F and pUASdd_R. Insert was cloned into the BamH1 cloning site by PPY mediated recombination.

6. Colony screening:

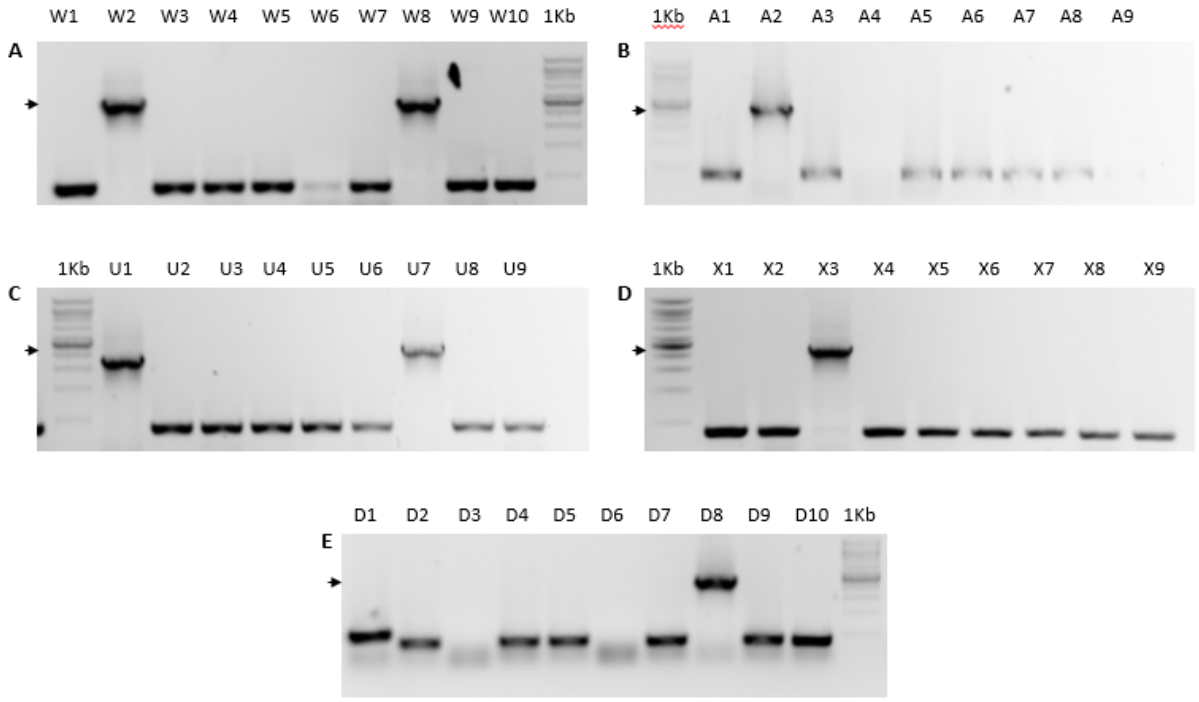

Gel images of colony screening PCR reactions performed for identifying the pUASP positive recombinants. A) W2 and W8 were identified as a positive recombinant for UAS-Casp^{wt} with a functional HA tag. Miniprep of the colony was sequenced. B) Colony A2 was identified for sequencing from the Casp$^{\Delta UBA}$ clones since it amplified a desired size product. C) Out of the two positives in case of Casp$^{\Delta UAS}$, only U7 amplicon was migrating at the expected product size. This was sequenced and identified as a proper recombinant. D) Panel shows colony X3 as a positive recombinant, amplifying a desired product at the expected size. E) D8 is a colony with proper recombination of the insert. The smaller amplicons indicate backbone end ligation without the insert incorporation. Arrowheads indicate the expected run size of each of the insert amplicons.

REFERENCES

1. Chu, K., Niu, X. & Williams, L. T. A Fas-associated protein factor, FAF1, potentiates Fas-mediated apoptosis. *Proceedings of the National Academy of Sciences* vol. 92 11894–11898 (1995).

2. Song, E. J., Yim, S.-H., Kim, E., Kim, N.-S. & Lee, K.-J. Human Fas-associated factor 1, interacting with ubiquitinated proteins and valosin-containing protein, is involved in the ubiquitin-proteasome pathway. *Mol. Cell. Biol.* 25, 2511–2524 (2005).

3. Lee, J.-J., Kim, Y. M., Jeong, J., Bae, D. S. & Lee, K.-J. Ubiquitin-associated (UBA) domain in human Fas associated factor 1 inhibits tumor formation by promoting Hsp70 degradation. *PLoS One* 7, e40361 (2012).

4. Kim, H.-J., Song, E. J., Lee, Y.-S., Kim, E. & Lee, K.-J. Human Fas-associated factor 1 interacts with heat shock protein 70 and negatively regulates chaperone activity. *J. Biol. Chem.* 280, 8125–8133 (2005).

5. Park, M.-Y., Jang, H. D., Lee, S. Y., Lee, K.-J. & Kim, E. Fas-associated Factor-1 Inhibits Nuclear Factor-κB (NF-κB) Activity by Interfering with Nuclear Translocation of the RelA (p65) Subunit of NF-κB. *Journal of Biological Chemistry* vol. 279 2544–2549 (2004).

6. Kim, H. *et al.* UAS domain of Ubxd8 and FAF1 polymerizes upon interaction with long-chain unsaturated fatty acids. *J. Lipid Res.* 54, 2144–2152 (2013).

7. Weigert, C., Brodbeck, K., Machicao, F., Hroing, H. U. & Schleicher, E. Proteasome-dependent induction of interleukin-6 by saturated fatty acids in human myotubes. *GBM Annual Spring meeting Mosbach 2004* vol. 2004 (2004).

8. Lee, J.-J. *et al.* Complex of Fas-associated factor 1 (FAF1) with valosin-containing protein (VCP)-Npl4-Ufd1 and polyubiquitinated proteins promotes endoplasmic reticulum-associated degradation (ERAD). *J. Biol. Chem.* 288, 6998–7011 (2013).

9. Shin, S.-W. *et al.* Mouse zygote-specific proteasome assembly chaperone important for maternal-to-zygotic transition. *Biol. Open* 2, 170–182 (2013).

10. Zhang, Z. *et al.* Ter94 ATPase complex targets k11-linked ubiquitinated ci to proteasomes for partial degradation. *Dev. Cell* 25, 636–644 (2013).

11. Adham, I. M. *et al.* Fas-associated factor (FAF1) is required for the early cleavage-stages of mouse embryo. *Mol. Hum. Reprod.* 14, 207–213 (2008).

12. Kim, M., Lee, J. H., Lee, S. Y., Kim, E. & Chung, J. Caspar, a suppressor of antibacterial immunity in *Drosophila*. *Proc. Natl. Acad. Sci. U. S. A.* 103, 16358–16363 (2006).

13. Nusslein-Volhard, C., Frohnhofer, H. & Lehmann, R. Determination of anteroposterior polarity in *Drosophila*. *Science* vol. 238 1675–1681 (1987).

14. Lu, X., Chou, T. B., Williams, N. G., Roberts, T. & Perrimon, N. Control of cell fate determination by p21ras/Ras1, an essential component of torso signaling in *Drosophila*. *Genes Dev.* 7, 621–632 (1993).

15. Zhou, H.-L., Geng, C., Luo, G. & Lou, H. The p97-UBXD8 complex destabilizes mRNA by promoting release of ubiquitinated HuR from mRNP. *Genes Dev.* 27, 1046–1058 (2013).

16. Xia, Y. *et al.* Pathogenic mutation of UBQLN2 impairs its interaction with UBXD8 and disrupts endoplasmic reticulum-associated protein degradation. *J. Neurochem.* 129, 99–106 (2014).

17. Fitch, K. R., Yasuda, G. K., Owens, K. N. & Wakimoto, B. T. 1 Paternal Effects in *Drosophila*: Implications for Mechanisms of Early Development. *Current Topics in Developmental Biology Volume 38* 1–34 (1997) doi:10.1016/s0070-2153(08)60243-4.

18. Wilson, K. L., Fitch, K. R., Bafus, B. T. & Wakimoto, B. T. Sperm plasma membrane breakdown during *Drosophila* fertilization requires sneaky, an acrosomal membrane protein. *Development* 133, 4871–4879 (2006).

19. Fuyama, Y. Genetics of Parthenogenesis in *DROSOPHILA* MELANOGASTER. I. the Modes of Diploidization in the Gynogenesis Induced by a Male-Sterile Mutant, ms(3)K81. *Genetics* 112, 237–248 (1986).

20. Yasuda, G. K., Schubiger, G. & Wakimoto, B. T. Genetic characterization of ms (3) K81, a paternal effect gene of *Drosophila* melanogaster. *Genetics* 140, 219–229 (1995).

21. Baker, B. S. Paternal loss (pal): a meiotic mutant in *Drosophila* melanogaster causing loss of paternal chromosomes. *Genetics* 80, 267–296 (1975).

22. Szabad, J., Máthé, E. & Puro, J. Horka, a dominant mutation of *Drosophila*, induces nondisjunction and, through paternal effect, chromosome loss and genetic mosaics. *Genetics* 139, 1585–1599 (1995).

23. Website. www.Quiagen.com/resources.

24. Kim, H., Kim, K., Kim, J., Kim, S.-H. & Yim, J. Mutagenesis by imprecise excision of the piggyBac transposon in *Drosophila* melanogaster. *Biochem. Biophys. Res. Commun.* 417, 335–339 (2012).

25. Ishino, Y., Shinagawa, H., Makino, K., Amemura, M. & Nakata, A. Nucleotide sequence of the iap gene, responsible for alkaline phosphatase isozyme conversion in Escherichia coli, and identification of the gene product. *J. Bacteriol.* 169, 5429–5433 (1987).

26. Barrangou, R. & Marraffini, L. A. CRISPR-Cas systems: Prokaryotes upgrade to adaptive immunity. *Mol. Cell* 54, 234–244 (2014).

27. Yosef, I., Goren, M. G. & Qimron, U. Proteins and DNA elements essential for the CRISPR adaptation process in Escherichia coli. *Nucleic Acids Research* vol. 40 5569–5576 (2012).

28. Makarova, K. S., Wolf, Y. I. & Koonin, E. V. Classification and Nomenclature of CRISPR-Cas Systems: Where from Here? *The CRISPR Journal* vol. 1 325–336 (2018).

29. Jinek, M. *et al.* Structures of Cas9 endonucleases reveal RNA-mediated conformational activation. *Science* 343, 1247997 (2014).

30. Gagnon, J. A. *et al.* Efficient mutagenesis by Cas9 protein-mediated oligonucleotide insertion and large-scale assessment of single-guide RNAs. *PLoS One* 9, e98186 (2014).

31. Chari, R., Mali, P., Moosburner, M. & Church, G. M. Unraveling CRISPR-Cas9 genome engineering parameters via a library-on-library approach. *Nat. Methods* 12, 823–826 (2015).

32. Fu, Y. *et al.* High-frequency off-target mutagenesis induced by CRISPR-Cas nucleases in human cells. *Nat. Biotechnol.* 31, 822–826 (2013).

33. Richardson, C. D., Ray, G. J., DeWitt, M. A., Curie, G. L. & Corn, J. E. Enhancing homology-directed genome editing by catalytically active and inactive CRISPR-Cas9 using asymmetric donor DNA. *Nat. Biotechnol.* 34, 339–344 (2016).

34. Jinek, M. *et al.* A programmable dual-RNA-guided DNA endonuclease in adaptive bacterial immunity. *Science* 337, 816–821 (2012).

35. Port, F., Chen, H.-M., Lee, T. & Bullock, S. L. Optimized CRISPR/Cas tools for efficient germline and somatic genome engineering in *Drosophila*. *Proc. Natl. Acad. Sci. U. S. A.* 111, E2967–76 (2014).

36. Website. http://www.crisprflydesign.org/wp-content/uploads/2014/06/Cloning-with-pCFD4.pdf.

37. Perkins, L. A. *et al.* The Transgenic RNAi Project at Harvard Medical School: Resources and Validation. *Genetics* 201, 843–852 (2015).

38. Giniger, E., Varnum, S. M. & Ptashne, M. Specific DNA binding of GAL4, a positive regulatory protein of yeast. *Cell* vol. 40 767–774 (1985).

39. Duffy, J. B. GAL4 system in D*rosophila*: A fly geneticist's swiss army knife. *genesis* vol. 34 1–15 (2002).

40. Zamore, P. D., Tuschl, T., Sharp, P. A. & Bartel, D. P. RNAi. *Cell* vol. 101 25–33 (2000).

41. Fire, A. *et al.* Potent and specific genetic interference by double-stranded RNA in Caenorhabditis elegans. *Nature* vol. 391 806–811 (1998).

42. Tabara, H. *et al.* The rde-1 Gene, RNA Interference, and Transposon Silencing in C. elegans. *Cell* vol. 99 123–132 (1999).

43. Paddison, P. J., Caudy, A. A. & Hannon, G. J. Stable suppression of gene expression by RNAi in mammalian cells. *Proc. Natl. Acad. Sci. U. S. A.* 99, 1443–1448 (2002).

44. Ni, J.-Q. *et al.* Vector and parameters for targeted transgenic RNA interference in *Drosophila* melanogaster. *Nat. Methods* 5, 49–51 (2008).

45. Xu, Y., Liu, Y., Lee, J.-G. & Ye, Y. A ubiquitin-like domain recruits an oligomeric chaperone to a retrotranslocation complex in endoplasmic reticulum-associated degradation. *J. Biol. Chem.* 288, 18068–18076 (2013).

46. Jones, D. L. *et al.* Kinetics of dCas9 target search in Escherichia coli. *Science* vol. 357 1420–1424 (2017).

47. Richardson, C. D., Ray, G. J., Bray, N. L. & Corn, J. E. Non-homologous DNA increases gene disruption efficiency by altering DNA repair outcomes. *Nat. Commun.* 7, 12463 (2016).

48. Kim, S., Kim, D., Cho, S. W., Kim, J. & Kim, J.-S. Highly efficient RNA-guided genome editing in human cells via delivery of purified Cas9 ribonucleoproteins. *Genome Res.* 24, 1012–1019 (2014).

49. Clarke, R. *et al.* Enhanced Bacterial Immunity and Mammalian Genome Editing via RNA-Polymerase-Mediated Dislodging of Cas9 from Double-Strand DNA Breaks. *Mol. Cell* 71, 42–55.e8 (2018).

50. Horlbeck, M. A. *et al.* Nucleosomes impede Cas9 access to DNA in vivo and in vitro. *Elife* 5, (2016).

51. Celniker, S. E. *et al.* Unlocking the secrets of the genome. *Nature* 459, 927–930 (2009).

52. Tadros, W. & Lipshitz, H. D. The maternal-to-zygotic transition: a play in two acts. *Development* 136, 3033–3042 (2009).

53. Wasbrough, E. R. *et al.* The *Drosophila* melanogaster sperm proteome-II (DmSP-II). *J. Proteomics* 73, 2171–2185 (2010).

54. Gao, G., Cheng, Y., Wesolowska, N. & Rong, Y. S. Paternal imprint essential for the inheritance of telomere identity in *Drosophila*. *Proc. Natl. Acad. Sci. U. S. A.* 108, 4932–4937 (2011).

55. Riparbelli, Maria Giovanna, et al. "Wolbachia-mediated male killing is associated with defective chromatin remodeling." PLoS One 7.1 (2012).

56. Schumann, Wolfgang. "Comperative studies with Culex pipiens egg rafts. Immunogenetic, electrophoretic and enzymatic analysis of unfertilized, compatible and incompatible fertilized eggs." Theoretical and Applied Genetics 44.4 (1974): 160-166.

57. Lassy, Craig W., and Timothy L. Karr. "Cytological analysis of fertilization and early embryonic development in incompatible crosses of Drosophila simulans." Mechanisms of development 57.1 (1996): 47-58.

58. Bressac, Christophe, and François Rousset. "The reproductive incompatibility system in Drosophila simulans: DAPI-staining analysis of the Wolbachia symbionts in sperm cysts." Journal of invertebrate pathology 61.3 (1993): 226-230

59. Clark, Michael E., et al. "Induced paternal effects mimic cytoplasmic incompatibility in Drosophila." Genetics 173.2 (2006): 727-734.